



Entergy Operations, Inc.
1448 S.R. 333
Russellville, AR 72801
Tel 501-858-4888

Craig Anderson
Vice President
Operations ANO

2CAN010304

January 29, 2003

U.S. Nuclear Regulatory Commission
Attn: Document Control Desk
Washington, DC 20555

SUBJECT: Arkansas Nuclear One, Unit 2
Docket No. 50-368
License Amendment Request to Change the Spent Fuel Pool (SFP)
Loading Restrictions

REFERENCE: Entergy Operations, Inc. letter to the NRC dated August 8, 2002, "Use of Metamic® In Fuel Pool Applications" (0CAN080201)

Dear Sir or Madam:

Pursuant to 10 CFR 50.90, Entergy Operations, Inc. (Entergy) hereby requests the following operating license amendment for Arkansas Nuclear One, Unit 2 (ANO-2). Currently, the ANO-2 SFP storage racks are divided into two regions: Region 1, which contains Boraflex®, and Region 2, which contains no poison panel inserts. ANO-2 Technical Specification (TS) 3.9.12.b, and TS Figure 3.9.2 describe the current loading restrictions for each of these regions. TS 3.9.12 Figure 3.9.1 depicts the SFP arrangement by showing the areas that are designated as Region 1 and Region 2. ANO-2 plans to modify a portion of the Region 2 SFP racks by inserting Metamic® poison panels. The new area will be defined as Region 3 and will allow storage of new and spent fuel without restriction. Upon approval of the proposed change, no credit will be taken for the Boraflex® in Region 1 of the SFP and new restrictions will be placed on the spent fuel loading pattern in Region 1 and Region 2. Changes to TS 3.9.12.b, TS Figures 3.9.1 and 3.9.2, TS 3.9.12.c, and Surveillance Requirement 4.9.12.b are proposed, as well as changes to the design features of the fuel storage racks which are included in TS 5.3.

Entergy submitted by letter dated August 8, 2002, a topical report prepared by Holtec International that describes the physical and chemical properties of Metamic® and the test results for the use of Metamic® in fuel pool applications. Approval of the topical report is required to support the requested plant specific TS changes addressed in the attachments to this letter.

The proposed changes have been evaluated in accordance with 10 CFR 50.91(a)(1) using criteria in 10 CFR 50.92(c) and it has been determined that this change involves no significant hazards considerations. The bases for these determinations are included in the attachments to this submittal.

Abol

The Nuclear Regulatory Commission (NRC) has not reviewed TS changes for other facilities regarding the use of Metamic® poison panels in wet storage applications.

Entergy requests approval of the proposed ANO-2 amendment by August 15, 2003, in order to support fuel re-arrangement in the ANO-2 SFP in late summer or early fall prior to the fall refueling outage. Based upon current Boraflex® degradation predictions, approval of this amendment will be required to maintain full core offload capability for the upcoming refueling outage. Once approved, the amendment shall be implemented within 60 days. Although this request is neither exigent nor emergency, your prompt review is requested.

Commitments associated with this submittal are documented in Attachment 6.

If you have any questions or require additional information, please contact Dana Millar at 601-368-5445.

I declare under penalty of perjury that the foregoing is true and correct. Executed January 29, 2003.

Sincerely,

A handwritten signature in black ink, appearing to read 'CGA/rhs', written in a cursive style.

CGA/rhs

Attachments:

1. Analysis of Proposed Technical Specification Change
2. Proposed Technical Specification Changes (mark-up)
3. Changes to TS Bases pages (for information only)
4. Holtec License Report
5. Evaluation of Spent Fuel Pool Structural Integrity for Increased Loads from Spent Fuel Racks
6. Commitments

**cc: Mr. Ellis W. Merschoff
Regional Administrator
U. S. Nuclear Regulatory Commission
Region IV
611 Ryan Plaza Drive, Suite 400
Arlington, TX 76011-8064**

**NRC Senior Resident Inspector
Arkansas Nuclear One
P. O. Box 310
London, AR 72847**

**U. S. Nuclear Regulatory Commission
Attn: Mr. Thomas W. Alexion MS O-7D1
Washington, DC 20555-0001**

**Mr. Bernard R. Bevill
Director Division of Radiation
Control and Emergency Management
Arkansas Department of Health
4815 West Markham Street
Little Rock, AR 72205**

Attachment 1

2CAN010304

Analysis of Proposed Technical Specification Change

1.0 DESCRIPTION

This letter is a request to amend Operating License NPF-6 for Arkansas Nuclear One, Unit 2 (ANO-2).

The proposed changes will revise the Technical Specifications (TS) to:

- Define Region 3 of the ANO-2 spent fuel pool (SFP) as the location in which Metamic® poison panel inserts will be installed.
- Redefine the loading pattern in the current Region 1, taking no credit for Boraflex®.
- Redefine the loading pattern in the current Region 2.
- Redefine the Surveillance Requirements (SR) associated with verification of fuel assembly placement.
- Delete Note 1 associated with TS 3.9.12.b.
- Redefine the design features associated with spent fuel storage rack criticality to specify that boron is credited to maintain K_{eff} less than or equal to 0.95.
- Increase the minimum boron concentration in the SFP to >2000 ppm.

Changes are proposed to the following ANO-2 TSs:

- TS 3.9.12.b and the associated Figures 3.9.1 and 3.9.2
- TS 3.9.12.c
- (SR) 4.9.12.b
- TS 5.3.1, Spent Fuel Storage Rack Criticality

To best reflect the loading restrictions in the two regions, a new figure will be added for Region 2 while the current Figure 3.9.2 will reflect the loading restrictions for Region 1.

Proposed changes to the TS Bases associated with TS 3.9.12 are included as Attachment 3 for information only.

Administrative changes are also being made to change the font on the pages that are included in the proposed change to Arial 11. This is a non-technical change and will not be discussed further in this submittal.

The changes are desired in order to address the degradation of Boraflex® in Region 1 and to support the creation of a new Region 3 in which Metamic® poison panel inserts will be installed. New loading restrictions will be imposed in Region 1 since the new reactivity balances will not take credit for the Boraflex® in that region.

2.0 PROPOSED CHANGES

ANO-2 TS 3.9.12.b and Figures 3.9.1 and 3.9.2 define the areas designated as Region 1 and Region 2 and define the loading restrictions for any fuel assemblies that are stored in Region 1 or 2 of the ANO-2 SFP. Region 1 contains Boraflex® and currently has fewer loading restrictions than Region 2 which does not contain any poison panel inserts. Calculations have shown that Boraflex® is degrading and will continue to degrade below the assumed value used in the current criticality analysis. Therefore, the proposed changes will take no credit for

Boraflex® in Region 1 and will include new loading restrictions for Region 1. Based on the new criticality analysis, new restrictions will also be imposed on Region 2. This will result in changes to TS 3.9.12.b and Figure 3.9.2. The new Figure 3.9.2 will depict loading restrictions for Region 1 and a new Figure 3.9.3 will be added for the loading restrictions in Region 2 such that loading restrictions for Region 1 and Region 2 are reflected on separate figures. In addition, a portion of the current Region 2 SFP racks will be modified by the installation of Metamic® poison panel inserts. This will result in the creation of a new Region 3 which will allow unrestricted storage of new and spent fuel. The creation of the new region will require a change to TS Figure 3.9.1. Entergy has submitted a topical report to allow the use of Metamic® in SFP applications. Approval of the topical report is required to support this submittal.

Note 1 associated with TS 3.9.12.b allows storage of fuel assemblies in the vacant spaces created in the most peripheral row/column of Region 1 as required by Curve A on TS Figure 3.9.2. The new criticality analysis redefines loading restrictions for Region 1; therefore, this note is no longer applicable and will be deleted.

TS 3.9.12.c currently requires that the boron concentration in the SFP be maintained at >1600 ppm. TS 5.3.1.b currently specifies that K_{eff} will be ≤ 0.95 if the SFP racks are fully flooded with unborated water. However, the new criticality analysis will take credit for boron to ensure K_{eff} remains ≤ 0.95 . Therefore, TS 3.9.12.c will be modified to require that the minimum boron concentration in the SFP be maintained at >2000 ppm to provide further assurance that K_{eff} remains below 0.95.

TS 5.3.1.b currently specifies that the effective multiplication factor (K_{eff}) will be less than or equal to 0.95 if the SFP racks are fully flooded with unborated water. The new criticality analysis will take credit for boron to ensure K_{eff} remains below 0.95. Subcriticality is maintained (K_{eff} less than 1.0) when the pool is fully flooded with unborated water and the fuel is loaded as designated in the proposed TS Figures 3.9.2 and 3.9.3. Therefore, TS 5.3.1.b will be modified to reflect that the presence of boron (400 ppm) is required to maintain the K_{eff} of the racks less than 0.95 and a new 5.3.1.c will be added to reflect that subcriticality ($K_{eff} < 1.0$) will be maintained without boron. The current 5.3.1.c, which describes the nominal center to center distance, will become 5.3.1.d.

SR 4.9.12.b requires verification that the fuel assemblies that will be placed in the SFP are within the limits of Figure 3.9.2. The proposed change will modify this SR to reflect the addition of a new curve to ensure that the current requirement is maintained.

In summary, the proposed changes will define Region 3 in which Metamic® poison panels will be inserted and impose new loading restrictions in Region 1 and Region 2. TS 5.3.1.b will also be modified.

Changes are also proposed to the TS Bases associated with TS 3.9.12. The proposed changes will reflect the newly defined Region 3 and modify the boron concentration required to maintain k_{eff} below 0.95 for the worst case accident condition to 825 parts per million (ppm). A soluble boron concentration of 825 ppm ensures k_{eff} remains below 0.95 if a misplacement of a fresh unburned fuel assembly of the highest permissible reactivity were to occur in a Region 1 or Region 2 storage cell. The loading patterns described in the bases will be modified to support the new SFP criticality analysis that does not credit the existing Boraflex® and the creation of Region 3 in which Metamic® poison panels will be installed.

3.0 BACKGROUND

3.1 Spent Fuel Pool Racks

The ANO-2 SFP provides 988 storage locations for spent fuel assemblies or other items (e.g. incore detectors) which require long term submerged storage. The racks are comprised of twelve free standing structures. Four modules contain 81 fuel storage locations each in a 9x9 array; four modules contain 90 fuel storage locations each in a 9x10 array; two modules contain 80 fuel storage locations in an 8x10 array; and, two modules contain 72 fuel storage locations in an 8x9 array. The SFP is lined with type 304L stainless steel and is designed to seismic Category I criteria.

Each fuel storage module is made up of rectangular storage cells which are capable of accepting one fuel assembly. The cells are open at the top and bottom to provide a flow path for convective cooling of spent fuel assemblies through natural circulation. The fuel storage cells are structurally connected to form storage modules which provide the assurance that the required minimum fuel assembly spacing is maintained for all design conditions including a design basis earthquake (DBE).

All welded construction is used in fabrication of the fuel storage cells and in the interconnection of cells to form modules. The fuel storage modules are constructed of type 304 stainless steel. The welded construction ensures the structural integrity of the storage modules and provides assurance of smooth snag-free paths in the storage cells so that it is highly improbable that a fuel assembly could become stuck in the racks.

ANO-2 Safety Analysis Report (SAR) Section 9.1.3 contains a detailed description of the ANO-2 SFP, the associated structural and seismic considerations, the fuel rack structural analysis, the pool structural analysis, the criticality analysis for Regions 1 and 2, the postulated spent fuel storage criticality analysis, and the testing and inspection requirements. Based on approval of the proposed changes, the appropriate section of the SAR will be revised.

TS 3.9.12.b currently defines two storage regions (Region 1 and Region 2), each of which has specified loading restrictions based on assembly average burnup in GWD/MTU and the initial assembly average U-235 loading per unit length (g/inch). TS Figure 3.9.2 was initially included in the ANO-2 TSs with the approval of TS Amendment 43 [NRC Safety Evaluation Report (SER) dated April 15, 1983]. The amendment allowed modification of the SFP racks which resulted in increased storage capacity in the pool and the addition of Region 1 which contains Boraflex®.

TS Figure 3.9.2 was subsequently modified with the approval of TS Amendment 178 (NRC SER dated January 14, 1997). This amendment allowed an increase in the initial fuel enrichment from 4.1 weight percent (w/o) to 5.0 w/o. The criticality analysis performed based on the higher initial enrichment resulted in changes to TS Figure 3.9.2. TS 3.9.12.a. was also modified.

TS Amendment 224 (NRC SER dated October 24, 2000) allowed an alternate storage configuration of fuel assemblies adjacent to the walls within Region 1 of the SFP provided they were less reactive than the area of the graph enclosed by Curve A on TS Figure 3.9.2. This change provided 17 additional storage locations. This allowance was incorporated with the insertion of Note 1.

The controls used in determining the storage location for new and irradiated fuel in the SFP are governed by procedure. The procedure currently contains guidelines pertaining to restricted and unrestricted fuel storage as reflected by TS Figure 3.9.2. The new loading pattern restrictions and the addition of Region 3 will continue to be governed by procedure. Checkerboard storage configurations will be procedurally controlled with the vacant spaces administratively controlled by procedure.

3.2 Spent Fuel Pool System

The fuel pool system is designed to:

- maintain the pool temperatures less than or equal to approximately 150°F during a full core discharge. The cooling system's heat removal capacity is a function of service water temperature. Refueling operations are administratively controlled in order to minimize the potential of exceeding a pool temperature of 150°F during a full core discharge whenever service water system temperature is elevated.
- maintain purity and optical clarity of the fuel pool water.
- maintain purity of the water in the refueling cavity and in the refueling water tank.
- maintain the water level a minimum of 9.5 feet above the top of the active fuel during fuel handling and storage operations.

The cooling portion of the fuel pool system is a closed loop system consisting of two half-capacity pumps for normal duty and one full-capacity heat exchanger. The fuel pool water is drawn from the fuel pool near the surface and is circulated by the fuel pool pumps through the fuel pool heat exchanger where heat is rejected to the service water system. From the outlet of the fuel pool heat exchanger, the cooled fuel pool water is returned to the top of the fuel pool via a distribution header at the end of the pool opposite from the intake.

The clarity and purity of the water in the fuel pool, refueling cavity, and refueling water tank are maintained by the purification portion of the fuel pool system. The purification loop consists of the fuel pool purification pump, ion exchanger, filters, and strainers. The purification flow is drawn from the bottom of the fuel pool. A basket strainer is provided in the purification line to the pump suction to remove any relatively large particulate matter. The fuel pool water is circulated by the pump through a filter which removes particulates and through an ion exchanger to remove ionic material. Connections to the refueling water tank and refueling water cavity are provided for purification and makeup.

Makeup to the fuel pool is provided from the Chemical and Volume Control System via the blending tee, the refueling water tank via the purification pumps, or the Boron Management System (BMS) holdup tanks if chemistry specifications are met. In an emergency, Seismic Category I makeup is available from either service water system loop. The boric acid makeup tanks are also available for boration of the SFP. Overflow protection is provided by transferring the fuel pool water to the refueling water tank or one of the BMS holdup tanks via the purification pump on high level alarm.

A detailed description of the SFP system is included in Section 9.1.3 of the ANO-2 SAR. No modifications are proposed to the SFP system in order to support the proposed change.

4.0 TOPICAL REPORT AND COUPON SAMPLING PROGRAM

Entergy submitted to the NRC by letter dated August 8, 2002, (Reference 1), a topical report that supports the use of Metamic® poison panel inserts in SFP applications. The topical report describes the manufacturing process, the material composition, the corrosion testing results, and the resistance of Metamic® to radiation damage. The report also describes various coupon sampling programs that have been established at test facilities to monitor the physical and chemical property changes over time. To ensure that the physical and chemical properties of Metamic® behave in a similar manner to that found at the test facilities, Entergy will establish a coupon sampling program. Coupons suspended on a mounting tree will be inserted into an empty fuel cell in an ANO-2 SFP rack that is surrounded by spent fuel assemblies. Ten coupons will be created from the same manufacturing lots that will be used to manufacture the Metamic® poison panels and inserted into the SFP. The coupon measurement program is intended to monitor for changes in the physical properties of the Metamic® absorber material by visual observation and photography. The physical changes observed will reflect the probable changes that are occurring in the Metamic® poison panel inserts and provide a method of verifying that the assumptions used in the SFP criticality analysis remain valid.

5.0 TECHNICAL ANALYSIS

Attachments 4 and 5 to this letter provide detailed technical analyses in support of the proposed changes. Below is a brief summary of these attachments.

5.1 Material Considerations

It is proposed that Metamic® be inserted in the newly defined Region 3. The physical and chemical properties of Metamic® have been submitted by letter to the NRC (Reference 1).

5.2 Criticality Considerations

A criticality safety evaluation was performed for storage of fresh and spent fuel in the ANO-2 SFP. The evaluation considered the three regions that are designated as Region 1, Region 2, and Region 3. The criticality analysis currently in place for Region 1 assumes the presence of Boraflex®. In the new analysis, no credit was taken for the Boraflex® in Region 1. The new analysis also assumes Metamic® poison panel inserts are installed in Region 3. It was concluded that in order to assure that K_{eff} remains less than 0.95 in the various storage configurations that are allowed, considering the storage of both spent and fresh fuel assemblies, a minimum soluble boron concentration is required. The requested change to TS 3.9.12.c requires a boron concentration in the SFP >2000 ppm. The boron concentrations for each region determined by analyses to assure K_{eff} remains below 0.95 are bounded by the requested TS value. The fuel loading patterns which are defined by the criticality safety evaluation will be governed by the proposed changes.

5.3 Thermal Hydraulic Considerations

A thermal hydraulic analysis conservatively demonstrated that natural circulation of the pool water for the proposed configuration provides adequate cooling of all fuel assemblies in the event of a loss of external cooling. Corrective actions can be taken prior to SFP boiling. The analysis also demonstrated that fuel cladding will not be subjected to departure from nucleate boiling under the postulated accident scenario of the loss of all SFP cooling and that cladding integrity would be maintained. None of the temperature limits or corrective actions for the SFP cooling system change.

5.4 Structural/Seismic Analysis

A structural analysis of the spent fuel racks with the new poison inserts was considered for all loadings postulated for normal and seismic conditions. The evaluation demonstrated that the structural integrity of all storage modules is maintained.

The structural integrity of the new poison inserts under normal and seismic conditions is essential to maintaining the assumptions of the criticality analysis. The poison insert design has been evaluated for normal and seismic conditions and all safety factors are greater than 1.0. However, it is expected that minor changes to the design will occur during product development and testing. All changes will be reflected in the finalized evaluation of the poison insert structural analysis.

5.5 Mechanical Accident

In line with the current approved philosophies, the postulated fuel assembly drop events for Region 3 of the SFP racks were conservatively evaluated and concluded that the poison inserts, as well as the cell wall of the impacted rack cell could be significantly damaged. Conservatively assuming that all poison inserts in Region 3 were damaged, the evaluation concluded that the racks would remain subcritical when credit was taken for a TS limit of >2000 ppm soluble boron in the pool.

5.6 SFP Structural Integrity for Increased Loads from SFP Racks

An evaluation of the SFP structural integrity for the effects of the increased loads from the SFP racks was performed. The evaluation demonstrated that the structural integrity of the pool structure is maintained.

6.0 REGULATORY ANALYSIS

6.1 Applicable Regulatory Requirements/Criteria

The proposed changes have been evaluated to determine whether applicable regulations and requirements continue to be met. The applicable regulations and requirements used to support the proposed changes and reflection of their continued compliance are included in the license report in Attachment 4.

Entergy has determined that the proposed changes do not require any exemptions or relief from regulatory requirements other than the TS changes described and do not affect conformance with any GDC differently than described in the SAR.

6.2 No Significant Hazards Consideration

The proposed change will modify the Arkansas Nuclear One, Unit 2 (ANO-2) Technical Specifications (TSs) related to fuel pool storage. The ANO-2 spent fuel pool (SFP) is currently divided into two regions (known as Region 1 and Region 2) in which specific loading restrictions are imposed based on assembly average burnup and initial assembly average uranium-235 (U-235) loading per unit length (up to five weight percent U-235). The SFP racks in Region 1 contain Boraflex® as a neutron absorber while the SFP racks in Region 2 contain no neutron absorbers. Based on calculations which indicate that the neutron absorption characteristics of Boraflex® are degrading, Entergy has determined that the reactivity worth of Boraflex® should no longer be credited in the reactivity analysis and that more stringent loading restrictions should be imposed in Region 1. Therefore, the proposed change includes modifications to the loading restrictions in Region 1. Changes to the loading restrictions in Region 2 are also proposed. In addition, a portion of the current Region 2 will be designated as a new Region 3. The new region will contain Metamic® poison panel inserts which will provide the neutron absorption capability required to allow storage of various combinations of fuel burnup and enrichment without loading restrictions. The above change also results in the design features of the SFP racks being changed. The criticality analysis associated with this change will require credit for boron in the SFP to assure that the SFP remains subcritical with an effective multiplication factor (K_{eff}) less than 0.95.

Entergy Operations, Inc. has evaluated whether or not a significant hazards consideration is involved with the proposed amendment by focusing on the three standards set forth in 10 CFR 50.92, "Issuance of Amendment," as discussed below:

1. Does the proposed change involve a significant increase in the probability or consequences of an accident previously evaluated?

Response: No.

Most accident conditions will not result in an increase in K-effective (K_{eff}) of the fuel stored in the rack. However, there are accidents that can be postulated to increase reactivity. For these accident conditions, the double contingency principle of ANS N16.1-1975 is applied. This states that it is unnecessary to assume two unlikely, independent, concurrent events to ensure protection against a criticality accident. Therefore, for accident conditions, the presence of soluble boron in the storage pool water can be assumed as a realistic initial condition since its absence would be a second unlikely event.

A vertical drop accident condition directly upon a cell will cause damage to the racks in the active fuel region. The proposed >2000 ppm TS limit will insure that K_{eff} does not exceed 0.95. A fuel assembly dropped on top of the rack will not deform the rack structure such that criticality assumptions are invalidated. The rack structure is such that an assembly positioned horizontally on top of the rack is more than eight inches away from the upper end of the active fuel region of the stored assemblies. This distance precludes interaction between the dropped assembly and the stored fuel. An inadvertent

drop of an assembly between the outside periphery of the rack and the pool wall is bounded by the worst case fuel misplacement accident condition of 825 ppm. The distance between all the rack modules and the pool walls is less than the width of a fuel assembly.

The fuel assembly misplacement accident was considered for all storage configurations. An assembly with high reactivity is assumed to be placed in a storage location which requires restricted storage based on initial U-235 loading and burnup. The presence of boron in the pool water assumed in the analysis has been shown to substantially offset the worst case reactivity effect of a misplaced fuel assembly for any configuration. The boron requirement of 825 ppm is less than the proposed >2000 ppm minimum boron TS limit. Therefore, a five percent subcriticality margin can be easily met for postulated accidents since any reactivity increase will be much less than the negative worth of the dissolved boron.

For fuel storage applications, water is present. An "optimum moderation" accident is not a concern in spent fuel pool storage racks because the rack design prevents the preferential reduction of water density between the cells of a rack (e.g., boiling between cells).

Therefore, the proposed change does not involve a significant increase in the probability or consequences of an accident previously evaluated.

2. Does the proposed change create the possibility of a new or different kind of accident from any accident previously evaluated?

Response: No.

The proposed changes will define a portion of the current Region 2 as Region 3. The new region will contain Metamic® poison panel inserts and will allow unrestricted storage of fuel assemblies with various enrichments and burnup. To support the proposed change, a new criticality analysis was performed. The analysis resulted in new loading restrictions in Region 1 and Region 2. The presence of boron in the pool water assumed in the analysis is less than the proposed ANO-2 TS minimum concentration of >2000 ppm. Therefore, a five percent subcriticality margin can be easily met for postulated accidents since any reactivity increase will be much less than the negative worth of the dissolved boron.

No new or different types of fuel assembly drop scenarios are created by the proposed change. During the installation of the Metamic® panels, the possible drop of a panel is bounded by the current fuel assembly drop analysis. No new or different fuel assembly misplacement accidents will be created. Administrative controls currently exist to assist in assuring that fuel misplacement does not occur.

Therefore, the proposed change does not create the possibility of a new or different kind of accident from any previously evaluated.

3. Does the proposed change involve a significant reduction in a margin of safety?

Response: No.

With the presence of a nominal boron concentration, the SFP storage racks are designed to assure that fuel assemblies of less than or equal to five weight percent U-235 enrichment when loaded in accordance with the proposed loading restrictions will be maintained within a subcritical array with a subcritical margin of five percent. This has been verified by criticality analyses.

Credit for soluble boron in the SFP water is permitted under accident conditions. The proposed change that will allow insertion of Metamic® poison panels does not result in the potential of any new misplacement scenarios. Criticality analyses have been performed to determine the required boron concentration that would ensure that the maximum K_{eff} does not exceed 0.95. By increasing the minimum boron concentration to >2000 ppm, the margin of safety currently defined by taking credit for soluble boron will be maintained.

The structural analysis of the spent fuel racks along with the evaluation of the SFP structure showed that the integrity of these structures will be maintained with the addition of the poison inserts. All structural requirements were shown to be satisfied, so all the safety margins were maintained.

Therefore, the proposed change does not involve a significant reduction in a margin of safety.

Based on the above, Entergy concludes that the proposed amendment presents no significant hazards consideration under the standards set forth in 10 CFR 50.92(c), and, accordingly, a finding of "no significant hazards consideration" is justified.

6.3 Environmental Considerations

The proposed amendment does not involve (i) a significant hazards consideration, (ii) a significant change in the types or significant increase in the amounts of any effluent that may be released offsite, or (iii) a significant increase in individual or cumulative occupational radiation exposure. Accordingly, the proposed amendment meets the eligibility criterion for categorical exclusion set forth in 10 CFR 51.22(c)(9). Therefore, pursuant to 10 CFR 51.22(b), no environmental impact statement or environmental assessment need be prepared in connection with the proposed amendment.

Attachment 2

2CAN010304

Proposed Technical Specification Changes (mark-up)

REFUELING OPERATIONS

FUEL STORAGE

LIMITING CONDITION FOR OPERATION

- 3.9.12.a Storage in the spent fuel pool shall be restricted to fuel assemblies having initial enrichment less than or equal to 5.0 w/o U-235. The provisions of Specification 3.0.3 are not applicable.
- 3.9.12.b Storage in Region 1 or Region 2 (as shown on Figure 3.9.1) of the spent fuel pool shall be further restricted by the limits specified in Figures 3.9.2 and 3.9.3. ~~In the event a cross-hatch storage configuration is deemed necessary for a portion of either Region 1 or Region 2, vacant spaces diagonal to the four corners of any fuel assembly or vacant spaces on two opposite faces of any fuel assembly shall be physically blocked before any such fuel assembly may be placed in that region (Note 1). Also, the Region 1 storage cells adjacent to the Region 2 interface are restricted to fuel assemblies that are outside of the area of the graph enclosed by Curve A on Figure 3.9.2. In the event a checkerboard storage configuration is deemed necessary for a portion of Region 2, vacant spaces adjacent to the four faces of any fuel assembly shall be physically blocked before any such fuel assembly may be placed in Region 2.~~ The provisions of Specification 3.0.3 are not applicable.
- 3.9.12.c The boron concentration in the spent fuel pool shall be maintained (at all times) at greater than ~~462000~~ parts per million.

APPLICABILITY: During storage of fuel in the spent fuel pool.

ACTION:

Suspend all actions involving the movement of fuel in the spent fuel pool if it is determined a fuel assembly has been placed in an incorrect location until such time as the correct storage location is determined. Move the assembly to its correct location before resumption of any other fuel movement.

Suspend all actions involving the movement of fuel in the spent fuel pool if it is determined the pool boron concentration is less than ~~462001~~ ppm, until such time as the boron concentration is increased to ~~462001~~ ppm or greater.

SURVEILLANCE REQUIREMENTS

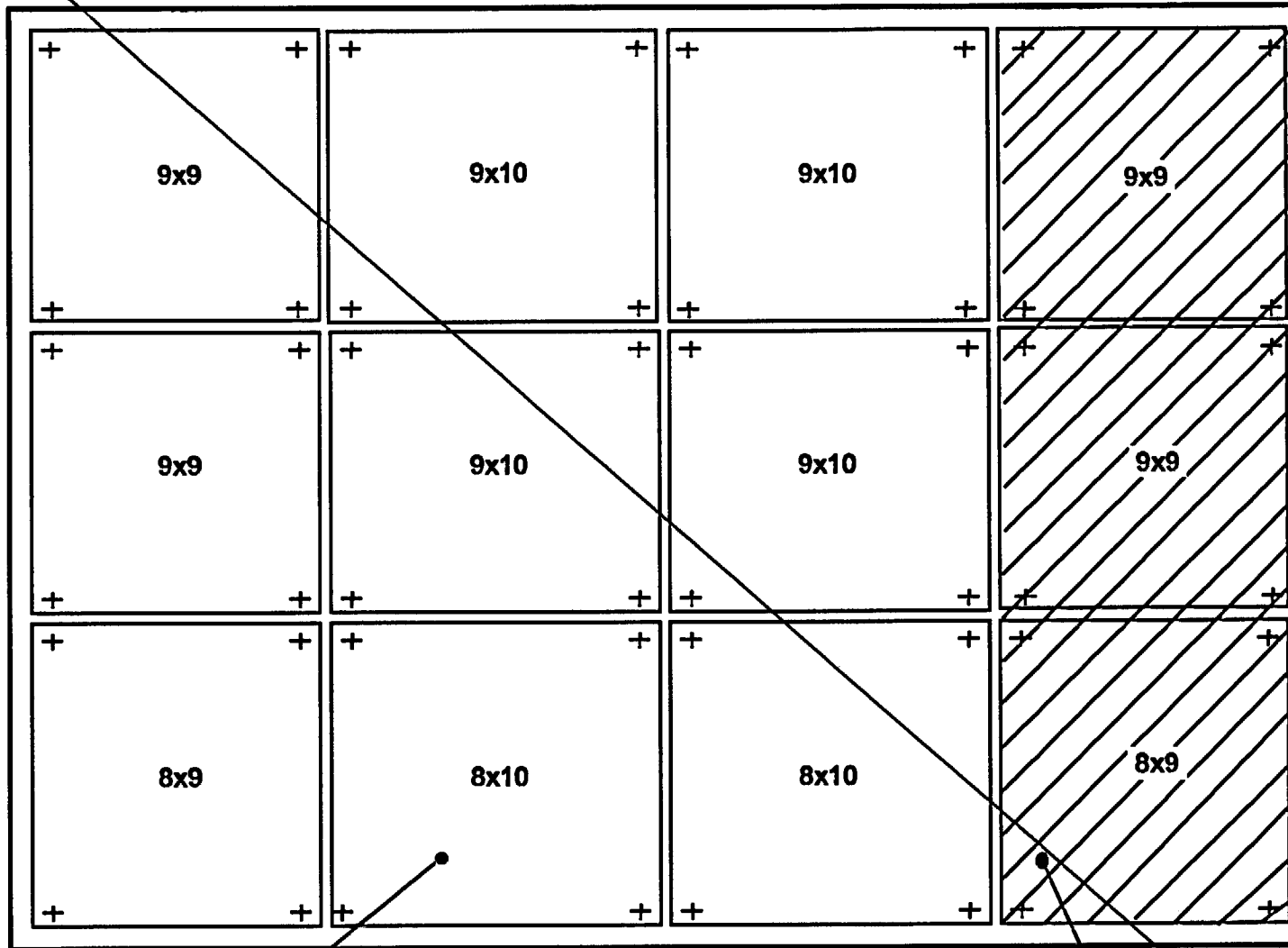
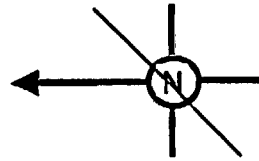
- 4.9.12.a Verify all fuel assemblies to be placed in the spent fuel pool have an initial enrichment of less than or equal to 5.0 w/o U-235 by checking the assemblies' design documentation.
- 4.9.12.b Verify all fuel assemblies to be placed in Region 1 and Region 2 ~~the spent fuel pool~~ are within the limits of Figures 3.9.2 and 3.9.3 by checking the assemblies' design and burnup documentation.
- 4.9.12.c Verify at least once per 31 days the spent fuel pool boron concentration is greater than ~~462000~~ ppm.

Note 1: ~~If the most peripheral row/column of the Region 1 contains vacant spaces in a cross-hatch storage configuration, these vacant spaces may be filled with fuel assemblies that are outside of the area of the graph enclosed by Curve A on Figure 3.9.2, provided that the most southwest and southeast corner locations remain empty.~~

ARKANSAS - UNIT 2

3/4 9-15

Amendment No. 43



REGION - 2

754 LOCATIONS (26 x 29)

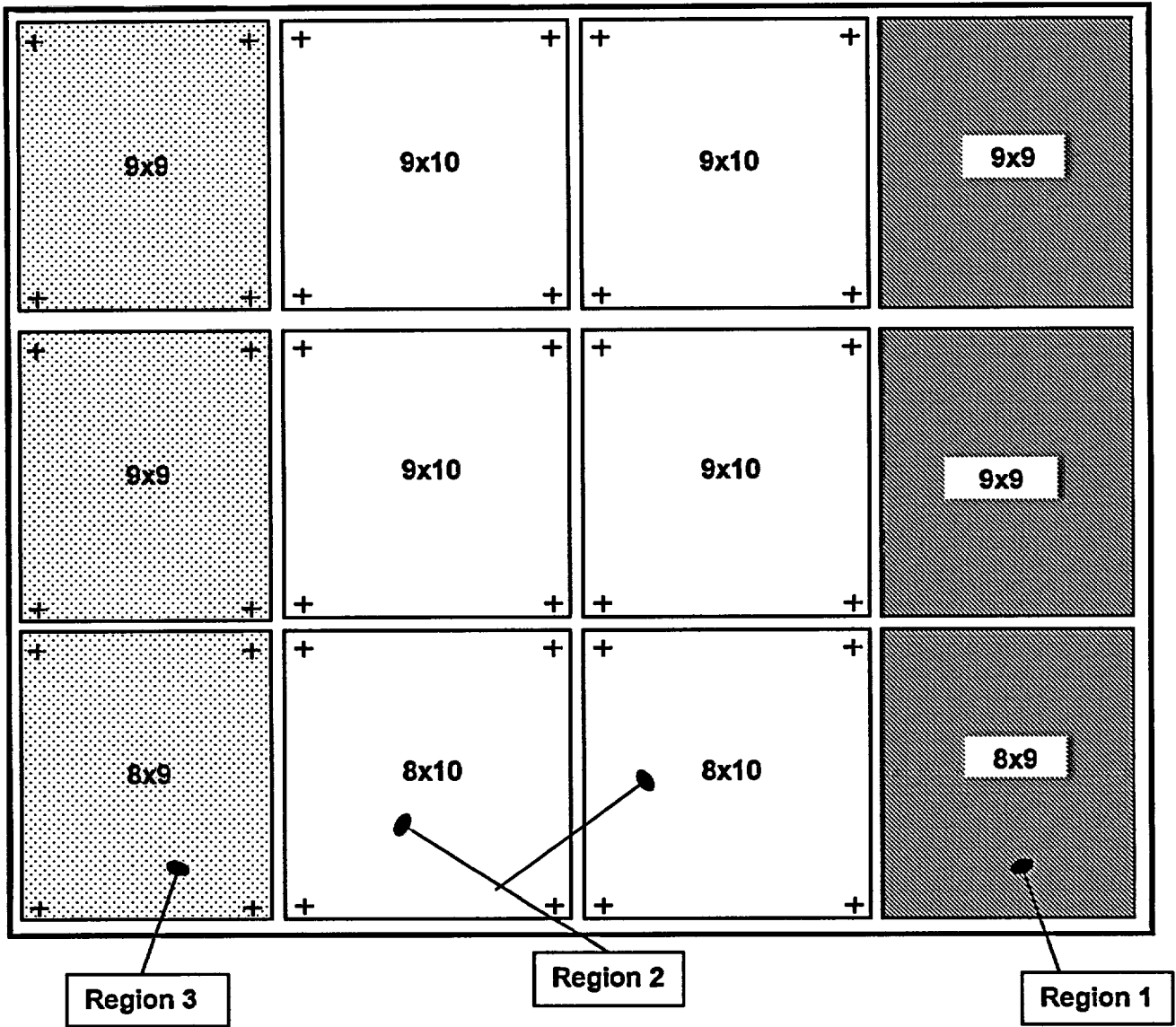
REGION - 1

234 LOCATIONS (9 x 26)

SPENT FUEL POOL ARRANGEMENT UNIT #2

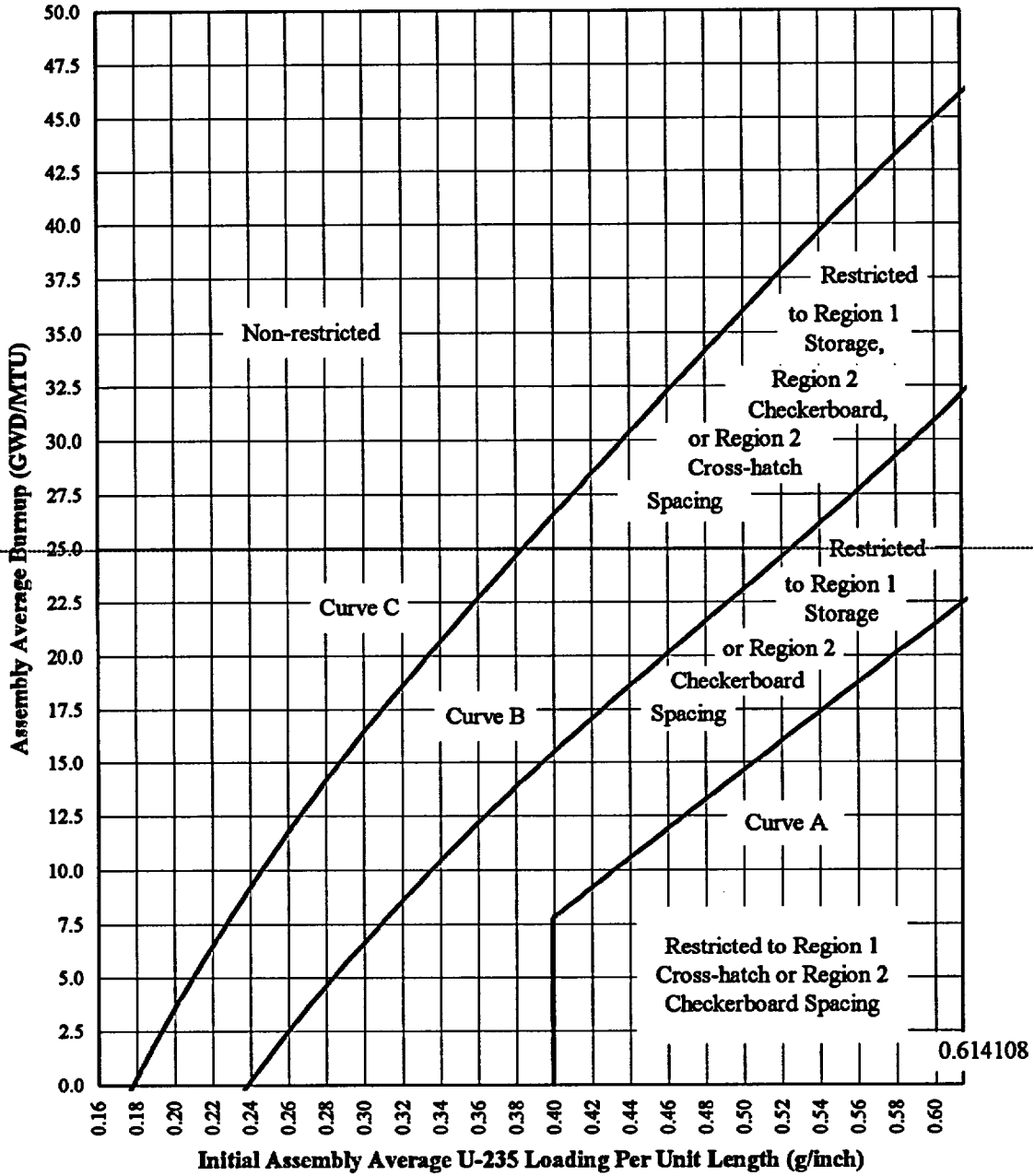
Figure 3.9.1

← N



**ANO-2 Spent Fuel Pool Arrangement
Figure 3.9.1**

FIGURE 3.9.2
MINIMUM BURNUP VS. INITIAL ASSEMBLY AVERAGE U-235 LOADING



Curve A = $68.008x - 19.366$ when $x > 0.399184$
 Curve B = $239.01x^3 - 347.75x^2 + 243.18x - 41.452$
 Curve C = $-714.35x^4 + 1335.80x^3 - 946.44x^2 + 394.52x - 47.040$

Figure 3.9.2
Bumup versus Initial Assembly Average U-235 Enrichment
Region 1

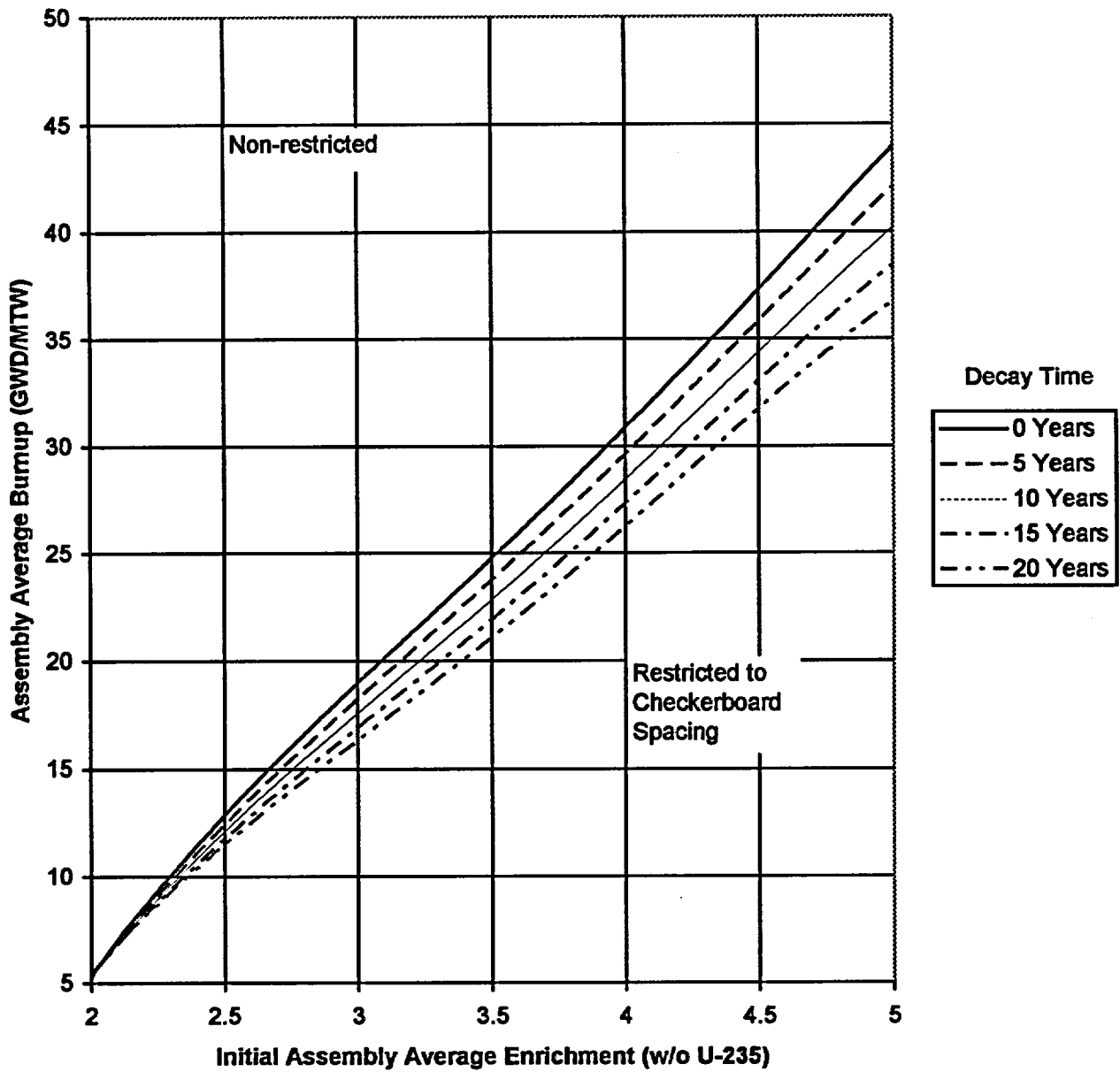
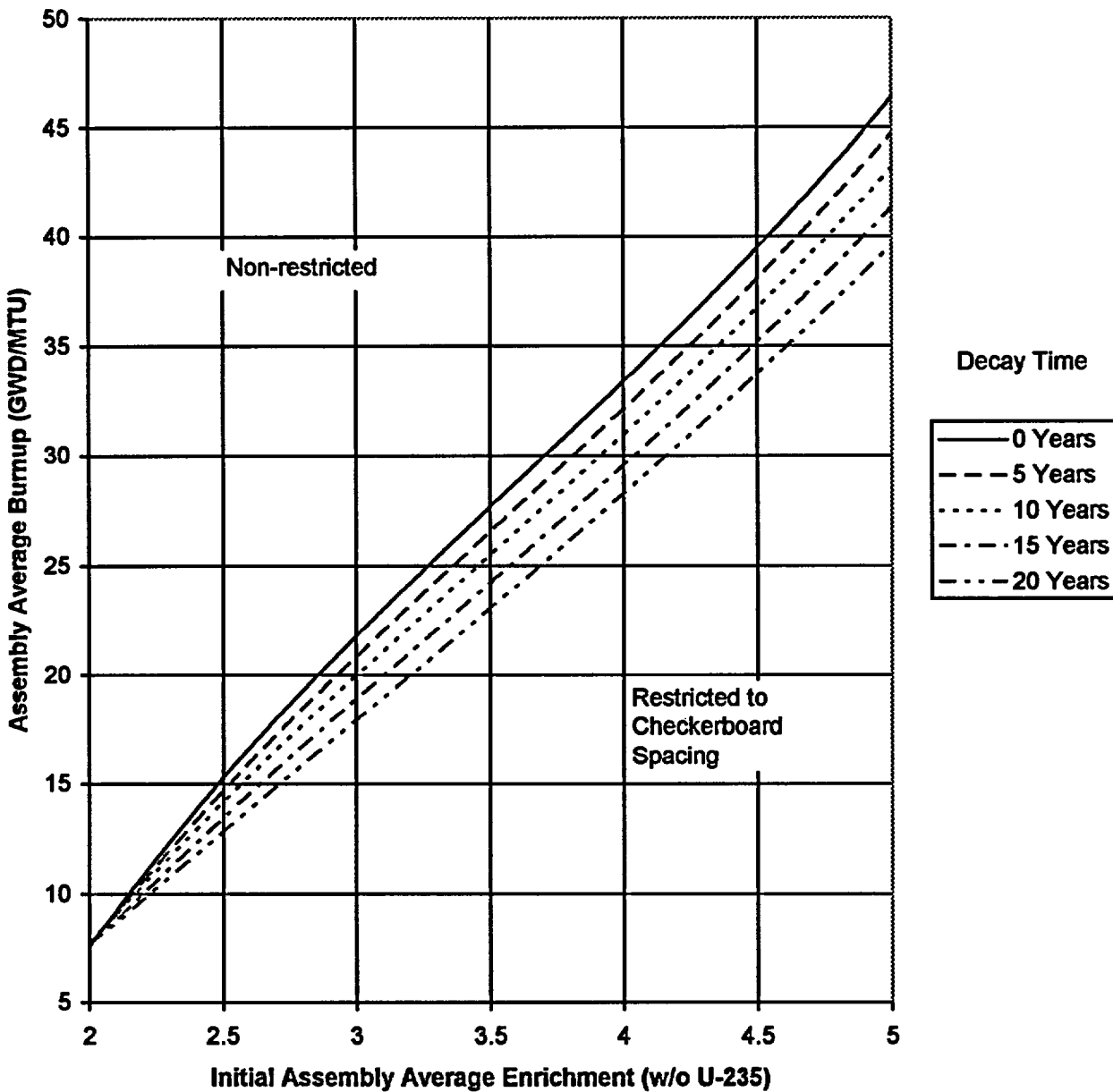


Figure 3.9.3
Burnup versus. Initial Assembly U-235 Enrichment
Region 2



DESIGN FEATURES

5.3 Fuel Storage

5.3.1 Spent Fuel Storage Rack Criticality

The spent fuel storage racks are designed and shall be maintained with:

- a. Fuel assemblies stored in the spent fuel pool in accordance with Specification 3.9.12;
- b. $k_{\text{eff}} \leq 0.95$ if fully flooded with 400 ppm unborated water, which includes an allowance for uncertainties as described in Section 9.1 of the SAR; and
- c. $k_{\text{eff}} < 1.0$ if fully flooded with unborated water, which includes an allowance for uncertainties as described in Section 9.1 of the SAR; and
- d. A nominal 9.8 inch center to center distance between fuel assemblies placed in the storage racks.

5.3.2 New Fuel Storage Rack Criticality

The new fuel storage racks are designed and shall be maintained with:

- a. Fuel assemblies having a maximum U-235 enrichment of 5.0 weight percent;
- b. $k_{\text{eff}} \leq 0.95$ if fully flooded with unborated water, which includes an allowance for uncertainties as described in Section 9.1 of the SAR;
- c. $k_{\text{eff}} \leq 0.98$ if moderated by aqueous foam, which includes an allowance for uncertainties as described in Section 9.1 of the SAR; and
- d. A nominal 26 inch center to center distance between fuel assemblies placed in the storage racks.

5.3.3 Drainage

The spent fuel storage pool is designed and shall be maintained to prevent inadvertent draining of the pool below elevation 399' 10½".

5.3.4 Capacity

The spent fuel storage pool is designed and shall be maintained with a storage capacity limited to no more than 988 fuel assemblies.

Attachment 3

2CAN010304

**Changes to Technical Specification Bases Pages
(For Information Only)**

REFUELING OPERATIONS

BASES

3/4.9.9 and 3/4.9.10 WATER LEVEL-REACTOR VESSEL AND SPENT FUEL POOL WATER LEVEL

The restrictions on minimum water level ensure that sufficient water depth is available to remove 99% of the assumed 12% iodine gas activity released from the rupture of an irradiated fuel assembly. The minimum water depth is consistent with the assumptions of the accident analysis.

3/4.9.11 FUEL HANDLING AREA VENTILATION SYSTEM

The limitations on the fuel handling area ventilation system ensure that all radioactive materials released from an irradiated fuel assembly will be filtered through the HEPA filters and charcoal adsorbers prior to discharge to the atmosphere. The operation of this system and the resulting iodine removal capacity are consistent with the assumptions of the accident analyses.

Acceptable removal efficiency is shown by methyl iodide penetration of less than 5.0% when tests are performed in accordance with ASTM D3803-1989, "Standard Test Method for Nuclear-Grade Activated Carbon," at a temperature of 30°C and a relative humidity of 95%. The penetration acceptance criterion is determined by the following equation:

$$\text{Allowable Penetration} = \frac{[100\% - \text{methyl iodide efficiency for charcoal credited in accident analysis}]}{\text{safety factor of 2}}$$

Applying a safety factor of 2 is acceptable because ASTM D3803-1989 is a more accurate and demanding test than older tests.

3/4.9.12 FUEL STORAGE

Region 1, Region 2, and Region 32 of the spent fuel storage racks are designed to assure fuel assemblies of less than or equal to 5.0 w/o U-235 enrichment can be stored in the pool with certain defined restrictions that are within the limits of Figure 3.9.2 will be maintained in a subcritical array with $K_{eff} \leq 0.95$ in unborated water. These conditions have been verified by criticality analyses and include calculational bias and manufacturing tolerance effects.

Region 1 and Region 2

Fresh unburned fuel with enrichments up to 5.0 w/o U-235 may be stored in a checkerboard pattern (alternate storage cells filled only with water or non-fuel bearing materials checkerboarded with cells containing fuel assemblies) in either Region 1 or Region 2 storage cells. Spent fuel may be stored in Region 1 and/or Region 2 per TS 3.9.12 Figures 3.9.2 (Region 1) and 3.9.3 (Region 2). The figures use initial U235 enrichment and burnup to determine loading restrictions. The five curves on each figure represent decay time in years. Decay time is based on the time at which an assembly is permanently placed in the pool (i.e., if an assembly is placed in the pool one cycle and then returned to the core, the initial time in the pool is not included in the decay time once the assembly is permanently removed from the core.) The following equations were used to generate the decay curves and may be used to interpolate fuel placement in restricted or non-restricted regions:

REFUELING OPERATIONS

BASES

Region 1 Decay Time Curves:

<u>Decay Time, Years</u>	<u>Burnup, GWD/MTU</u>
<u>0</u>	$(-0.2906 \cdot E^4) + (4.5902 \cdot E^3) - (26.239 \cdot E^2) + (76.516 \cdot E) - 74.8$
<u>5</u>	$(-0.3306 \cdot E^4) + (5.0873 \cdot E^3) - (28.413 \cdot E^2) + (79.862 \cdot E) - 76.21$
<u>10</u>	$(-0.362 \cdot E^4) + (5.463 \cdot E^3) - (29.978 \cdot E^2) + (81.9 \cdot E) - 76.48$
<u>15</u>	$(-0.402 \cdot E^4) + (5.9607 \cdot E^3) - (32.152 \cdot E^2) + (85.245 \cdot E) - 77.82$
<u>20</u>	$(-0.4375 \cdot E^4) + (6.3977 \cdot E^3) - (34.034 \cdot E^2) + (87.983 \cdot E) - 78.6$

Region 2 Decay Time Curves:

<u>Decay Time, Years</u>	<u>Burnup, GWD/MTU</u>
<u>0</u>	$(0.68 \cdot E^3) - (7.449 \cdot E^2) + (38.56 \cdot E) - 45.20$
<u>5</u>	$(0.5489 \cdot E^3) - (5.9344 \cdot E^2) + (32.496 \cdot E) - 38.05$
<u>10</u>	$(0.4153 \cdot E^3) - (4.3948 \cdot E^2) + (26.356 \cdot E) - 30.75$
<u>15</u>	$(0.2867 \cdot E^3) - (2.9045 \cdot E^2) + (20.367 \cdot E) - 23.80$
<u>20</u>	$(0.153 \cdot E^3) - (1.3649 \cdot E^2) + (14.227 \cdot E) - 16.60$

Region 1 and Region 2 Restricted Loading Pattern

If restricted loading is required by Figures 3.9.2 or 3.9.3, then a checkerboard loading arrangement is required. If a checkerboard loading arrangement is not desirable, then the fuel assembly may be stored in Region 3.

Region 1 is comprised of three separate modules and Region 2 has six separate modules with a water gap separating each module from the others. If it is desired to load part of a module in the checkerboard loading pattern and part of the module without loading restrictions, then a single row of empty cells (cells filled only with water or non-fuel bearing materials) must be maintained as a barrier between the two loading patterns. The row of empty cells serves as the water gap between the modules to prevent neutron interaction between the two loading patterns and thereby ensures proper criticality control.

Region 3

Fresh fuel assemblies with enrichments up to a maximum of 5 w/o U-235 or spent fuel of any burnup may be stored in any cell in Region 3 without restriction.

TS 3.9.12.c includes the requirement for > 2000 ppm boron concentration is to assure the fuel assemblies will be maintained in a subcritical array with $K_{eff} \leq 0.95$ in the event of a postulated drop accident. Analysis has shown that, during a postulated misplacement accident with the fuel stored within the limits of this specification, that a K_{eff} of ≤ 0.95 will be maintained when the boron concentration is at or above 4000 ppm.

~~Normally, fuel stored in a cross-hatch storage configuration must have all four diagonal spaces or at least two adjacent faces remain vacant to meet the criticality safety analysis mentioned above. However, the spent fuel pool walls may be credited as a neutron leakage path. Therefore, vacant spaces face adjacent to the walls of the Region I cross-hatch configured assemblies may be used to store fuel assemblies that are outside of the area of the graph enclosed by Curve A on Figure 3.9.2, excluding the most southeast and southwest corner spaces of Region 1 which must remain empty.~~

Attachment 4

2CAN010304

**Spent Fuel Pool Rack Modifications with Poison Material Inserts
in
ANO Unit-2**

**SPENT FUEL POOL RACKS MODIFICATIONS
WITH POISON MATERIAL INSERTS
IN ANO UNIT-2**

**FOR
ENTERGY**

Holtec Report No: HI-2022868

Holtec Project No: 1196

Report Class: SAFETY RELATED

TABLE OF CONTENTS

1.0	INTRODUCTION	1-1
1.1	References	1-4
2.0	SPENT FUEL RACK FLUX TRAP GAP POISON INSERT DESIGN	2-1
2.1	Introduction	2-1
2.2	Summary of Principal Design Criteria	2-1
2.3	Applicable Codes and Standards	2-2
2.4	Quality Assurance Program	2-10
2.5	Mechanical Design	2-10
2.6	Fabrication	2-11
2.7	Installation	2-12
3.0	MATERIAL CONSIDERATIONS	3-1
3.1	Introduction	3-1
3.2	Structural Materials	3-1
3.3	Neutron Absorbing Material	3-1
3.3.1	Metamic Material Characteristics	3-3
3.4	Compatibility with Environment	3-3
3.5	Heavy Load Considerations	3-4
3.6	References	3-4
4.0	CRITICALITY SAFETY EVALUATION	4-1
4.1	Design Bases	4-1
4.2	Summary of Criticality Analyses	4-5
4.2.1	Normal Operating Conditions	4-5
4.2.1.1	Region 1	4-5
4.2.1.2	Region 2	4-6
4.2.1.3	Region 3	4-7
4.3	Reference Design Input Data	4-7
4.3.1	Reference Fuel Assembly	4-7
4.3.2	Region 1 Fuel Storage Cells	4-7
4.3.3	Region 2 Fuel Storage Cells	4-8
4.3.4	Region 3 Fuel Storage Cells	4-8
4.4	Analytical Methodology	4-8
4.4.1	Reference Design Calculations	4-8
4.4.2	Fuel Burnup Calculations and Uncertainties	4-9
4.4.3	Effect of Axial Burnup Distribution	4-10
4.4.4	MCNP4a Temperature Correction	4-11
4.4.5	Long -Term Changes in Reactivity	4-11
4.5	Region 1 Criticality Analyses and Tolerances	4-11
4.5.1	Nominal Design Case	4-11
4.5.2	Uncertainties Due to Tolerances	4-11
4.5.3	Eccentric Fuel Positioning	4-12
4.6	Region 2 Criticality Analyses and Tolerances	4-12
4.6.1	Nominal Design Case	4-12

TABLE OF CONTENTS

4.6.2	Uncertainties Due to Tolerances.....	4-12
4.6.3	Eccentric Fuel Positioning.....	4-12
4.7	Region 3 Criticality Analyses and Tolerances.....	4-13
4.7.1	Nominal Design Case.....	4-13
4.7.2	Uncertainties Due to Tolerances.....	4-13
4.7.3	Eccentric Fuel Positioning.....	4-13
4.8	Abnormal and Accident Conditions in the Spent Fuel Pool Racks.....	4-13
4.8.1	Temperature and Water Density Effects.....	4-13
4.8.2	Lateral Rack Movement.....	4-14
4.8.3	Abnormal Location of a Fuel Assembly.....	4-14
4.8.4	Dropped Fuel Assembly.....	4-15
4.9	Soluble Boron Dilution Evaluation.....	4-16
4.10	References for Section 4.0.....	4-19
Appendix 4A	“Benchmark Calculations”(Total of 25 Pages including 6 figures).....	4-36
4A.1	Introduction and Summary.....	4A-1
4A.2	Effect of Enrichment.....	4A-3
4A.3	Effect of ¹⁰ B Loading.....	4A-4
4A.4	Miscellaneous and Minor Parameters.....	4A-5
4A.4.1	Reflector Material and Spacings.....	4A-5
4A.4.2	Fuel Pellet Diameter and Lattice Pitch.....	4A-5
4A.4.3	Soluble Boron Concentration Effects.....	4A-5
4A.5	MOX Fuel.....	4A-6
4A.6	References.....	4A-7
5.0	THERMAL-HYDRAULIC CONSIDERATIONS.....	5-1
5.1	Introduction.....	5-1
5.2	Cooling System Description.....	5-2
5.3	Spent Fuel Pool Decay Heat Loads.....	5-3
5.4	Minimum Time-to-Boil and Maximum Boiloff Rate.....	5-4
5.5	Maximum SFP Local Water Temperature.....	5-6
5.6	Fuel Rod Cladding Temperature.....	5-8
5.7	Results.....	5-10
5.7.1	Decay Heat.....	5-10
5.7.2	Minimum Time-to-Boil and Maximum Boiloff Rate.....	5-10
5.7.3	Local Water and Fuel Cladding Temperatures.....	5-10
5.8	References.....	5-12
6.0	STRUCTURAL/SEISMIC CONSIDERATIONS.....	6-1
6.1	Introduction.....	6-1
6.2	Overview of Rack Structural Analysis Methodology.....	6-1
6.2.1	Background of Analysis Methodology.....	6-2
6.3	Description of Racks.....	6-5
6.4	Synthetic Time-Histories.....	6-6
6.5	WPMR Methodology.....	6-6

TABLE OF CONTENTS

6.5.1	Model Details for Spent Fuel Racks	6-7
6.5.1.1	Assumptions	6-7
6.5.1.2	Element Details	6-9
6.5.2	Fluid Coupling Effect	6-10
6.5.2.1	Multi-Body Fluid Coupling Phenomena	6-11
6.5.3	Stiffness Element Details	6-12
6.5.4	Coefficients of Friction	6-13
6.5.5	Governing Equations of Motion	6-13
6.6	Structural Evaluation of Spent Fuel Rack Design	6-15
6.6.1	Kinematic and Stress Acceptance Criteria	6-15
6.6.2	Stress Limit Evaluations	6-16
6.6.3	Dimensionless Stress Factors	6-19
6.6.4	Loads and Loading Combinations for Spent Fuel Racks	6-20
6.7	Parametric Simulations	6-21
6.8	Time History Simulation Results	6-22
6.8.1	Rack Displacements	6-23
6.8.2	Pedestal Vertical Forces	6-23
6.8.3	Pedestal Friction Forces	6-23
6.8.4	Rack Impact Loads	6-23
6.8.4.1	Rack to Rack Impacts	6-24
6.8.4.2	Rack to Wall Impacts	6-24
6.8.4.3	Fuel to Cell Wall Impact Loads	6-24
6.9	Rack Structural Evaluation	6-25
6.9.1	Rack Stress Factors	6-25
6.9.2	Pedestal Thread Shear Stress	6-26
6.9.3	Local Stresses Due to Impacts	6-26
6.9.4	Weld Stresses	6-27
6.10	Poison Insert Structural Evaluation	6-29
6.11	Level A Evaluation	6-30
6.12	Hydrodynamic Loads on Pool Walls	6-30
6.13	Local Stress Considerations	6-30
6.13.1	Cell Wall Buckling	6-30
6.13.2	Thermal Loads	6-31
6.14	Evaluation of Postulated Stuck Fuel Assembly	6-31
6.15	Conclusion	6-31
6.16	References	6-33
7.0	MECHANICAL ACCIDENTS	7-1
7.1	Introduction	7-1
7.2	Description of Mechanical Accidents	7-1
7.3	Evaluation of Mechanical Accidents	7-1
7.4	Conclusion	7-2
7.5	References	7-2

TABLE OF CONTENTS

Tables

3.3.1	Chemical Composition and Physical Properties of Aluminum (6061 Alloy).....	3-5
3.3.2	Chemical Composition and Physical Properties of Boron Carbide.....	3-6
4.1.1	Fuel Assembly Specifications	4-21
4.2.1	Summary of Criticality Safety Analyses for Storage of 4.95%±0.05 wt% ²³⁵ U Enriched Spent Fuel Assemblies in Region 1 Racks.....	4-22
4.2.2	Minimum Burnup Required for Storage of Spent Fuel Assemblies in the Region 1 Racks.....	4-23
4.2.3	Bounding Polynomial Fits to Determine Minimum Acceptable Burnup for Storage of Spent Fuel Assemblies Storage in Region 1 Racks as a Function of Initial Average Enrichment.....	04-24
4.2.4	Summary of the Criticality Safety Analyses for a 2-of-4 Checkerboard Storage of Fresh Fuel Assemblies and Empty Cells in Region 1 Racks.....	4-25
4.2.5	Summary of the Criticality Safety Analyses for Storage of Spent Fuel Assemblies in Region 2 Racks.....	4-26
4.2.6	Minimum Burnup Required for Storage of Spent Fuel Assemblies in Region 2 Racks.....	4-27
4.2.7	Bounding Polynomial Fits to Determine Minimum Acceptable Burnup for Storage of Spent Fuel Assemblies Storage in Region 2 Racks as a Function of Initial Enrichment.....	4-28
4.2.8	Summary of the Criticality Safety Analyses for 2-of-4 Checkerboard Storage of Fresh Fuel Assemblies and Empty Cells in Region 2 Racks.....	4-29
4.2.9	Summary of the Criticality Safety Analyses for Storage of Fresh Fuel Assemblies in ANO Unit 2 Region 3 Racks.....	4-30
4.9.1	Required Soluble Boron Concentrations in the SFP Water.....	4-31
4A.1	Summary of Criticality Benchmark Calculations.....	4A-9 thru 4A-13
4A.2	Comparison of MCNP4a and Keno5a Calculated Reactivities for Various Enrichments	4A-14
4A.3	MCNP4a Calculated Reactivities for Critical Experiments with Neutron Absorbers.....	4A-15
4A.4	Comparison of MCNP4a and KENO5a Calculated Reactivities for Various ¹⁰ B Loadings.....	4A-16
4A.5	Calculations for Critical Experiments with Thick Lead and Steel Reflectors	4A-17
4A.6	Calculations for Critical Experiments with Various Soluble Boron Concentrations.....	4A-18
4A.7	Calculations for Critical Experiments with MOX Fuel.....	4A-19
5.3.1	Key Input Data for Decay Heat Computations	5-13
5.3.2	Theoretical Bounding Fuel Discharge History.....	5-14
5.4.1	Key Input Data for Time-To-Boil Evaluation.....	5-15
5.5.1	Key Input Data for Local Temperature Evaluation.....	5-16
5.7.1	Result of SFP Decay Heat Calculations.....	5-17

TABLE OF CONTENTS

5.7.2	Results of Loss-of-Forced Cooling Evaluations.....	5-18
5.7.3	Results of Maximum Local Water and Fuel Cladding Temperature Evaluations.....	5-19
6.2.1	Partial Listing of Fuel Rack Applications Using DYNARACK	6-36 through 6-38
6.3.1	Rack Material Data (150°F).....	6-39
6.4.1	Time-History Statistical Correlation Results.....	6-40
6.5.1	Degrees-of-Freedom.....	6-41
6.9.1	Comparison of Bounding Calculated Loads/Stresses vs. Code Allowables at Impact Locations and at Welds	6-42

TABLE OF CONTENTS

Figures

- 1.1 Location of the Different Rack Types in the Spent Fuel Pool.
- 2.5.1 Schematic of the Poison Insert Mechanism
- 2.5.2 Lead-in Device
- 4.1.1 3-Dimensional Plot of Minimum Fuel Burnups for Fuel in Unit 2 Region 1 for Enrichments and/or Cooling Times
- 4.1.2 3-Dimensional Plot of Minimum Fuel Burnups for Fuel in Unit 2 Region 2 for Enrichments and/or Cooling Times
- 4.3.1 A Cross-Sectional View of the Calculational Model Used for the Region 1 Rack Analysis
- 4.3.2 A Cross-Sectional View of the Calculational Model Used for the Region 2 Rack Analysis
- 4A.1 MCNP Calculated k-eff Values for Various Values of the Spectral Index
- 4A.2 KENO5a Calculated k-eff Values for Various Values of the Spectral Index
- 4A.3 MCNP Calculated k-eff Values at Various U-235 Enrichments
- 4A.4 KENO5a Calculated k-eff Values at Various U-235 Enrichments
- 4A.5 Comparison of MCNP and KENO5a Calculations for Various Fuel Enrichments
- 4A.6 Comparison of MCNP and KENO5a Calculations for Various Boron-10 Areal Densities
- 5.5.1 Schematic of the CFD Model of the ANO Unit 2 SFP.
- 5.7.1 ANO Unit 2 Pool Decay Heat Plot (Partial Core Discharge)
- 5.7.2 ANO Unit 2 Decay Heat Curve (Full Core Discharge)
- 5.7.3 Contours of Static Temperature in a Vertical Plane Through the Center of the SFP
- 5.7.4 Velocity Vector Plot In a Vertical Plane Through the Center of the SFP
- 6.1.1 ANO Unit 2 Spent Fuel Pool Layout
- 6.4.1 ANO Unit 2, DBE, 5% Damping , 362' Elevation E-W Time Acceleration
- 6.4.2 ANO Unit 2, DBE, 5% Damping, 362' Elevation N-S Time Acceleration
- 6.4.3 ANO Unit 2, DBE, 5% Damping, 362' Elevation Vert Time Acceleration
- 6.4.4 ANO Unit 2, OBE, 2% Damping, 362' Elevation E-W Time Acceleration
- 6.4.5 ANO Unit 2. OBE, 2% Damping, 362' Elevation N-S Time Acceleration
- 6.4.6 ANO Unit 2, OBE, 2% Damping, 362' Elevation Vert Time Acceleration
- 6.5.1 Schematic of the Single Rack Dynamic Model Used in DYNARACK
- 6.5.2 Fuel-to-Rack Gap/Impact Elements at Level of Rattling Mass
- 6.5.3 Two Dimensional View of the Spring-Mass Simulation
- 6.5.4 Shear and Bending Springs Representing Rack Elasticity in X-Z and Y-Z Planes
- 6.5.5 Rack Periphery Gap/Impact Elements
- 6.11.1 Maximum Instantaneous Hydrodynamic Pressures

1.0 INTRODUCTION

Arkansas Nuclear One, Unit 2 (ANO-2) operated by Entergy Operations and in commercial operation since 1980, is located approximately 70 miles northwest of Little Rock, Arkansas and about five miles west of Russellville, Arkansas. ANO-2 is a Combustion Engineering pressurized water reactor (PWR) with a licensed thermal power level of 3026 megawatts. The reactor core contains 177 fuel assemblies and the spent fuel pool (SFP) is licensed for the storage of 988 fuel assemblies.

The racks in the SFP of ANO-2 are free-standing and self supporting racks of Westinghouse design. The principal fabrication materials are ASTM A-240, Type 304 stainless steel for the structural members and shapes. "Boraflex", a product of BISCO (a division of Brand, Inc.) was originally used to augment reactivity control.

The SFP was designed to hold spent fuel assemblies (or rod cluster control assemblies) in underwater storage for long-term decay after their removal from the reactor core. The structure is seismic Category I, heavy walled, reinforced concrete pool, located on grade outside the containment structure. The interior of the pool is lined with stainless steel plate (Type 304L).

The ANO-2 spent fuel racks consist of individual cells with a square pitch of 9.8 inches, each of which accommodates a single Combustion Engineering 16x16 fuel assembly or equivalent. The ANO-2 SFP uses two types of racks of different designs, designated Region 1 and Region 2. Region 1 racks employed Boraflex as the poison material and are presently qualified to store fresh fuel assemblies with a maximum enrichment up to 5.0 weight percent (wt%) ^{235}U . Region 2 racks are designed with flux-traps and are currently used to store spent fuel assemblies with various initial enrichments that have accumulated certain minimum burn-ups. These racks do not have any poison material. Some of the Region 2 racks will be modified by the insertion of Metamic[®] absorber panels into the flux trap region to create a Region 3. These different regions are depicted in Figure 1-1. These poison inserts will have two borated Aluminum (Metamic[®]) panels as neutron absorbers. Each poison insert panel will be held in the flux trap along the cell wall by a spring mechanism. The insertion of the Metamic[®] poison panels into the new region, as shown by analyses later in this report, will continue to allow the storage of fresh fuel with a maximum enrichment up to 5.0 wt% in the ANO-2 SFP. The Region 3 flux traps will be fitted with lead-ins on the top of the flux traps, which will act to prevent any possible uplifting of the poison panel insert. The lead-in devices will also help guide the fuel assemblies into the storage cells.

The existing Region 1 racks have been reanalyzed to establish new fuel storage requirements without crediting the presence of Boraflex. The Region 2 racks, which will not be converted to Region 3 racks, were re-analyzed to establish more flexible fuel storage requirements. These racks have been re-analyzed to establish their capability for fresh fuel storage in a 2-of-4 checkerboard arrangement or to store spent fuel assemblies of specified enrichment-burnup limits. The New Fuel Vault and fuel handling equipment is currently analyzed for storage of fresh fuel with a maximum enrichment up to 5.0 wt% and is not addressed in this analysis.

Sections 2.0 and 3.0 of this report provide an abstract of the design and material information on the poison inserts and the racks.

Section 4.0 provides a summary of the methods and results of the criticality evaluations performed for the spent fuel storage racks. Credit for soluble boron in the pool has been taken, in accordance with 10CFR50.68, to assure the criticality safety of the spent fuel storage racks. The analyses show that the neutron multiplication factors (k_{eff}) for the stored fuel arrays are subcritical under assumed condition of the loss of all soluble boron in the pool water. Additional analyses are required to determine the soluble boron requirements to maintain k_{eff} below 0.95 for both normal storage and accident conditions. The criticality safety analysis sets the requirements on the Metamic[®] poison insert panel length and the amount of B₄C (i.e., loading density) of the Metamic[®] inserts for the Region 3 SFP racks.

Thermal-hydraulic considerations require that fuel cladding will not fail due to excessive thermal stress. The thermal-hydraulic analyses carried out in support of the modification of some of the existing Region 2 racks are described in Section 5.0.

Rack module structural criteria require that the primary stresses in the rack module structure will remain below the ASME B&PV Code (Subsection NF) [1] allowables. Demonstrations of seismic and structural adequacy are presented in Section 6.0. The structural qualification also requires that the subcriticality of the stored fuel be maintained under all postulated mechanical accident scenarios. The structural consequences of these postulated mechanical accidents are evaluated in Section 7.0 of this report.

Results of the analyses presented in this report establish acceptable restrictions on combinations of initial enrichment and discharge burnups for Region 1 and Region 2, as well as showing that the insertion of poison inserts into the newly defined Region 3 racks will permit storage of fresh fuel assemblies in these racks. The storage racks meet all requirements of the applicable

USNRC guidelines and regulations (References 2 - 6). The analysis methodologies employed are a direct evolution of previous license applications reviewed and approved by the USNRC, including nuclear subcriticality, thermal-hydraulic safety, seismic and structural adequacy, and mechanical integrity.

All computer programs utilized to perform the analyses documented in Section 1.0 through 7.0 are benchmarked and verified. These programs have been utilized by Holtec International in numerous license applications over the past decade. The analyses presented herein clearly demonstrate that the rack module arrays with the addition of the poison inserts and the lead-ins possess wide margins of safety in respect to all considerations of safety specified in the OT Position Paper [3], namely, nuclear subcriticality, thermal-hydraulic safety, seismic and structural adequacy, and mechanical integrity.

1.1 References

- [1] American Society of Mechanical Engineers (ASME), Boiler & Pressure Vessel Code, Section III, 1989 Edition, Subsection NF, and Appendices.
- [2] General Design Criterion 62, Prevention of Criticality in Fuel Storage and Handling.
- [3] USNRC, "OT Position for Review and Acceptance of Spent Fuel Storage and Handling Applications, April 14, 1978, and Addendum dated January 18, 1979.
- [4] Code of Federal Regulations 10 CFR 50.68, Criticality Accident Requirements
- [5] ANSI-8.17-1984, Criticality Safety Criteria for the Handling, Storage and Transportation of LWR Fuel Outside Reactors.
- [6] L. Kopp, "Guidance on the Regulatory Requirements for Criticality Analysis Of Fuel Storage At Light-Water Reactor Plants", USNRC Internal Memorandum L. Kopp to Timothy Collins, August 19 1998.

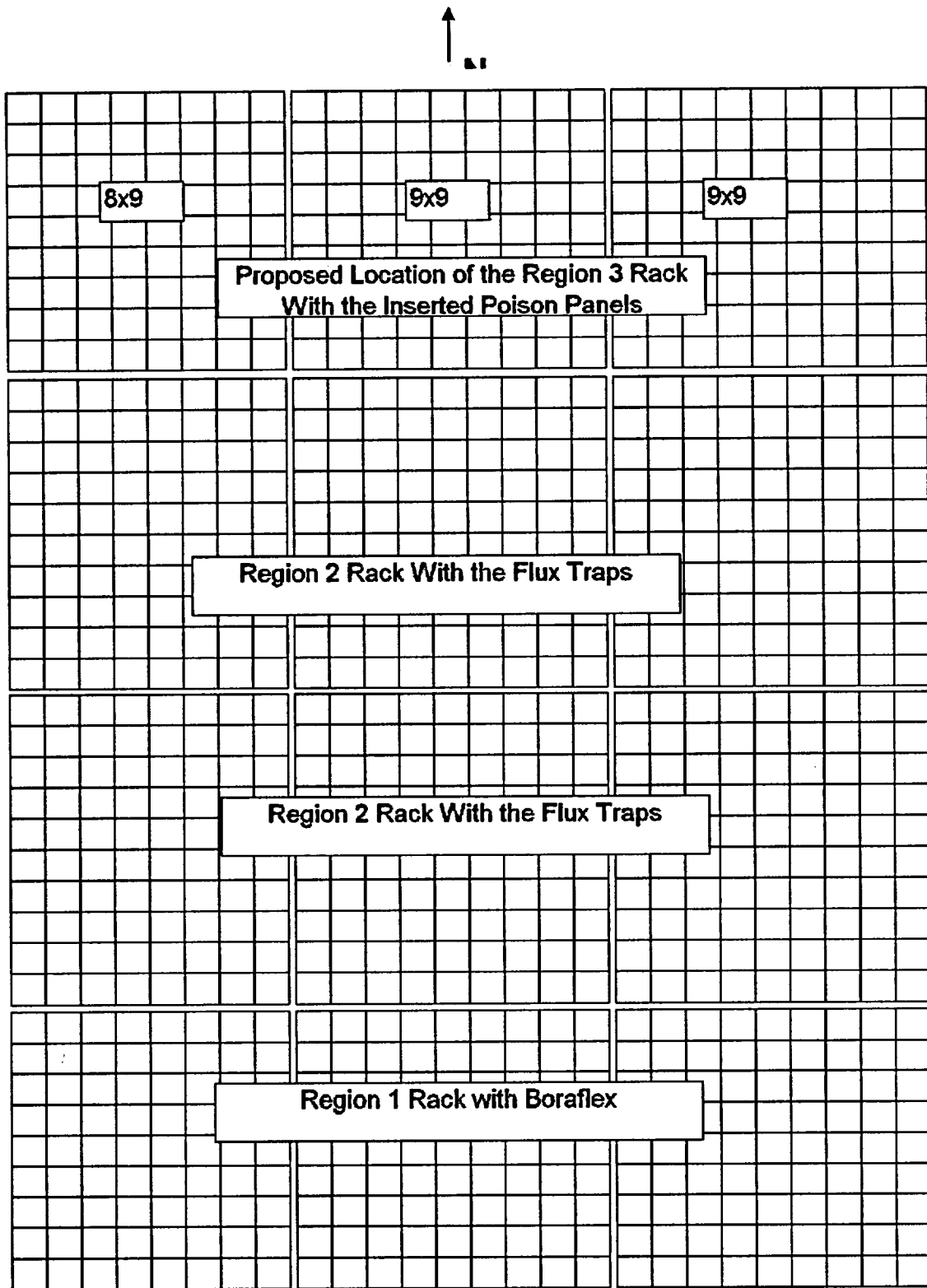


Figure 1.1: Location of the Different Rack Types in the Spent Fuel Pool.

2.0 SPENT FUEL RACK FLUX TRAP GAP POISON INSERT DESIGN

2.1 INTRODUCTION

The ANO-2 SFP contains twelve fuel racks with a total storage capacity of 988 fuel assemblies. As described in Section 1.0, there are currently two regions in the ANO-2 SFP that are designated as Region 1, which contains Boraflex, and Region 2, which does not contain poison inserts. A portion of Region 2 will be designated as Region 3 in which panels of Metamic® containing a high areal loading of the B₄C (up to 40% by weight of B₄C) will be inserted into the flux traps to provide appropriate neutron attenuation between adjacent storage cells. With the insert of Metamic®, it is proposed to allow unrestricted storage of fresh fuel in the Region 3 racks with a maximum enrichment of 5.0 wt%.

In addition to the poison inserts, the Region 3 racks will also be fitted with independent lead-in devices to help guide the fuel assemblies into the storage cells and prevent debris from entering the flux trap.

2.2 SUMMARY OF PRINCIPAL DESIGN CRITERIA

The key design criteria for the spent fuel racks are set forth in the USNRC memorandum entitled "OT Position for Review and Acceptance of Spent Fuel Storage and Handling Applications", dated April 14, 1978 as modified by amendment dated January 18, 1979. The individual sections of this report expound on the specific design bases derived from the above-mentioned "OT Position Paper". The design bases for the racks with the poison inserts in them are summarized below:

- a. Kinematic Stability: All freestanding modules must be kinematically stable (against tipping or overturning) if a seismic event is imposed on any module.
- b. Structural Compliance: All primary stresses in the rack modules must satisfy the limits postulated in Section III subsection NF of the ASME B & PV Code.
- c. Thermal-Hydraulic Compliance: The spatial average bulk pool temperature is required to remain below 150 °F. No localized boiling is permitted.

- d. **Criticality Compliance:** The New Fuel Storage Racks (NFSR) and the (Spent Fuel Storage Racks) SFSR must be able to store Zircaloy clad fuel of 5.0 weight percent (wt%) maximum enrichment while maintaining the reactivity (k_{eff}) less than 0.95.
- e. **Accident Events:** In the event of postulated drop events (uncontrolled lowering of a fuel assembly, for instance), it is necessary to demonstrate that the stored fuel remains subcritical.

The foregoing design bases are further articulated in Sections 4.0 through 7.0 of this licensing report.

2.3 APPLICABLE CODES AND STANDARDS

The following codes, standards and practices are used as applicable for the design, construction, and assembly of the poison inserts. Additional specific references related to detailed analyses are given in each section.

- a. **Design Codes**
 - (1) ASME B & PV Code Section III, 1998 Edition.
 - (2) American Society for Nondestructive Testing SNT-TC-1A, June 1980, Recommended Practice for Personnel Qualifications and Certification in Non-destructive Testing.
 - (3) ASME Y14.5M, Dimensioning and Tolerancing.
 - (4) ASME B & PV Code, Section II-Parts D, 1998 Edition.

b. Standards of American Society for Testing and Materials (ASTM)

- (1) ASTM A240 - Standard Specification for Heat-Resisting Chromium and Chromium-Nickel Stainless Steel Plate, Sheet and Strip for Pressure Vessels.**
- (2) ASTM A262 - Standard Practices for Detecting Susceptibility to Intergranular Attack in Austenitic Stainless Steel.**
- (3) ASTM C750 - Standard Specification for Nuclear-Grade Boron Carbide Powder.**
- (4) ASTM A380 - Standard Practice for Cleaning, Descaling, and Passivation of Stainless Steel Parts, Equipment and Systems.**
- (5) ASTM C992 - Standard Specification for Boron-Based Neutron Absorbing Material Systems for Use in Nuclear Spent Fuel Storage Racks.**
- (6) ASTM E3 - Standard Practice for Preparation of Metallographic Specimens.**
- (7) ASTM E190 - Standard Test Method for Guided Bend Test for Ductility of Welds.**

c. Welding Code:

- (1) ASME B & PV Code, Section IX - Welding and Brazing Qualifications, latest applicable edition and addenda.**

d. Quality Assurance, Cleanliness, Packaging, Shipping, Receiving, Storage, and Handling

- (1) ANSI N45.2.1 - Cleaning of Fluid Systems and Associated Components during Construction Phase of Nuclear Power Plants - 1980 (R.G. 1.37).
- (2) ANSI N45.2.2 - Packaging, Shipping, Receiving, Storage and Handling of Items for Nuclear Power Plants - 1978 (R.G. 1.38).
- (3) ANSI N45.2.6 - Qualifications of Inspection, Examination, and Testing Personnel for the Construction Phase of Nuclear Power Plants - 1973 (R.G. 1.58).
- (4) ANSI N45.2.8 - Supplementary Quality Assurance Requirements for Installation, Inspection and Testing of Mechanical Equipment and Systems for the Construction Phase of Nuclear Plants - 1975 (R.G. 1.116).
- (5) ANSI N45.2.11 - Quality Assurance Requirements for the Design of Nuclear Power Plants - 1978 (R.G. 1.64).
- (6) ANSI N45.2.12 - Requirements for Auditing of Quality Assurance Programs for Nuclear Power Plants - 1977 (R.G. 1.144).
- (7) ANSI N45.2.13 - Quality Assurance Requirements for Control of Procurement of Items and Services for Nuclear Power Plants - 1976 (R. G. 1.123).
- (8) ANSI N45.2.23 - Qualification of Quality Assurance Program Audit Personnel for Nuclear Power Plants - 1978 (R.G. 1.146).
- (9) ASME B & PV Code, Section V, Nondestructive Examination, 1983 Edition.

- (10) ANSI N16.9-75 - Validation of Calculation Methods for Nuclear Criticality Safety.
- (11) ASME NQA-1 – Quality Assurance Program Requirements for Nuclear Facilities.
- (12) ASME NQA-2 – Quality Assurance Requirements for Nuclear Power Plants.

e. USNRC Documents

- (1) "OT Position for Review and Acceptance of Spent Fuel Storage and Handling Applications," dated April 14, 1978, and the modifications to this document of January 18, 1979.
- (2) NUREG 0612, "Control of Heavy Loads at Nuclear Power Plants", USNRC, Washington, D.C., July, 1980.
- (3) NUREG 0800, "Standard Review Plan for the Review of Safety Analysis Reports for Nuclear Power Plants", USNRC, Washington, D.C., July, 1981.

f. Other ANSI Standards (not listed in the preceding)

- (1) ANSI/ANS 8.1 - Nuclear Criticality Safety in Operations with Fissionable Materials Outside Reactors, 1983.
- (2) ANSI N45.2.9 - Requirements for Collection, Storage and Maintenance of Quality Assurance Records for Nuclear Power Plants - 1974.
- (3) ANSI N45.2.10 - Quality Assurance Terms and Definitions - 1973.
- (4) ANSI/ASME N626-3 - Qualification and Duties of Specialized Professional Engineers, 1977.

g. Code-of-Federal Regulations (CFR)

- (1) 10CFR20 - Standards for Protection Against Radiation.
- (2) 10CFR21 - Reporting of Defects and Non-compliance.
- (3) 10CFR50 Appendix A - General Design Criteria for Nuclear Power Plants.
- (4) 10CFR50 Appendix B - Quality Assurance Criteria for Nuclear Power Plants and Fuel Reprocessing Plants.
- (5) 10CFR100 – Reactor Site Criteria.

h. Regulatory Guides (RG)

- (1) RG 1.13 - Spent Fuel Storage Facility Design Basis (Revision 2 Proposed).
- (2) RG 1.25 - Assumptions Used for Evaluating the Potential Radiological Consequences of a Fuel Handling Accident in the Fuel Handling and Storage Facility for Boiling and Pressurized Water Reactors, Rev. 0 - March, 1972.
- (3) RG 1.28 - Quality Assurance Program Requirements - Design and Construction, Rev. 2 - February, 1979 (endorses ANSI N45.2).
- (4) RG 1.33 – Quality Assurance Program Requirements.
- (5) RG 1.29 - Seismic Design Classification, Rev. 2 - February, 1976.
- (6) RG 1.31 - Control of Ferrite Content in Stainless Steel Weld Metal, Rev. 3.

- (7) RG 1.38 - Quality Assurance Requirements for Packaging, Shipping, Receiving, Storage and Handling of Items for Water-Cooled Nuclear Power Plants, Rev. 2 - May, 1977 (endorses ANSI N45.2.2).
- (8) RG 1.44 - Control of the Use of Sensitized Stainless Steel.
- (9) RG 1.58 - Qualification of Nuclear Power Plant Inspection, Examination, and Testing Personnel, Rev. 1 - September 1980 (endorses ANSI N45.2.6).
- (10) RG 1.60 - Design Response Spectra for Seismic Design of Nuclear Power Plants.
- (11) RG 1.61 - Damping Values for Seismic Design of Nuclear Power Plants, Rev. 0, 1973.
- (12) RG 1.64 - Quality Assurance Requirements for the Design of Nuclear Power Plants, Rev. 2 - June, 1976 (endorses ANSI N45.2.11).
- (13) RG 1.71 - Welder Qualifications for Areas of Limited Accessibility.
- (14) RG 1.74 - Quality Assurance Terms and Definitions, Rev. 2 - February, 1974 (endorses ANSI N45.2.10).
- (15) RG 1.85 - Materials Code Case Acceptability - ASME Section III, Division 1.
- (16) RG 1.88 - Collection, Storage and Maintenance of Nuclear Power Plant Quality Assurance Records, Rev. 2 - October, 1976 (endorses ANSI N45.2.9).
- (17) RG 1.92 - Combining Modal Responses and Spatial Components in Seismic Response Analysis, Rev. 1 - February, 1976.

- (18) **RG 1.116 - Quality Assurance Requirements for Installation, Inspection and Testing of Mechanical Equipment and Systems, Rev. 0-R - May, 1977 (endorses ANSI N45.2.8-1975).**
- (19) **RG 1.123 - Quality Assurance Requirements for Control of Procurement of Items and Services for Nuclear Power Plants, Rev. 1 - July, 1977 (endorses ANSI N45.2.13).**
- (20) **RG 1.124 - Service Limits and Loading Combinations for Class 1 Linear-Type Component Supports, Rev. 1, - January, 1978.**
- (21) **RG 1.144 - Auditing of Quality Assurance Programs for Nuclear Power Plants, Rev. 1 - September, 1980 (endorses ANSI N45.2.12-1977).**
- (22) **RG 8.8 - Information Relative to Ensuring that Occupational Radiation Exposures at Nuclear Power Stations will be as Low as Reasonably Achievable (ALARA).**
- (23) **IE Information Notice 83-29 - Fuel Binding Caused by Fuel Rack Deformation.**
- (24) **RG 8.38 - Control of Access to High and Very High Radiation Areas in Nuclear Power Plants, June, 1993.**

i. **Branch Technical Position**

- (1) **CPB 9.1-1 - Criticality in Fuel Storage Facilities.**
- (2) **ASB 9-2 - Residual Decay Energy for Light-Water Reactors for Long-Term Cooling - November, 1975.**

j. American Welding Society (AWS) Standards

- (1) AWS D1.1 - Structural Welding Code - Steel.
- (2) AWS D1.3 - Structure Welding Code - Sheet Steel.
- (3) AWS D9.1 - Sheet Metal Welding Code.
- (4) AWS A2.4 - Standard Symbols for Welding, Brazing and Nondestructive Examination.
- (5) AWS A3.0 - Standard Welding Terms and Definitions.
- (6) AWS A5.12 - Specification for Tungsten and Tungsten Alloy Electrodes for Arc-Welding and Cutting.
- (7) AWS QC1 - Standard for AWS Certification of Welding Inspectors.
- (8) AWS 5.4 – Specification for Stainless Steel Electrodes for Shielded Metal Arc Welding.
- (9) AWS 5.9 – Specification for Bare Stainless Steel Welding Electrodes and Rods.

k. Other References

- (1) ANO Unit 1 & 2 Operating Licenses and Technical Specifications, License No. DPR-51 & NPF-6.
- (2) ANO Unit 1 & 2 Updated Final Safety Analysis Report (UFSAR).

2.4 QUALITY ASSURANCE PROGRAM

The governing quality assurance requirements for design and fabrication of the poison inserts are stated in 10CFR50 Appendix B. Holtec's Nuclear Quality Assurance program complies with this regulation and is designed to provide a system for the design, analysis, and licensing of customized components in accordance with various codes, specifications, and regulatory requirements.

The Quality Assurance System that will be used by Entergy Operations to install the poison inserts is also controlled by the ANO-2 Quality Assurance Program.

2.5 MECHANICAL DESIGN

The mechanical design of the poison insert consists of two poison panels separated by a mechanism to maintain the water gap specified by criticality considerations. The poison panels are independent flat panels sized to cover the active fuel region. The poison panels will extend all the way to the SFP rack base plate. The poison panels will be nominally 0.10 inch thick 6061 aluminum plus boron carbide metal matrix manufactured by Metamic®. The poison panels will be held together with a frame that is fabricated from SA240-304 stainless steel. A schematic of the arrangement is shown in Figure 2.5.1. The poison panels and the mechanical frame work form the poison insert. The poison insert will be able to collapse smaller than the flux trap opening prior to installation. Figure 4.3.2 depicts the current Region 2 cell with four flux traps. The insert is designed to expand in the flux trap once fully inserted.

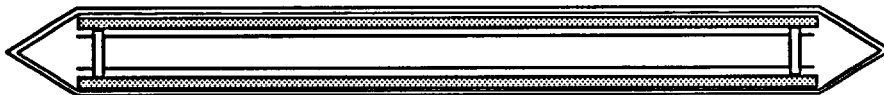


Figure 2.5.1 Schematic of the Poison Insert Mechanism

The lead-in device, which is depicted in Figure 2.5.2, is fabricated from SA240-304 stainless steel. The device is designed to rest on top of the flux trap, and it is secured in place by two slotted plates, which straddle the cell wall at the corners external to the flux trap. The size and shape of the lead-in is such that it will not interfere with the square opening of the cell. Each lead-in device weighs less than 3 lb. The lead-in contains flow holes in the mounting plate to provide an uninterrupted flow path for the water entering at the bottom of the flux trap and exiting at the top of the flux trap.

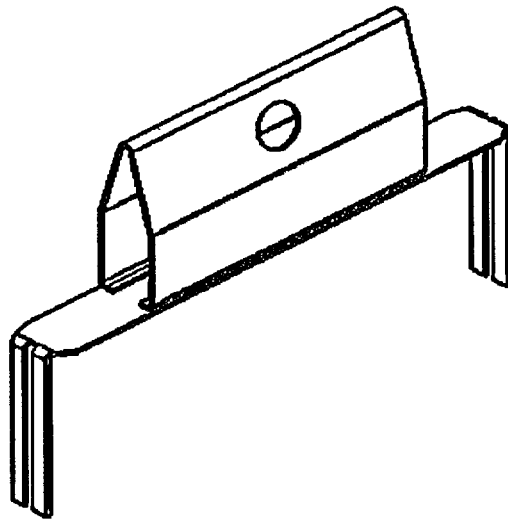


Figure 2.5.2 Lead-in Device

2.6 FABRICATION

The object of this section is to provide a brief description of the poison insert construction activities, which enable an independent appraisal of the adequacy of design. The pertinent methods used in manufacturing the poison inserts may be stated as follows:

1. The poison panels are extruded and rolled from a powder metallurgy billet then cut to the specified rectangular size.
2. The fabrication process involves operational sequences that permit immediate accessibility for verification by the inspection staff.

3. The poison inserts are fabricated per the manufacturer's Appendix B Quality Assurance program, which ensures, and documents, that the fabricated poison inserts meet all of the requirements of the design and fabrication documents.

2.7 INSTALLATION

The poison insert is placed in an upending cradle on the fuel bridge. The poison insert is then upended and connected to the poison insert handling tool. All installation activities will be performed remotely, from the fuel bridge, using a long handled installation tool. Subsequent to the upending process, the poison insert is lowered into the spent fuel pool and guided into the appropriate flux trap with installation tools. Then, the lead-ins are installed onto a flux trap that received a poison insert.

3.0 MATERIAL CONSIDERATIONS

3.1 INTRODUCTION

Safe storage of nuclear fuel in the pool requires that the materials utilized in the poison inserts be of proven durability and compatible with the pool water environment. This section provides a synopsis of the considerations with regard to long-term design service life of 60 years.

3.2 STRUCTURAL MATERIALS

The only structural material utilized in the fabrication of the poison inserts is SA240 Type 304 stainless steel.

3.3 NEUTRON ABSORBING MATERIAL

In addition to the structural materials, the poison inserts employ Metamic[®], a patented product of Metamic[®], Inc., as the neutron absorber material. A brief description of Metamic[®] follows.

Metamic[®] is a neutron absorber material developed by the Reynolds Aluminum Company in the mid-1990s for spent fuel reactivity control in dry and wet storage applications [3.3.1]. Metallurgically, Metamic[®] is a metal matrix composite (MMC) consisting of a high purity 6061 aluminum matrix reinforced with Type 1 ASTM C750-89, isotopically graded boron carbide (B₄C).

Metamic[®] is characterized by an extremely fine aluminum spherical powder (325 mesh or better) and boron carbide powder (average particle size under 10 microns). The high performance reliability of Metamic[®] derives from the particle size distribution of its constituents, namely, high purity Aluminum 6061 alloy powder and isotopically graded B₄C particulate, rendered into an isotropic metal matrix composite state by the powder metallurgy process which yields excellent homogeneity, and which prevents B₄C from clustering in the final product.

The powders are carefully blended together without binders, chelating agents, or other additives that could potentially become retained in the final product and deleteriously influence performance. The maximum percentage of B₄C that will be dispersed in the aluminum alloy 6061

matrix is 25% by weight. The pure blend of powders is cold isostatically compacted into a green billet and vacuum sintered to a high theoretical density¹. An extrusion process is used to bring the matrix into final density. Billets can vary in diameter, size and weight depending on a number of variables including loading and final panel dimensions.

Metamic[®] has been subjected to an extensive array of tests sponsored by the Electric Power Research Institute (EPRI) that evaluated the functional performance of the material at elevated temperatures (up to 900°F) and radiation levels (1E+11 rads gamma). The results of the tests documented in an EPRI report [3.3.2] indicate that Metamic[®] maintains its physical and neutron absorption properties with little variation in its properties from the unirradiated state. The main conclusions provided in the above-referenced EPRI report are summarized below:

- The isotropic metal matrix configuration produced by the powder metallurgy process with a complete absence of interconnected internal porosity in Metamic[®] ensures that its density is essentially equal to the maximum theoretical density.
- Measurements of boron carbide particle distribution show extremely small particle-to-particle distance² and near-perfect homogeneity.
- The physical and neutronic properties of Metamic[®] are essentially unaltered under exposure to elevated temperatures (750°F - 900°F).
- No detectable change in the neutron attenuation characteristics under accelerated test conditions has been observed.

Holtec International's Q.A. program ensures that Metamic[®] is manufactured under the control and surveillance of a Quality Assurance/Quality Control Program that conforms to the requirements of 10CFR50 Appendix B, "Quality Assurance Criteria for Nuclear Power Plants".

¹ The theoretical density of Metamic[®], before being hot worked, is 82% to 98% depending on the B₄C content.

² Medium measured neighbor-to-neighbor distance is 10.08 microns according to the article, "METAMIC Neutron Shielding" [3.3.3].

3.3.1 METAMIC® Material Characteristics

Aluminum: Aluminum is a silvery-white, ductile metallic element. The 6061 alloy aluminum is used extensively in heat exchangers, pressure and storage tanks, chemical equipment, reflectors and sheet metal work.

It has high resistance to corrosion in industrial and marine atmospheres. Aluminum has atomic number of 13, atomic weight of 26.98, specific gravity of 2.69 and valence of 3. The physical, mechanical and chemical properties of the 6061 alloy aluminum are listed in Table 3.3.1.

The excellent corrosion resistance of the 6061 alloy aluminum is provided by the protective oxide film that quickly develops on its surface from exposure to the atmosphere or water. This film prevents the loss of metal from general corrosion or pitting corrosion.

Boron Carbide: The boron carbide contained in Metamic® is a fine granulated powder that conforms to ASTM C750-89 nuclear grade Type I. The material conforms to the chemical composition and properties listed in Table 3.3.2.

References [3.3.1] and [3.3.2] provide further discussion as to the suitability of these materials for use in spent fuel storage applications.

3.4 COMPATIBILITY WITH ENVIRONMENT

All materials used in the construction of the poison inserts have been determined to be compatible with the ANO Spent Fuel Pools. Austenitic stainless steel (e.g., Type 304) is a widely used stainless alloy in nuclear power plants, and it has an established history of in-pool usage. Metamic® is likewise an excellent material for spent fuel applications based on its high resistance to corrosion and its functional performance at elevated temperatures and radiation levels.

3.5 HEAVY LOAD CONSIDERATIONS

There are no heavy loads involved in the proposed installation of poison inserts. The estimated weight of a single poison insert is less than 40 pounds.

3.6 REFERENCES

[3.3.1] "Use of METAMIC in Fuel Pool Applications," Holtec International, HI-2022871, Revision 1, August 2002.

[3.3.2] "Qualification of METAMIC for Spent Fuel Storage Application," EPRI, 1003137, Final Report, October 2001.

[3.3.3] K. Anderson et al., "METAMIC Neutron Shielding," EPRI Boraflex Conference, November 19-20, 1998.

Table 3.3.1	
Chemical Composition and Physical Properties of Aluminum (6061 Alloy)	
Chemical Composition	
0.8-1.2%	Magnesium
0.40-0.8%	Silicone
0.15-0.40%	Copper
0.15% max.	Iron
0.25% max.	Zinc
0.15% max.	Titanium
50 ppm max.	Nickel
10 ppm max.	Cobalt
10 ppm max.	Manganese
10 ppm max.	Chromium
0.15% max.	Other
Remainder	Aluminum
Physical Properties	
Density	0.098 lb/in ³ 2.71 g/cm ³
Melting Range	1080°F - 1205°F 582° - 652°C
Thermal Conductivity (77°F)	1250 BTU/hr-ft ² -°F/in 1.55 kcal/hr-cm ² -°C/cm

Table 3.3.2	
Chemical Composition and Physical Properties	
of Boron Carbide	
Chemical Composition (Weight Percentage)	
Total boron	76.5 min.
B ¹⁰ isotope	19.9 ± 0.30 a/o
HNO ₃ soluble boron	0.5 max.
Water soluble boron	0.2 max.
Fluoride	25 µg/g max.
Chloride	75 µg/g max.
Calcium	0.3 max.
Iron	1.0 max.
Total boron plus total carbon	98.0 min.
Physical Properties	
Chemical formula	B ₄ C
Boron content (weight percent)	78.28%
Carbon content (weight percent)	21.72%
Crystal structure	rhombohedral
Density	0.0907 lb/in ³ 2.51 g/cm ³
Melting Point	4442°F 2450°C
Boiling Point	6332°F 3500°C

4.0 CRITICALITY SAFETY EVALUATION

4.1 Design Bases

This section of the report documents the criticality safety evaluation for the storage of fresh and spent nuclear fuel assemblies in the ANO-2 high-density spent fuel storage racks. The ANO-2 SFP currently has two regions of storage which are currently licensed to store a maximum enrichment of 5.0 wt% or nominally 4.95 ± 0.05 wt%.

1. Region 1 racks: These racks were originally designed with Boraflex as the poison material in a flux-trap configuration.
2. Region 2 racks: These racks are designed to store spent fuel assemblies of a specified combination of initial enrichment and discharge burnup. These racks do not have any poison material between cells.

Due to the Boraflex degradation in the Region 1 racks, future credit for the Boraflex neutron absorber is not feasible in these racks. The proposed resolution is to re-evaluate the criticality safety of the racks without credit for Boraflex and to insert poison material strips into the flux trap region of some of the Region 2 racks (These modified Region 2 racks are identified as Region 3 racks). The new Region 3 racks will enable unrestricted fresh fuel storage capability in that region. The calculations are performed under the assumed loss of all Boraflex in the Region 1 racks and with poison inserts in the Region 3 racks. All racks, including the remaining Region 2 racks were re-evaluated under the provisions of 10CFR50.68.

Specifically, the following evaluations were performed for ANO-2:

- ◆ Region 1 racks were evaluated for storage of spent fuel assemblies with specific burnup requirements for the spent fuel assemblies, as a function of initial enrichments and decay times (up to 20 years). Results are summarized in Figure 4.1.1 and tabulated in Table 4.2.1, 4.2.2 and 4.2.3.

- ◆ Fresh fuel storage in Region 1 was assessed based on a "2 of 4" checkerboard loading with empty storage cells (i.e., filled only with water or non-fuel bearing materials). Results are shown in Table 4.2.4 for fuel of 4.95 ± 0.05 wt% ^{235}U enrichment.
- ◆ Region 2 racks were evaluated for storage of spent fuel assemblies with specific burnup requirements for the spent fuel assemblies, determined as a function of initial enrichments and decay times (up to 20 years). Results are summarized in Figure 4.1.2 and Tables 4.2.5, 4.2.6 and 4.2.7.
- ◆ Fresh fuel storage in the Region 2 racks was assessed based on a "2 of 4" checkerboard loading with empty storage cells (i.e., filled only with water or non-fuel bearing materials). Results are shown in Table 4.2.8 for fuel of 4.95 ± 0.05 wt% ^{235}U enrichment.
- ◆ Region 3 racks were evaluated, with Metamic® panels inserted in the water gap, for storage of fresh unburned fuel assemblies, with ^{235}U enrichments up to 4.95 ± 0.05 wt%. Results are shown in Table 4.2.9. Region 3 may also accommodate spent fuel of any burnup for fuel assemblies up to 4.95 ± 0.05 wt% ^{235}U enrichment.

The racks are evaluated for Combustion Engineering (CE) 16x16 spent and fresh fuel assemblies with an initial average uniform enrichment up to 4.95 ± 0.05 wt% ^{235}U enrichment. Credit is taken for poison inserts, fuel burnup, cooling time, and soluble boron in pool water as applicable per 10 CFR 50.68 and Reference 4.1.2.

The objective of this analysis is to ensure, per 10 CFR 50.68, that the racks shall remain subcritical under normal conditions with no credit for soluble boron and less than or equal to 0.95 when partial credit is taken for soluble boron in the pool water, including calculation uncertainties and effects of mechanical tolerances. Reactivity effects of abnormal and accident conditions have also been evaluated to determine the required soluble boron concentration in the pool to assure that under all credible abnormal and accident conditions, the reactivity will not exceed the regulatory limit of 0.95. The required soluble boron concentrations are summarized in Table 4.9.1. In this context "abnormal" refers to conditions, which may reasonably be expected to occur during the lifetime of the plant and "accident" refers to conditions, which are not expected to occur but nevertheless must be protected against. The double contingency principle of ANSI N-16.1-1975 and of the April 1978 NRC letter allows full credit for soluble boron under other abnormal or accident

conditions, since only a single independent accident need be considered at one time.

Applicable codes, standards, and regulations or pertinent sections thereof, include the following:

- Code of Federal Regulations, Title 10, Part 50, Appendix A, General Design Criterion 62, "Prevention of Criticality in Fuel Storage and Handling."
- Code of Federal Regulation 10CFR50.68, Criticality Accident Requirements
- USNRC Standard Review Plan, NUREG-0800, Section 9.1.2, Spent Fuel Storage, Rev. 3 - July 1981.
- USNRC letter of April 14, 1978, to all Power Reactor Licensees - OT Position for Review and Acceptance of Spent Fuel Storage and Handling Applications, including modification letter dated January 18, 1979.
- L. Kopp, "Guidance on the Regulatory Requirements for Criticality Analysis of Fuel Storage at Light-Water Reactor Power Plants," NRC Memorandum from L. Kopp to T. Collins, August 19, 1998.
- USNRC Regulatory Guide 1.13, Spent Fuel Storage Facility Design Basis, Rev. 2 (proposed), December 1981.
- ANSI ANS-8.17-1984, "Criticality Safety Criteria for the Handling, Storage and Transportation of LWR Fuel Outside Reactors."

To assure the true reactivity will always be less than the calculated reactivity, the following conservative design criteria and assumptions were employed:

- ◆ Criticality safety analyses were based upon an infinite radial array of cells; i.e., no credit was taken for radial neutron leakage, except for evaluating accident conditions along the rack outer boundary where neutron leakage is inherent.
- ◆ Minor structural materials were neglected; i.e., spacer grids were conservatively assumed

to be replaced by water.

- ◆ Because the temperature coefficient of reactivity is positive in the absence of neutron absorber panels, the analyses for Region 1 (no credit is taken in the current evaluations for the existing Boraflex poison material in these racks) and Region 2 (no poison material currently exists in these racks) type racks assumed a temperature of 150 °F. This is the design basis maximum pool water temperature. Higher temperatures would be an accident condition for which full soluble boron credit is permitted and the reactivity effects would be mitigated by the presence of the large amounts of soluble boron in the pool water.
- ◆ For Region 3 type racks, the moderator is assumed to be un-borated water at a temperature within the operating range (4 °C) that results in the highest reactivity. Criticality calculations were performed at 20 °C and temperatures below 20 °C were assumed to be abnormal events and the reactivity effects combined additively with other uncertainties.
- ◆ The analyses used a CE 16x16 fuel assembly, with a maximum enrichment of 5.0 wt% ²³⁵U.
- ◆ No axial blankets were assumed to be present in the fuel rods. The entire active fuel length was assumed to be of uniform enrichment.
- ◆ In-core depletion calculations assume conservative operating conditions, highest fuel and moderator temperature, and an allowance for the average soluble boron concentrations during in-core operations.
- ◆ Manufacturing tolerances of the Metamic® neutron absorber (width, thickness and B₄C loading) is included in the criticality safety evaluations. Steel components associated with the inserts are replaced with water in the analysis.

The spent fuel storage racks are designed to accommodate the fuel assembly type listed in Table 4.1.1 with a maximum nominal initial enrichment of 4.95 ± 0.05 wt% ^{235}U .

4.2 Summary of Criticality Analyses

4.2.1 Normal Operating Conditions

The criticality analyses for each of the three separate regions of the spent fuel storage pool for the design basis storage conditions are summarized in Tables 4.2.1 to 4.2.9. For the fuel acceptance criteria defined in the previous section, the maximum effective multiplication factor (k_{eff}) values are shown to be less than 1.0 (95% probability at the 95% confidence level) in each of the regions when no credit is taken for the presence of soluble boron in the pool. Credit for soluble boron is required to ensure k_{eff} is maintained less than 0.95 and the required soluble boron concentrations are summarized in Table 4.9.1.

4.2.1.1 Region 1

The maximum k_{eff} values for storage of spent fuel were determined assuming an infinite radial array of storage cells with a finite axial length, water reflected. For each spent fuel cooling time, minimum burnup values were determined that assure the maximum k_{eff} , including calculational and manufacturing uncertainties, remains subcritical under the assumed accident condition of the loss of all soluble boron. Table 4.2.1 summarizes the results of these analyses at zero cooling time for spent fuel assemblies with an initial enrichment of 4.95 ± 0.05 wt% ^{235}U . Figure 4.1.1 and Table 4.2.2 show the minimum acceptable burnup for storage of fuel assemblies of various initial enrichments and cooling times in the spent fuel. The calculated maximum reactivity includes the reactivity effect of the axial distribution in burnup and provides an additional margin of uncertainty for the depletion calculations. The minimum soluble boron concentration required to maintain k_{eff} below 0.95, including all manufacturing and calculational tolerances, for the storage of spent fuel in the Region 1 racks is 240 ppm.

For convenience, the minimum (limiting) burnup data shown in Table 4.2.2 may be described as a function of the nominal initial enrichment, E , in wt% ^{235}U by bounding polynomial expressions as shown in Table 4.2.3. Fuel assemblies with enrichments less than 2.0 wt% ^{235}U will conservatively be required to meet the burnup requirements of 2.0 wt% ^{235}U assemblies. Since

the data is nearly linear, linear interpolation between the points listed in Table 4.2.2 is acceptable.

The maximum k_{eff} for storage of fresh fuel assemblies of 4.95 ± 0.05 wt% ^{235}U initial enrichment in the Region 1 racks in a 2-of-4 checkerboard pattern with the alternate cells remaining empty of fuel, is 0.9233. Table 4.2.4 summarizes the results of this analysis. Based on these results, this arrangement is acceptable for storage of fresh fuel with no credit for soluble boron or for spent fuel regardless of burnup.

4.2.1.2 Region 2

The maximum k_{eff} values for storage of spent fuel were determined assuming an infinite radial array of storage cells with a finite axial length, water reflected. For each spent fuel cooling time, minimum burnup values were determined that assure the maximum k_{eff} , including calculational and manufacturing uncertainties, remains subcritical under the assumed accident condition of the loss of all soluble boron. Table 4.2.5 summarizes the results of these analyses at zero cooling time for spent fuel assemblies with an initial enrichment of 4.95 ± 0.05 wt% ^{235}U . Figure 4.1.2 and Table 4.2.6 shows the minimum acceptable burnup for storage of fuel assemblies of various initial enrichments and cooling times. The calculated maximum reactivity includes the reactivity effect of the axial distribution in burnup and provides an additional margin of uncertainty for the depletion calculations. The minimum soluble boron concentration required to maintain k_{eff} below 0.95, including all manufacturing and calculational tolerances, for the storage of spent fuel allowed in the Region 2 racks is 240 ppm.

For convenience, the minimum (limiting) burnup data shown in Table 4.2.6 may be described as a function of the nominal initial enrichment, E , in wt% ^{235}U by a bounding polynomial expression as shown in Table 4.2.7. Fuel assemblies with enrichments less than 2.0 wt% ^{235}U will conservatively be required to meet the burnup requirements of 2.0 wt% ^{235}U assemblies. Since the data is nearly linear, linear interpolation between the points listed in Table 4.2.6 is acceptable.

The maximum k_{eff} for storage of fresh unburned fuel assemblies in the Region 2 racks in a 2-of-4 checkerboard pattern with the alternate cells remaining empty of fuel, is 0.9392, which is below the 0.95 limit, including all manufacturing and calculational tolerances. Table 4.2.8 summarizes the results of this analysis and confirms that this arrangement is acceptable for storage of fresh

fuel or spent fuel regardless of burnup, without requiring any credit for soluble boron.

4.2.1.3 Region 3

The Region 3 racks were analyzed for the storage of 4.95 ± 0.05 wt% fresh fuel assemblies. The maximum k_{eff} for storage of fresh fuel assemblies in the Region 3 racks is 0.9971. Table 4.2.9 summarizes the results of this analysis, and confirms that this arrangement is acceptable for storage of fresh unburned fuel or spent fuel regardless of burnup. The minimum soluble boron concentration required in Region 3 to maintain k_{eff} below 0.95, including all manufacturing and calculational tolerances, is 400 ppm.

4.3 Reference Design Input Data

4.3.1 Reference Fuel Assembly

The spent fuel storage racks are designed to accommodate Combustion Engineering (CE) 16x16 fuel assemblies. The design specifications for the CE fuel assemblies, as used for this analysis, are given in Table 4.1.1.

4.3.2 Region 1 Fuel Storage Cells

Figure 4.3.1 shows the calculational model of the nominal Region 1 spent fuel storage cell. The Region 1 storage cells are composed of stainless steel boxes separated by a gap. The 0.075 ± 0.0040 thick steel walls define the storage cells, which have a $8.58 +0.050/-0.025$ inch nominal inside dimension. A 0.020 inch stainless steel sheath is around the gap and defines the boundary of the flux-trap water-gap used to augment reactivity control. The cells are located on a lattice spacing of 9.80 inches in both directions. Stainless steel channels connect the storage cells in a rigid structure and define the flux-trap of 0.806 ± 0.010 inches, between the sheathing of adjacent cells.

4.3.3 Region 2 Fuel Storage Cells

Figure 4.3.2 shows the calculational model of the nominal Region 2 spent fuel storage cell. The Region 2 storage cells area also have a flux trap between adjacent cells and are composed of stainless steel boxes separated by a gap. The straight portion of the flux trap is 7.2 inches. The measured flux trap water gap of $0.097 +0.12/-0.08$ inches was used in the analysis. The 0.075 ± 0.0040 thick steel walls define the storage cells, which have a $8.58 +0.050/-0.025$ inch nominal inside dimension. The measured value of the flux trap water gap corresponded to a Box ID of 8.68 inches because of the bow in the cell walls. This value of the Box ID was used in the analysis. The cells are located on a lattice spacing of 9.80 inches in both directions. No additional water gaps exist between adjacent Region 2 cells in a rack.

4.3.4 Region 3 Fuel Storage Cells

The Region 3 storage cells are identical to Region 2 storage cells except that the Metamic® poison panels will be inserted into the flux trap gaps. The poison panels are designed to be 7.00 ± 0.0625 inches wide with minimum Boron Carbide (B_4C) content of 39.5 weight percent. These Metamic® panels are held by appropriate mechanisms to remain close to the straight portion of the flux trap walls.

4.4 Analytical Methodology

4.4.1 Reference Design Calculations

The principal methods for the criticality analyses of the storage racks include the following codes: (1) MCNP4a [4.4.1], (2) KENO5a [4.4.2], and (3) CASMO-4 [4.4.5-4.4.7]. MCNP4a is a continuous energy three-dimensional Monte Carlo code developed at the Los Alamos National Laboratory. KENO5a is a three-dimensional multi-group Monte Carlo code developed at the Oak Ridge National Laboratory as part of the SCALE 4.3 package [4.4.3]. The KENO5a calculations used the 238-group SCALE cross-section library and NITAWL [4.4.4] for ^{238}U resonance shielding effects (Nordheim integral treatment). Benchmark calculations, presented in Appendix 4A, indicate a bias of 0.0009 with an uncertainty of ± 0.0011 for MCNP4a and 0.0030 ± 0.0012 for KENO5a, both evaluated with the 95% probability at the 95% confidence level [4.1.1].

Fuel depletion analyses during core operation were performed with CASMO-4, a two-dimensional multi-group transport theory code based on capture probabilities [4.4.5 - 4.4.7]. Restarting the CASMO-4 calculations in the storage rack geometry yields the two-dimensional infinite multiplication factor (k_{∞}) for the storage rack. CASMO-4 was also used to determine the reactivity uncertainties (differential calculations) of manufacturing tolerances and the reactivity effects of variations in the water temperature and density.

In the geometric models used for the calculations, each fuel rod and its cladding were described explicitly and reflecting boundary conditions were used in the radial direction, which has the effect of creating an infinite radial array of storage cells. Monte Carlo calculations inherently include a statistical uncertainty due to the random nature of neutron tracking. To minimize the statistical uncertainty of the MCNP4a and KENO5a calculated reactivities and to assure convergence, a minimum of 1 million neutron histories were accumulated in each calculation. Three-dimensional MCNP calculations were necessary to describe the geometry of the checkerboard cases. However, MCNP cannot perform depletion calculations, thus depletion calculations were performed with CASMO4. Explicit description of the fission product nuclide concentrations in the spent fuel was determined from the CASMO4 calculations and used in the MCNP calculations. To compensate for those few fission product nuclides that are not in the MCNP library, an equivalent boron-10 concentration in the fuel was determined which produced the same reactivity in MCNP as the CASMO4 result. This methodology explicitly incorporates approximately 40 of the most important fission products, accounting for all but about 1% in k . The remaining ~1 % in k is included by the equivalent B-10 concentration in the fuel.

4.4.2 Fuel Burnup Calculations and Uncertainties

CASMO-4 was used for burnup calculations in the hot operating condition. To the extent possible, CASMO-4 has been benchmarked [4.4.6, 4.4.7] against cold, clean, critical experiments (including plutonium-bearing fuel) and also by comparison with Monte Carlo calculations.

In the CASMO-4 geometric models, each fuel rod and its cladding were described explicitly and reflective boundary conditions were used in the axial direction and between storage cells. These boundary conditions have the effect of creating an infinite array of storage cells in both the radial and axial directions.

Conservatively bounding moderator and fuel temperatures and the average operating soluble boron concentrations (900ppm) were used to assure the highest plutonium production and hence conservatively high values of reactivity. Since critical experiment data with spent fuel is not available for determining the uncertainty in depletion calculations, an allowance for uncertainty in reactivity was assigned based upon other considerations [4.1.2]. Assuming the uncertainty in depletion calculations is less than 5% of the total reactivity decrement; a burnup dependent uncertainty in reactivity for burnup calculations was assigned. Thus, the burnup uncertainty varies (increases) with burnup. This allowance for burnup uncertainty was included in determination of the acceptable burnup versus enrichment combinations.

4.4.3 Effect of Axial Burnup Distribution

Initially, fuel loaded into the reactor will burn with a slightly skewed cosine power distribution. As burnup progresses, the burnup distribution will tend to flatten, becoming more highly burned in the central regions than in the upper and lower regions. At high burnups, the more reactive fuel near the ends of the fuel assembly (less than average burnup) occurs in regions of high neutron leakage. Consequently, it is expected that over most of the burnup history, fuel assemblies with distributed burnups will exhibit a slightly lower reactivity than that calculated for the uniform average burnup. As burnup progresses, the distribution, to some extent, tends to be self-regulating as controlled by the axial power distribution, precluding the existence of large regions of significantly reduced burnup.

Among others, Turner [4.4.8] has provided generic analytic results of the axial burnup effect based upon calculated and measured axial burnup distributions. These analyses confirm the minor and generally negative reactivity effect of the axially distributed burnups at values less than about 30 GWD/MTU with small positive reactivity effects at higher burnup values. Calculations were performed based upon a burnup distribution provided by ANO. These calculations were performed in MCNP4a with 10 zone axial calculations, using specific (CASMO) concentrations of actinides and fission product nuclides in each zone. Results of these calculations, therefore, inherently include the effect of the axial distribution in burnup.

4.4.4 MCNP4a Temperature Correction

The reactivity for non-poisoned racks in the spent fuel pool increases with pool water temperature. The maximum bulk pool water temperature is 150 °F. However, since the Doppler treatment and cross-sections in MCNP4a are valid only at 20 °C, the Δk determined in CASMO-4 from 20 °C to 150 °F is included as a bias in the final k_{eff} calculation.

4.4.5 Long-Term Changes in Reactivity

At reactor shutdown, the reactivity of the fuel initially decreases due to the growth of Xe-135. Subsequently, the Xenon decays and the reactivity increases to a maximum at about a hundred hours when the Xenon is gone. Therefore, for conservatism, the Xenon is set to zero in the calculations to assure maximum reactivity. During the next 50 years, the reactivity continuously decreases due primarily to ^{241}Pu decay and ^{241}Am growth. Credit for this decay and for changes in fission product concentration is included in calculations of the decrease in reactivity in long term storage (up to 20 years). The CASMO4 code includes the capability of tracking the decay of the actinides and the most significant fission product nuclides during long term storage.

4.5 Region 1 Criticality Analyses and Tolerances

4.5.1 Nominal Design Case

For the nominal storage cell design in Region 1, the criticality safety analyses for the two different storage patterns are summarized in Tables 4.2.1, 4.2.2 and 4.2.4. This data confirms that the maximum reactivity in Region 1 remains subcritical (less than the regulatory limit $k_{\text{eff}} \leq 1.0$) under the assumed condition of the loss of all soluble boron in the pool water. Figure 4.1.1 shows the limiting burnup values for fuel of other enrichments and cooling times (see also Table 4.2.2).

4.5.2 Uncertainties Due to Tolerances

The reactivity effects of manufacturing tolerances are tabulated in Tables 4.2.1 and 4.2.4. All of the individual reactivity allowances were separately calculated for the reference fuel assembly and a statistical combination of uncertainties was used.

4.5.3 Eccentric Fuel Positioning

The fuel assembly is assumed to be normally located in the center of the storage rack cell. However, calculations were also made with the fuel assemblies assumed to be in the corner of the storage rack cell (four-assembly cluster at closest approach). These calculations indicated that the reactivity effect is slightly positive. Therefore, the uncertainty for eccentricity is included in the calculations for the final k_{eff} in Tables 4.2.1 and 4.2.4.

4.6 Region 2 Criticality Analyses and Tolerances

4.6.1 Nominal Design Case

For the nominal storage cell design in Region 2, the criticality safety analyses are summarized in Tables 4.2.5, 4.2.6 and 4.2.8. This data confirms that the maximum reactivity in Region 2 remains subcritical (less than the regulatory limit $k_{\text{eff}} \leq 1.0$) under the assumed condition of the loss of all soluble boron in the pool water. Figure 4.1.2 (and Table 4.2.6) summarizes the limiting fuel burnups for fuel assemblies of other enrichments and cooling times.

4.6.2 Uncertainties Due to Tolerances

The reactivity effects of manufacturing tolerances are tabulated in Tables 4.2.5 and 4.2.8. All of the individual reactivity allowances were separately calculated for the reference fuel assembly and a statistical combination of uncertainties was used.

4.6.3 Eccentric Fuel Positioning

The fuel assembly is assumed to be normally located in the center of the storage rack cell. However, calculations were also made with the fuel assemblies assumed to be in the corner of the storage rack cell (four-assembly cluster at closest approach). These calculations indicate that the reactivity effect is slightly positive. Therefore, the uncertainty for eccentricity is included in the calculations for the final k_{eff} in Tables 4.2.5 and 4.2.8.

4.7 Region 3 Criticality Analyses and Tolerances

4.7.1 Nominal Design Case

For the nominal storage cell design in Region 3, the criticality safety analyses are summarized in Table 4.2.9. This data confirms that the maximum reactivity in Region 3 remains subcritical (less than the regulatory limit $k_{\text{eff}} \leq 1.0$) under the assumed condition of the loss of all soluble boron in the pool water.

4.7.2 Uncertainties Due to Tolerances

The reactivity effects of manufacturing tolerances are tabulated in Table 4.2.9. All of the individual reactivity allowances were separately calculated for the reference fuel assembly and a statistical combination of uncertainties was used.

4.7.3 Eccentric Fuel Positioning

The fuel assembly is assumed to be normally located in the center of the storage rack cell. However, calculations were also made with the fuel assemblies assumed to be in the corner of the storage rack cell (four-assembly cluster at closest approach). These calculations indicate that the reactivity effect is slightly negative.

4.8 Abnormal and Accident Conditions in the Spent Fuel Pool Racks

4.8.1 Temperature and Water Density Effects

The moderator temperature coefficient of reactivity in both Region 1 and Region 2 is positive. Therefore, a moderator temperature of 20 °C (39.2 °F) was assumed for the reference MCNP4a calculations and the increase in reactivity to the maximum bulk pool water temperature of 150 °F is included (CASMO4 calculation) as a bias in the calculation of the maximum k_{eff} . This assures that the true reactivity will always be lower over the expected range of water temperatures. The reactivity effects of the pool water temperature effects on reactivity have been evaluated using CASMO-4.

The moderator temperature coefficient of reactivity for the Region 3 racks is negative, and, therefore,

the reference MCNP4a calculation provides the maximum reactivity. The effect of a reduction in pool water temperature to 4 °C is included as an uncertainty in Table 4.2.9.

4.8.2 Lateral Rack Movement

Lateral motion of the storage racks under postulated seismic conditions could potentially alter the spacing between racks. Under these conditions, credit for the soluble boron (permitted under accident conditions) would maintain the k_{eff} at a value well below the maximum allowable. Nevertheless, the separation (water-gap) between rack modules is sufficiently large that even for the maximum movement expected under seismic excitation, the water gap remains larger than the water gap within the Region 1 modules. In the Region 2 and Region 3 racks, the k_{eff} is independent of the inter-module water gap and is not sensitive to any potential seismic induced movement of the modules. The water gap structure in each cell is included in the analysis and precludes any closer proximity between modules.

4.8.3 Abnormal Location of a Fuel Assembly

The misplacement of a fresh unburned fuel assembly of the highest permissible reactivity could, in the absence of soluble poison, result in exceeding the regulatory limit ($k_{\text{eff}} \leq 1.0$). This could occur if a fresh fuel assembly of the highest permissible initial enrichment ($4.95 \pm 0.05 \text{ wt\% } ^{235}\text{U}$) were to be inadvertently loaded into a Region 1 or Region 2 storage cell, which is intended to store spent fuel assemblies or remain empty. Calculations confirmed that the highest reactivity, including uncertainties, for the worst case postulated accident condition (fresh fuel assembly in Region 2 cell intended to remain empty) would exceed the limit on reactivity in the absence of soluble boron. Soluble boron in the spent fuel pool water, for which credit is permitted under these accident conditions, would assure that the reactivity is maintained substantially less than the design limitation. Calculations indicate that a soluble boron concentration of 825 ppm is adequate to assure that the maximum k_{eff} does not exceed 0.95. Proposed ANO-2 Technical Specifications will require that a concentration of at least 2000 ppm boron is maintained in the SFP.

In addition, the mislocation of a fresh unburned fuel assembly could occur if a fresh fuel assembly of the highest permissible initial enrichment ($4.95 \pm 0.05 \text{ wt\% } ^{235}\text{U}$) were to be accidentally mis-located outside of a Region 1 or Region 2 storage rack, with the rack fully loaded. However, this is an area of high neutron leakage and the reactivity effect would be bounded by that of a fuel assembly

accidentally mis-loaded internal to a Region 1 or Region 2 storage module.

4.8.4 Dropped Fuel Assembly

For the case in which a fuel assembly is assumed to be dropped on top of a rack and the fuel assembly comes to rest horizontally on top of the rack with a minimum separation distance from the active fuel region of more than 12 inches, which is sufficient to preclude neutron coupling (with fuel in the storage rack). Consequently, the horizontal fuel assembly drop accident will not result in a significant increase in reactivity. Furthermore, the soluble boron in the spent fuel pool water assures that the true reactivity is always less than the limiting value for this dropped fuel accident.

Analyses were performed to evaluate the potential loss of Metamic® poison panels in the Region 3 racks by means of a dropped fuel assembly. A very conservative bounding accident condition was analyzed postulating the loss of all Metamic® absorber material throughout the entire Region 3 storage racks. For this accident analysis, the proposed Technical Specification limit of 2000 ppm soluble boron was assumed. The results of this postulated accident condition shows that the maximum k_{eff} is 0.93, including bias and tolerance uncertainties, which is well below 0.95. This is a very conservative evaluation since an actual dropped assembly at most would be expected to only damage a maximum of eight Metamic® panels.

It is also possible to vertically drop an assembly into a location occupied by another assembly. Such a vertical impact, would, at most cause a small compression of the stored assembly, reducing the water-to-fuel ratio and thereby reducing reactivity. In addition the distance between the active fuel regions of both assemblies will be more than sufficient to ensure no neutron interaction between the two assemblies.

Dropping of an assembly into an unoccupied cell could result in a localized deformation of the base plate of the rack. The immediate eight surrounding fuel cells could also be affected. However, the amount of deformation for these cells would be considerably less. The resultant effect would be the lowering a few fuel assemblies in the area near the deformation. The Metamic poison panel inserts in the Region 3 type racks are designed to sit on the base plate and could potentially move downward and uncover a portion of the active fuel. The resulting geometry is bound by the previously discussed configuration in which a complete loss of all

Metamic[®] inserts was assumed with no change in the active fuel region alignment. Therefore, the presence of the proposed Boron concentration assures the maximum k_{eff} is will below the 0.95 acceptance criteria.

4.9 Soluble Boron Dilution Evaluation

The soluble boron in the spent fuel pool water is normally a minimum of 2000 ppm under operating conditions. Significant loss or dilution of the soluble boron concentration is extremely unlikely, if not incredible. Nonetheless, an evaluation was performed based on the ANO spent fuel pool data. The minimum required soluble boron concentration in the spent fuel pool water for various conditions are summarized in Table 4.9.1.

The required minimum soluble boron concentration is 400 ppm under normal conditions and 825 ppm for the most serious credible accident scenario. The volume of water in the pool is 199,200 gallons. Large amounts of unborated water would be necessary to reduce the boron concentration from 2000 ppm to 825 ppm or 400 ppm. Abnormal or accident conditions are discussed below for either low dilution rates (abnormal conditions) or high dilution rates (accident conditions). It should be noted that routine surveillances to measure the soluble boron concentrations in the pool water is required by Technical Specifications.

Small failures or mis-aligned values could possibly occur in the normal soluble boron control system or related systems. Such failures might not be immediately detected. These flow rates would be of the order of 2 gpm (comparable to normal evaporative loss) and the increased frequency of makeup flow might not be observed. However, an assumed loss flow-rate of 2 gpm dilutions flow rate would require some 111 days to reduce the boron concentration to the minimum required 400 ppm required under normal conditions or 61 days to reach the 825 ppm required for the most severe fuel handling accident. Routine surveillance measurements of the soluble boron concentration would readily detect the reduction in soluble boron concentration with ample time for corrective action.

Under certain accident conditions, it is conceivable that a high flow rate of unborated water could flow onto the top of the pool. Such an accident scenario could result from rupture of an unborated water supply line or possibly the rupture of a fire protection system header, both events potentially allowing unborated water to spray onto the pool. A flow rate of up to 2500 gpm

could possibly flow onto the spent fuel pool as a result of a rupture of the fire protection line. This would be the most serious condition and bounds all other accident scenarios. Conservatively assuming that all the unborated water from the break poured onto the top of the pool and further assuming instantaneous mixing of the unborated water with the pool water, it would take approximately 128 minutes to dilute the soluble boron concentration to 400 ppm, which is the minimum required concentration to maintain k_{eff} below 0.95 under normally operating conditions. In this dilution accident, some 320,000 gallons of water would spill on the auxiliary building floor and into the air-conditioning duct system. Well before the spilling of such a large volume of water, multiple alarms would have alerted the control room of the accident consequences (including the fuel pool high-level alarm, the fire protection system pump operation alarm, and the floor drain receiving tank high level alarm). For this high flow rate condition, 71 minutes would be required to reach the 825 ppm required for the most severe fuel handling accident.

Instantaneous mixing of pool water with the water from the rupture of the demineralized water supply line is an extremely conservative assumption. Water falling on to the pool surface would mix with the top layers of pool water and the portions of the mixed volumes would continuously spill out of the pool. The density difference between water at 150 °F (maximum permissible pool bulk water temperature) and at the temperature of the demineralizer water supply is small. This density difference will not cause the water falling on to the pool surface to instantaneously sink down into the racks overcoming the principal driving force for the flow in the pool, which is the buoyancy force generated in the spent fuel pool racks region due to the heat generation from the spent fuel in the racks. This would further enhance the mixing process between the pool water and spilled water above the racks.

For the fire control line break, upon the initial break, the fire protection system header pressure would drop to the auto start setpoint of the fire protection pumps. The start is accompanied with an alarm in the main control room. The enunciator response is to dispatch an operator to find the source of the pump start. Approximately 5 minutes into the event, a Spent Fuel Pool high level alarm would be received in the main control room, assuming that the Spent Fuel Pool level started at the low alarm. The enunciator response for high Spent Fuel Pool level is to investigate the cause. The coincidence of the 2 alarms would quickly lead to the discovery of the failure of the fire protection system and sufficient time to isolate the failure.

The maximum flow rate for a failure of the demineralized water header would provide approximately 400 gpm into the Spent Fuel Pool. Failure of the demineralized water header is not accompanied with an alarm; however, the time to dilute the Spent Fuel Pool from 2000 ppm to 400 ppm is greater than the bounding case described above. In this scenario, there is sufficient time to isolate the failure and to prevent the spilling of some 320,000 gallons of water.

The analysis assume that for a double-ended break in the fire control piping, the stream of water will arch through the air some 40 feet falling on top of the pool. This is virtually an incredible event. Should the stream of water fall upon the pool deck, a 3 inch high curb would channel some of the water to the pool drain and prevent all of the water from reaching the pool. Furthermore, the evaluation also assumes at least 3 independent and concurrent accidents occur simultaneously:

- ◆ Large amount of water flowing from the double-ended pipe break would remain undetected and is ignored.
- ◆ Pool water high level alarms either fail or are ignored.
- ◆ Alarms indicating large amounts of water flowing into the floor drain have failed or are ignored.

Considering all related facts, a significant dilution of the pool soluble boron concentration in a short period of time without corrective action is not considered a credible event.

It is not considered credible that multiple alarms would fail or be ignored or that the spilling of large volumes of water would not be observed. Therefore, such a major failure would be detected in sufficient time for corrective action to avoid violation of an administrative guideline and to assure that the health and safety of the public is protected.

4.10 References for Section 4.0

- [4.1.1] M. G. Natrella, Experimental Statistics, National Bureau of Standards Handbook 91, August 1963.
- [4.1.2] L.I. Kopp, "Guidance on the Regulatory Requirements for Criticality Analysis of Fuel Storage at Light-Water Reactor Power Plants," NRC Memorandum from L. Kopp to T. Collins, August 19, 1998.
- [4.4.1] J.F. Briesmeister, Editor, "MCNP - A General Monte Carlo N-Particle Transport Code, Version 4A," LA-12625, Los Alamos National Laboratory (1993).
- [4.4.2] L.M. Petrie and N.F. Landers, "KENO Va - An Improved Monte Carlo Criticality Program with Supergrouping," Volume 2, Section F11 from "SCALE: A Modular System for Performing Standardized Computer Analysis for Licensing Evaluation" NUREG/CR-0200, Rev. 4, January 1990.
- [4.4.3] "SCALE 4.3: A Modular System for Performing Standardized Computer Analysis for Licensing Evaluation For Workstations and Personal Computers, Volume 0," CCC-545, ORNL-RSICC, Oak Ridge National Laboratory (1995).
- [4.4.4] N.M. Greene, L.M. Petrie and R.M. Westfall, "NITAWL-II: Scale System Module for Performing Shielding and Working Library Production," Volume 1, Section F1 from "SCALE: A Modular System for Performing Standardized Computer Analysis for Licensing Evaluation" NUREG/CR-0200, Rev. 4, January 1990.
- [4.4.5] M. Edenius, K. Ekberg, B.H. Forssén, and D. Knott, "CASMO-4 A Fuel Assembly Burnup Program User's Manual," Studsvik/SOA-95/1, Studsvik of America, Inc. and Studsvik Core Analysis AB (proprietary).
- [4.4.6] D. Knott, "CASMO-4 Benchmark Against Critical Experiments", SOA-94/13, Studsvik of America, Inc., (proprietary).

- [4.4.7] D. Knott, "CASMO-4 Benchmark Against MCNP," SOA-94/12, Studsvik of America, Inc., (proprietary).
- [4.4.8] S.E. Turner, "Uncertainty Analysis - Burnup Distributions", presented at the DOE/SANDIA Technical Meeting on Fuel Burnup Credit, Special Session, ANS/ENS Conference, Washington, D.C., November 2, 1988.

**Table 4.1.1
Fuel Assembly Specifications**

Assembly Data	
Rod Array Size	16x16
Rod Pitch (inches)	0.506
Total Width (inches)	8.130–8.149
Total Length (inches)	176.803
Active Fuel Length (inches)	149.61–150
Fuel Rod Data	
Total Number of Fueled Rods	Up to 236
Fuel Rod Total Length (inches)	161.318–161.868
Fuel Rod Outer Diameter (inches)	0.382
Fuel Rod Inner Diameter (inches)	0.332
Cladding Thickness (inches)	0.025
Cladding Material	Zircalloy
Pellet Diameter (inches)	0.325
UO ₂ Stack Density, gms/cc	10.522
Guide Tube Data	
Number of Tubes	5
Tube Outer Diameter (inches)	0.980
Tube Thickness (inches)	0.040
Tube Material	Zircalloy

Table 4.2.1
Summary of the Criticality Safety Analyses for Storage of 4.95 ±0.05
wt% ²³⁵U Enriched Spent Fuel Assemblies in Region 1 Racks.

Reference k_{eff}	0.9689
Burnup, MWD/KgU	43.0
MCNP4a Bias	0.0009
Temperature Bias	0.0092
MCNP4a Bias Uncertainty	0.0011
MCNP4a Statistical (95/95) Uncertainty	0.0007
Manufacturing Tolerance Uncertainty	0.0038
Enrichment Tolerance Uncertainty	0.0031
Depletion Uncertainty	0.0144
Fuel Eccentric Positioning Uncertainty	0.0027
Statistical Combination of Uncertainties	0.0155
Maximum k_{eff}	0.9945
Regulatory Limiting k_{eff}	1.0000

Table 4.2.2

Minimum Burnup Required for Storage of Spent Fuel Assemblies in the Region 1 Racks.

BURNUP, MWD/ KgU					
Average Enrichment, wt% ²³⁵U	0 Years Cooling Time	5 Years Cooling Time	10 Years Cooling Time	15 Years Cooling Time	20 Years Cooling Time
2	5.16	5.12	5.08	5.04	5.00
2.5	12.50	12.25	12.00	11.75	11.50
3.0	18.90	18.05	17.20	16.35	15.50
3.5	24.67	23.75	22.84	21.92	21.00
4.0	30.27	29.20	28.14	27.07	26.00
4.5	37.30	35.78	34.25	32.73	31.20
4.95	43.00	41.25	39.50	37.75	36.00

Table 4.2.3

Bounding Polynomial Fits to Determine Minimum Acceptable Burnup for Storage of Spent Fuel Assemblies Storage in Region 1 Racks as a Function of Initial Average Enrichment.

Decay Time, Years	Burnup, MWD/KgU
0	$-0.2906 \cdot E^4 + 4.5902 \cdot E^3 - 26.239 \cdot E^2 + 76.516 \cdot E - 74.8$
5	$-0.3306 \cdot E^4 + 5.0873 \cdot E^3 - 28.413 \cdot E^2 + 79.862 \cdot E - 76.21$
10	$-0.362 \cdot E^4 + 5.463 \cdot E^3 - 29.978 \cdot E^2 + 81.9 \cdot E - 76.48$
15	$-0.402 \cdot E^4 + 5.9607 \cdot E^3 - 32.152 \cdot E^2 + 85.245 \cdot E - 77.82$
20	$-0.4375 \cdot E^4 + 6.3977 \cdot E^3 - 34.034 \cdot E^2 + 87.983 \cdot E - 78.6$

Note: E = Initial average enrichment in wt% ²³⁵U

Table 4.2.4

**Summary of the Criticality Safety Analyses for a 2-of-4
Checkerboard Storage of Fresh Fuel Assemblies and Empty Cells
in Region 1 Racks.**

Reference k_{eff}	0.9072
MCNP4a Bias	0.0009
Temperature Effect	0.0103
Axial Burnup Distribution Penalty	Not Applicable
MCNP4a Bias Uncertainty	0.0011
MCNP4a Statistics (95/95) Uncertainty	0.0007
Manufacturing Tolerance Uncertainty	0.0042
Enrichment Tolerance Uncertainty	0.0020
Depletion Uncertainty	Not Applicable
Fuel Eccentric Positioning Uncertainty	0.0005
Statistical Combination of Uncertainties	0.0049
Maximum k_{eff}	0.9233
Regulatory Limiting k_{eff}	1.0000

Table 4.2.5

Summary of the Criticality Safety Analyses for Storage of Spent Fuel Assemblies in Region 2 Racks.

Initial Enrichment, wt% ²³⁵ U	4.95 ±0.05
Burnup, MWD/KgU	45.0
Cooling Time, years	0
Reference k _{eff}	0.9682
MCNP4a Bias	0.0009
Temperature Effect	0.0092
MCNP4a Bias Uncertainty	0.0011
MCNP4a Statistics (95/95) Uncertainty	0.0007
Manufacturing Tolerance Uncertainty	0.0097
Enrichment Tolerance Uncertainty	0.0031
Depletion Uncertainty	0.0166
Fuel Eccentric Positioning Uncertainty	0.0021
Statistical Combination of Uncertainties	0.0196
Maximum k _{eff}	0.9979
Regulatory Limiting k _{eff}	1.0000

Table 4.2.6

Minimum Burnup Required for Storage of Spent Fuel Assemblies in the Region 2 Racks.

BURNUP, MWD/KgU					
Average Enrichment, wt% ²³⁵ U	0 Years Cooling Time	5 Years Cooling Time	10 Years Cooling Time	15 Years Cooling Time	20 Years Cooling Time
2	7.56	7.56	7.56	7.56	7.56
2.5	14.94	14.21	13.47	12.74	12.00
3.0	21.30	20.30	19.30	18.30	17.30
3.5	27.10	25.95	24.80	23.65	22.50
4.0	32.67	31.38	30.09	28.79	27.50
4.5	39.30	37.73	36.15	34.58	33.00
4.95	45.00	43.33	41.65	39.98	38.30

Table 4.2.7

Bounding Polynomial Fits to Determine Minimum Acceptable Burnup for Storage of Spent Fuel Assemblies Storage in Region 2 Racks as a Function of Initial Enrichment.

Decay Time, Years	Burnup, MWD/KgU
0	$0.68 \cdot E^3 - 7.449 \cdot E^2 + 38.56 \cdot E - 45.20$
5	$0.5489 \cdot E^3 - 5.9344 \cdot E^2 + 32.496 \cdot E - 38.05$
10	$0.4153 \cdot E^3 - 4.3948 \cdot E^2 + 26.356 \cdot E - 30.75$
15	$0.2867 \cdot E^3 - 2.9045 \cdot E^2 + 20.367 \cdot E - 23.80$
20	$0.153 \cdot E^3 - 1.3649 \cdot E^2 + 14.227 \cdot E - 16.60$

Note: E = Initial average enrichment in wt% ²³⁵U

Table 4.2.8

Summary of the Criticality Safety Analyses for 2-of-4 Checkerboard Storage
of Fresh Fuel Assemblies and Empty Cells in Region 2 Racks

Reference k_{eff}	0.9151
MCNP4a Bias	0.0009
Temperature Effect	0.0101
MCNP4a Bias Uncertainty	0.0011
MCNP4a Statistical (95/95) Uncertainty	0.0007
Manufacturing Tolerance Uncertainty	0.0129
Enrichment Tolerance Uncertainty	0.0019
Depletion Uncertainty	Not Applicable
Fuel Eccentricity Uncertainty	0.0002
Statistical Combination of Uncertainties	0.0131
Maximum k_{eff}	0.9392
Regulatory Limiting k_{eff}	1.0000

Table 4.2.9

Summary of the Criticality Safety Analyses for Storage of Fresh Fuel Assemblies in ANO Unit 2 Region 3 Racks

Reference k_{eff}	0.9839
MCNP4a Bias	0.0009
MCNP4a Bias Uncertainty	0.0011
MCNP4a Statistical (95/95) Uncertainty	0.0007
Manufacturing Tolerance Uncertainty	0.0120
Enrichment Tolerance Uncertainty	0.0017
Depletion Uncertainty	Not Applicable
Fuel Eccentric Positioning Uncertainty	Negative
Pool Water Temperature Uncertainty	0.0014
Statistical Combination of Uncertainties	0.0123
Maximum k_{eff}	0.9971
Regulatory Limiting k_{eff}	1.0000

Table 4.9.1

Required Soluble Boron Concentrations in the SFP Water

Condition	<u>Soluble Boron Required for k<1</u>	<u>Soluble Boron Required for k<0.95 (ppm)</u>
Region 1: All Spent Fuel Assemblies	0	240
Region 1: Accident condition of 1 fresh fuel assembly mis-placed into a cell intended to store spent fuel	-	490
Region 1: Accident condition of 1 fresh fuel assembly mis-placed into a cell intended to remain empty	-	740
Region 2: All Spent Fuel Assemblies	0	240
Region 2: Accident condition of 1 fresh fuel assembly mis-placed into a cell intended to store spent fuel	-	490
Region 2: Accident condition of 1 fresh fuel assembly mis-placed into a cell intended to remain empty	-	825
Region 3: All Fresh Fuel Assemblies	-	400
Region 3: Dropped fuel assembly with all fresh fuel assemblies with no poison inserts.		2000

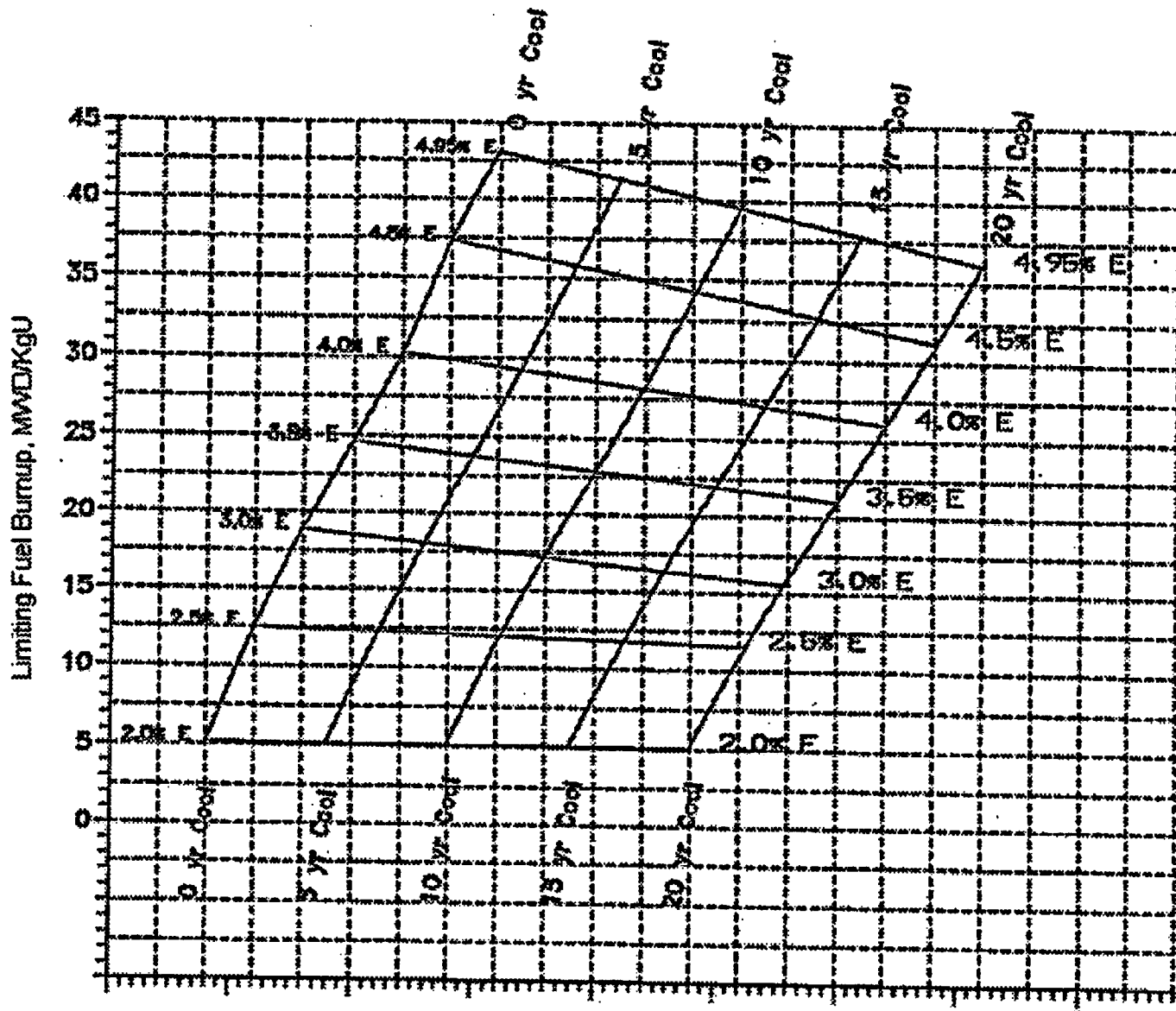


Figure 4.1.1: 3-Dimensional Plot of Minimum Fuel Burnups for Fuel in Unit 2 Region 1 for Enrichments and/or Cooling Times.

(Use Enrichment or Decay Time, as Appropriate, for Interpolation Along the x-axis)

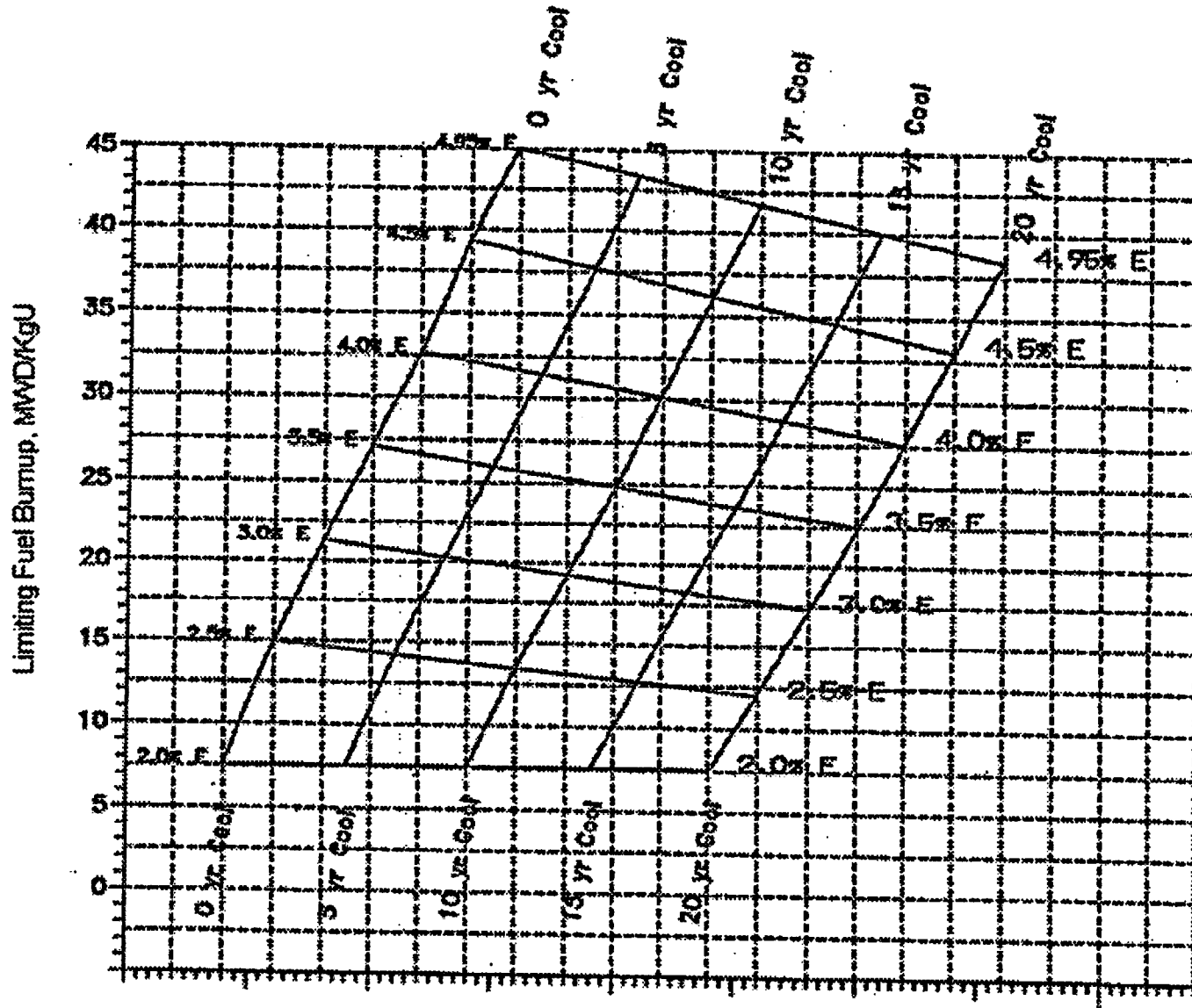


Figure 4.1.2: 3-Dimensional Plot of Minimum Fuel Burnups for Fuel in Unit 2 Region 2 for Enrichments and/or Cooling Times.

(Use Enrichment or Decay Time, as Appropriate, for Interpolation Along the x-axis)

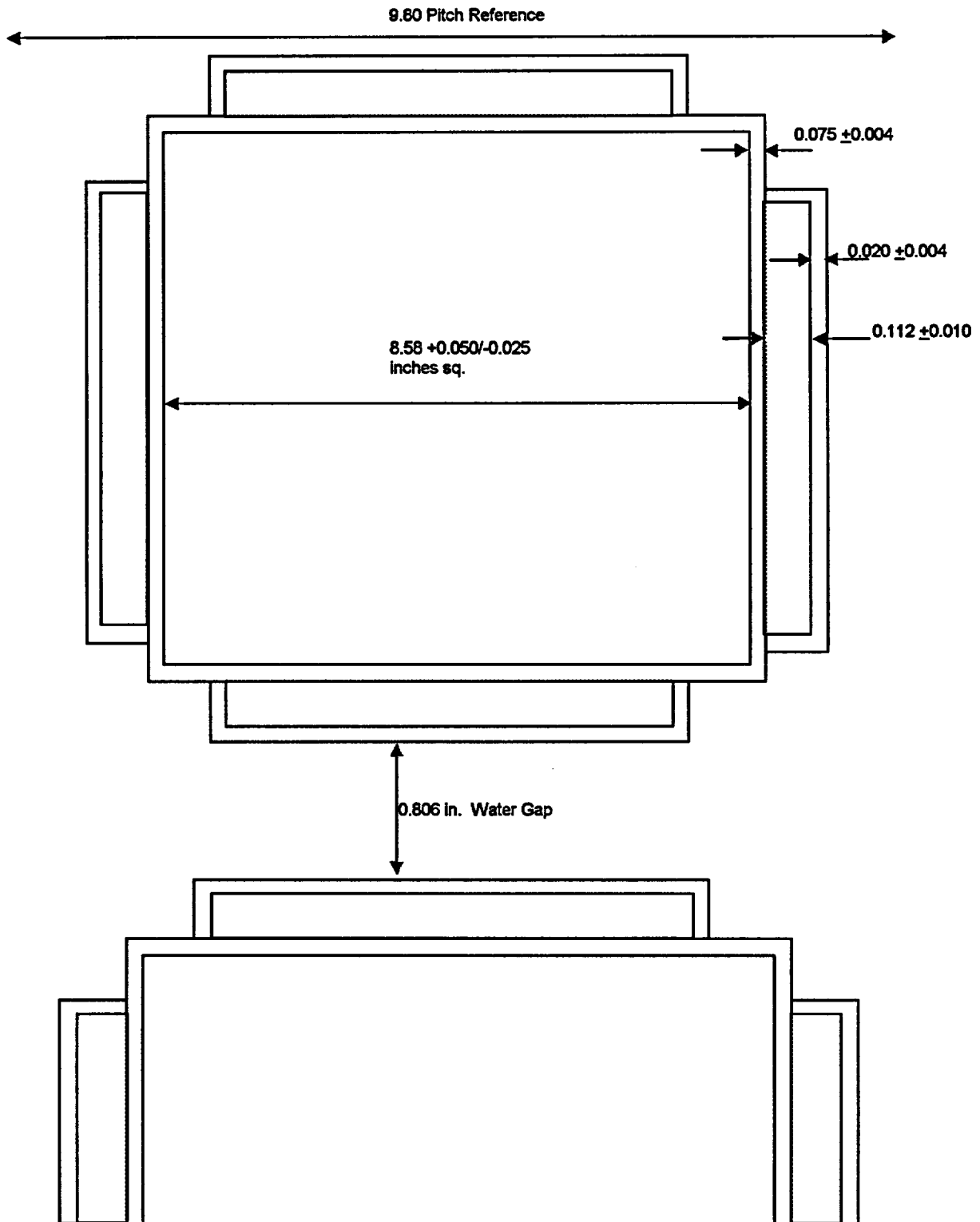


Figure 4.3.1: A Cross-Sectional View of the Calculational Model Used for the Region 1 Rack Analysis (NOT TO SCALE).

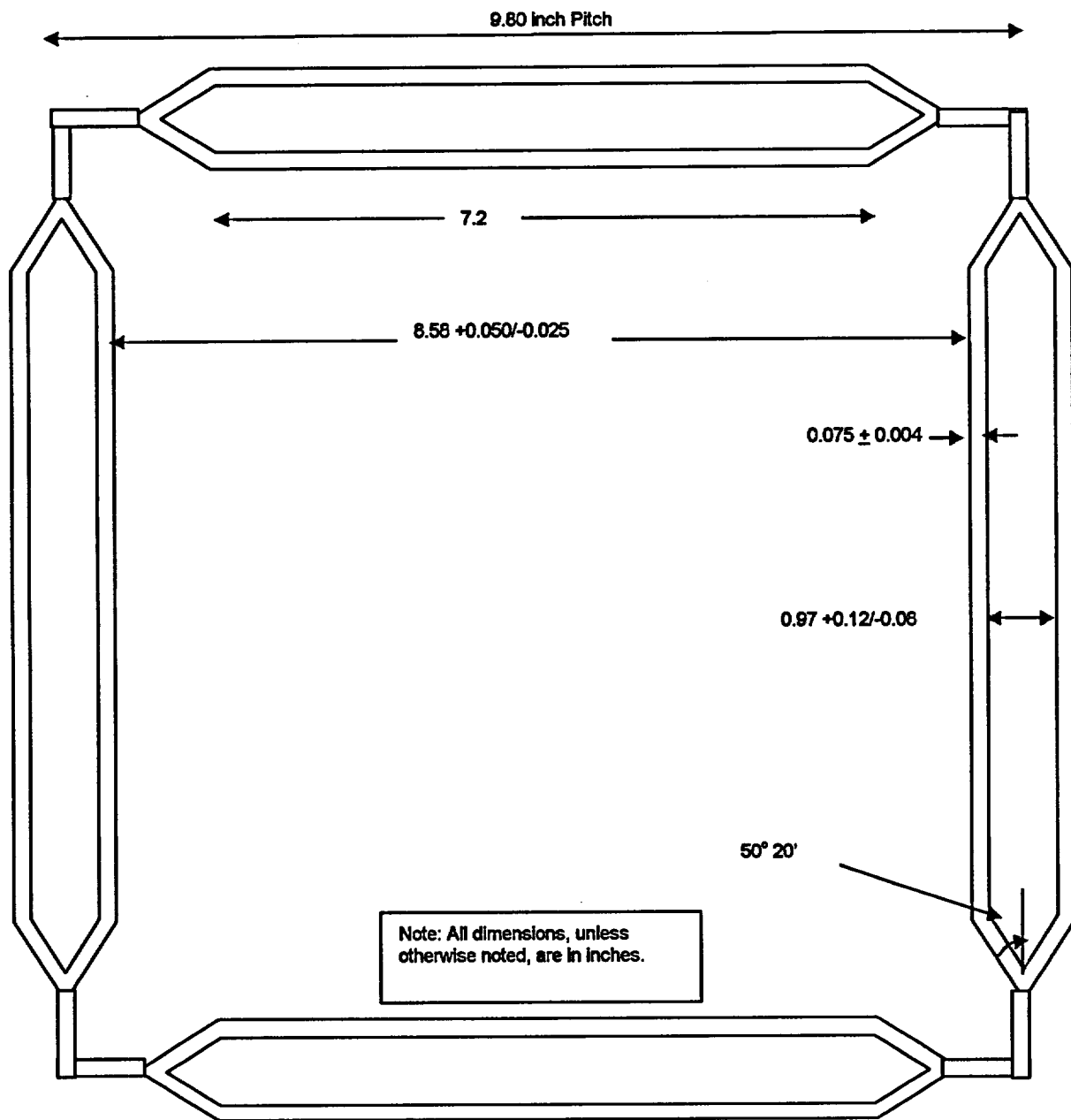


Figure 4.3.2: A Cross-Sectional View of the Calculational Model Used for the Region 2 Rack Analysis (NOT TO SCALE).

Note: In order to preserve the pitch due to a conservative reduction of the flux trap gap width from a design reference value of 1.07 inches to 0.97 inches (based on measurements), the cell ID was modeled as $8.68 +0.050/-0.025$ inches.

5.0 THERMAL-HYDRAULIC CONSIDERATIONS

5.1 INTRODUCTION

This document requests an operating license amendment to modify the ANO-2 SFP storage capacity. The modification will preserve the fresh fuel storage capability of the SFP racks. As discussed in Section 1.0, this will be achieved by placing poison inserts into the flux trap area of some of the existing Region 2 spent fuel storage racks (SFSRs). This section provides a summary of the analyses performed to demonstrate the compliance of the SFP and its attendant cooling system with the provisions of USNRC Standard Review Plan (SRP) 9.1.3 (Spent Fuel Pool Cooling and Cleanup System, Rev. 1, July 1981) and Section III of the USNRC "OT Position Paper for Review and Acceptance of Spent Fuel Storage and Handling Applications," (April 14, 1978). Similar methods of thermal-hydraulic analysis have been used in the licensing evaluations for other SFP capacity expansion projects.

The thermal-hydraulic qualification analyses for the modified rack array may be broken down into the following categories:

- i. Evaluation of bounding maximum decay heat versus time profiles, used as input to subsequent analyses.
- ii. Evaluation of loss-of-forced cooling scenarios, to establish minimum times to perform corrective actions and the associated makeup water requirements.
- iii. Determination of the maximum local water temperature, at the instant when the pool decay heat reaches its maximum value, to establish that localized boiling in the SFSRs is not possible while forced cooling is operating. The bulk pool temperature is postulated to be at the maximum limit.
- iv. Evaluation of the maximum fuel rod cladding temperature, at the instant when the pool decay heat reaches its maximum value, to establish that nucleate boiling is not possible while forced cooling is operating. The co-incident bulk pool temperature is postulated to be at the maximum limit.

The following sections present plant system descriptions, analysis methodologies and assumptions, a synopsis of the input data employed and summaries of the calculated results.

5.2 COOLING SYSTEMS DESCRIPTION

The Spent Fuel Cooling (SFC) System is designed to maintain the water quality and clarity and to remove the decay heat from the stored fuel in the spent fuel pool. It is designed to maintain the spent fuel pool water less than or equal to 150 °F. Refueling operations are administratively controlled in order to minimize the potential of exceeding a pool temperature of 150°F during a full core discharge whenever service system temperature is elevated. The decay heat removal process is accomplished by recirculating spent fuel coolant water from the spent fuel pool through the pumps and cooler and back to the pool. The ANO Unit 2 fuel pool cooling is a closed loop system consisting of two pumps (only one normal operation) and one full capacity shell and tube heat exchanger. The fuel pool water is drawn from the fuel pool near the surface and is circulated by the operating fuel pool pump through the tube side of the fuel pool heat exchanger where heat is rejected to the service water system flowing on the shell side. From the outlet of the fuel pool heat exchanger, the cooled fuel pool water is returned to the top of the fuel pool via distribution header at the opposite end of the pool from the intake.

The clarity and purity of the water in the fuel pool, refueling cavity, and refueling water tank are maintained by the purification portion of the fuel pool system. The purification loop consists of the fuel pool purification pump, ion exchanger, filters, strainers, and an installed connection for a floating skimmer. The purification flow is drawn from the bottom of the fuel pool. A basket strainer is provided in the purification line to the pump suction to remove any relatively large particulate matter. The pump circulates the fuel pool water through a filter, which removes particulates larger than 5 micron size, and through an ion exchanger to remove ionic material. Connections to the refueling water tank and refueling water cavity are provided for purification and makeup.

Makeup to the fuel pool is provided from the CVCS (Chemical and Volume Control System) via the blending tee, the refueling water tank via the purification pumps, or the BMS (Borated Makeup System) holdup tanks if chemistry specifications are met. In an emergency, Seismic Category I makeup is available from either service water system loop. The boric acid makeup tanks are also available for boration of the spent fuel pool. Overflow protection is provided by

transferring the fuel pool water on high level alarm to the refueling water tank or one of the BMS holdup tanks via the purification pump.

5.3 SPENT FUEL POOL DECAY HEAT LOADS

The decay heat in the SFP is generated in the spent fuel assemblies stored therein. The total spent fuel pool decay heat is the sum of decay heat contributions from two groups of assemblies:

- i. Fuel assemblies from previous offloads already stored in the SFP
- ii. Fuel assemblies that are being offloaded from the reactor to the SFP

The fuel assemblies in the first group are referred to as previously offloaded fuel. Over the relatively short transient evaluation periods of this report the heat generation rate of these assemblies reduces very slowly with time, due to the exponential nature of radioactive decay and their relatively long decay periods. The decay heat contribution of these assemblies can therefore be conservatively treated as constant, neglecting any reduction in their decay heat contribution during the evaluation period. The fuel assemblies in the second group are referred to as recently offloaded fuel. The heat generation rate of these assemblies reduces rapidly with time, so the decay heat contribution of these assemblies is treated as time varying. The following equation defines the total decay heat generation in the SFP.

$$Q_{GEN}(\tau) = Q_P + F(\tau) \times Q_R(\tau) \quad (5-1)$$

where:

$Q_{GEN}(\tau)$ is the total time-varying decay heat generation rate in SFP, Btu/hr

Q_P is the decay heat contribution of the previously offloaded fuel, Btu/hr

$F(\tau)$ is the fraction of the recently offloaded fuel transferred to the SFP

$Q_R(\tau)$ is the decay heat contribution of the recently offloaded fuel, Btu/hr

τ is the fuel decay time after reactor shutdown, hrs

Prior to the start of fuel transfer from the reactor to the SFP, $F(\tau)$ is equal to zero and the total decay heat in the SFP will be equal to the invariant portion Q_P . During the fuel transfer, $F(\tau)$ will increase linearly from zero to one, and the total decay heat in the SFP will increase to $Q_P + Q_R(\tau)$.

Following the completion of fuel transfer, the total decay heat in the SFP will decrease as $Q_R(\tau)$

decreases.

The decay heat contributions of both the previously and recently offloaded fuel are determined using the Holtec QA validated computer program DECOR [5.3.1]. This computer program incorporates the Oak Ridge National Laboratory (ORNL) ORIGEN2 computer code [5.3.2] for performing decay heat calculations. The ORIGEN2 code is not modified for its incorporation into the Holtec program and should give the same results as the DECOR.

Based on the input data provided in Tables 5.3.1 and 5.3.2, the fuel decay heat is determined for the following two bounding offload scenarios:

1. **Partial Core Offload** - A refueling batch of 90 assemblies is offloaded from the plant's reactor into the SFP, completely filling all storage locations. The total SFP inventory prior to the offload is 900 fuel assemblies, for a final post-offload inventory of 990 fuel assemblies. This slightly exceeds the storage capacity of the ANO-2 SFP and is used for calculation of decay heat loads, which is conservative.
2. **Full Core Offload** - The full core of 177 assemblies is offloaded from the plant's reactor into the SFP, completely filling all storage locations. The total SFP inventory prior to the offload is 900 fuel assemblies, for a final post-offload inventory of 1077 fuel assemblies. This slightly exceeds the storage capacity of the ANO-2 SFP and is used for calculation of decay heat loads, which is conservative.

5.4 MINIMUM TIME-TO-BOIL AND MAXIMUM BOILOFF RATE

In this section, we present the methodology for calculating the minimum time-to-boil and corresponding maximum boil off rate. The following conservatisms and assumptions are applied in the time-to-boil and boil off rate calculations:

- The thermal inertia (thermal capacity) of the SFP is based on the water volume above the fuel pool racks. This conservatively neglects the considerable thermal inertia of the fuel assemblies, stainless steel racks and stainless steel SFP liners.

- During the loss of forced cooling evaluations, it is assumed that makeup water is not available. This minimizes the thermal capacity of the SFP as water is boiled off, thus increasing the water level drop rate.
- The loss of forced cooling is postulated for the most adverse combination of conditions assumed to occur co-incidentally, viz. the maximum SFP bulk temperature and the maximum pool decay heat (Q_{max}) computed when the fuel batch is transferred to the pool. Maximizing the initial temperature and the pool decay heat will conservatively minimize the calculated time-to-boil.
- The time-to-boil (τ_{boil}) is computed assuming Q_{max} and an adiabatic heatup from an initial temperature to normal boiling temperature

Key input data for these calculations is provided in Table 5.4.1. The following equation is used to determine the time to boil:

$$\tau_{boil} = \frac{C_w(T_b - T_o)}{Q_{max}} \quad [5-1]$$

where:

- C_w = pool water thermal capacity (Btu/°F)
- T_o = initial pool water temperature (120 °F normal offload, 150 °F full core offload)
- T_b = normal boiling temperature of water (= 212 °F)

The post boiling water height attenuation function is conservatively obtained based on the maximum water inventory loss rate (Q_{max} / latent heat of evaporation). By mass balance, the water height is computed as:

$$h(\tau) = h_o - \frac{Q_{max}}{A_p \rho \lambda} (\tau - \tau_{boil}) \quad [5-2]$$

where:

- $h(\tau)$ = pool water height (ft) as a function of time τ after loss of forced cooling (hr)
- h_o = initial pool water height (ft)
- A_p = pool area (ft²)
- ρ = water density
= 59.8 lb/ft³ @ 212 °F [5.4.1]

λ = latent heat of vaporization
= 970.3 Btu/lb @ 212 °F [5.4.1]

5.5 MAXIMUM SFP LOCAL WATER TEMPERATURE

In this section, a summary of the methodology for evaluating the maximum SFP local water temperature is presented. The results of these evaluations are maximum local water temperatures.

In order to determine an upper bound on the maximum local water temperature, a series of conservative assumptions are made. The most important of these assumptions are:

- The walls and floor of the SFP are all modeled as adiabatic surfaces, thereby neglecting conduction heat loss through these items.
- Heat losses by thermal radiation and natural convection from the hot SFP surface to the environment are neglected.
- No downcomer flow is assumed to exist between the rack modules.
- The hydraulic resistance of the rack cells is conservatively overstated
- The bottom plenum heights used in the model are less than the actual heights.
- The hydraulic resistance of every SFSR cell is determined based on the most restrictive water inlet geometry of the cells over rack support pedestals (i.e., all baseplate holes are completely blocked). These cells have a reduced water entrance area, caused by the pedestal blocking the baseplate hole, and a correspondingly increased hydraulic resistance.
- The hydraulic resistance of every SFSR cell includes the effects of blockage due to an assumed dropped fuel assembly lying horizontally on top of the SFSRs.

The objective of this study is to demonstrate that the thermal-hydraulic criterion of ensuring local subcooled conditions in the SFP is met for all postulated fuel offload scenarios. The local thermal-hydraulic analysis is performed such that slight fuel assembly variations are bounded. An outline of the Computational Fluid Dynamics (CFD) approach is described in the following.

There are several significant geometric and thermal-hydraulic features of the ANO-2 SFP that need to be considered for a rigorous CFD analysis. From a fluid flow modeling standpoint, there are two regions to be considered. One region is the SFP bulk region where the classical Navier-Stokes equations [5.5.1] are solved, with turbulence effects included. The other region is the SFSRs containing heat generating fuel assemblies, located near the bottom of the SFP. In this region, water flow is directed vertically upwards due to buoyancy forces through relatively small flow channels formed by the CE 16x16 fuel assemblies in each SFSR cell. This situation is modeled as a porous region with pressure drop in the flowing fluid governed by Darcy's Law as:

$$\frac{\partial P}{\partial X_i} = -\frac{\mu}{K(i)} V_i - C \rho |V| \frac{V_i}{2} \quad (5-3)$$

where $\partial P/\partial X_i$ is the pressure gradient, $K(i)$, V_i and C are the corresponding permeability, velocity and inertial resistance parameters and μ is the fluid viscosity. These terms are added as sink terms to the classic Navier-Stokes equations. The permeability and inertial resistance parameters for the rack cells loaded with CE 16x16 fuel assemblies are determined based on friction factor correlations for the laminar flow conditions that would exist due to the low buoyancy induced velocities and the small size of the flow channels.

The ANO-2 SFP geometry requires an adequate portrayal of both large scale and small scale features, spatially distributed heat sources in the SFSRs and water inlet/outlet piping. Relatively cooler bulk water normally flows down between the fuel racks outline and wall liner, a clearance known as the downcomer. Near the bottom of the racks the flow turns from a vertical to horizontal direction into the bottom plenum, supplying cooling water to the rack cells. Heated water issuing out of the top of the racks mixes with the bulk water. An adequate modeling of these features on the CFD program involves meshing the large scale bulk SFP region and small scale downcomer and bottom plenum regions with sufficient number of computational cells to capture both the global and local features of the flow field.

The distributed heat sources in the spent fuel pool racks are modeled by identifying distinct heat generation zones considering recently offloaded fuel, bounding peaking effects, and the presence of background decay heat from previous offloads. Two heat generating zones are modeled. The first consists of background fuel from previous offloads. The second zone consists of fuel from recently offloaded fuel assemblies. This is a conservative model, since all of the hot fuel assemblies from the recent offload are placed in a contiguous area. A uniformly distributed heat generation rate was applied throughout each distinct zone (i.e., there were no variations in heat generation rate within a single zone).

The CFD analysis was performed on the commercially available FLUENT [5.5.2] computational fluid dynamics program, which has been benchmarked under Holtec's QA program. The FLUENT code enables buoyancy flow and turbulence effects to be included in the CFD analysis. Buoyancy forces are included by specifying a temperature-dependent density for water and applying an appropriate gravity vector. Turbulence effects are modeled by relating time-varying Reynolds' Stresses to the mean bulk flow quantities with the standard k- ϵ turbulence model.

Some of the major input values for this analysis are summarized in Table 5.5.1. An isometric view of the assembled CFD model is presented in Figure 5.5.1.

5.6 FUEL ROD CLADDING TEMPERATURE

In this section, the method to calculate the temperature of the fuel rod cladding is presented. The maximum fuel rod cladding temperature is determined to establish that nucleate boiling is not possible while forced cooling is operating. This requires demonstrating that the highest fuel rod cladding temperatures are less than the local saturation temperature of the adjacent SFP water. The maximum fuel cladding superheat above the local water temperature is calculated for two different peak fuel rod heat emission rates.

A fuel rod can produce F_z times the average heat emission rate over a small length, where F_z is the axial peaking factor. The axial heat distribution in a rod is generally a maximum in the central region, and tapers off at its two extremities. Thus, peak cladding heat flux over an infinitesimal rod section is given by the equation:

$$q_c = \frac{Q \times F_z}{A_c} \quad (5-4)$$

where Q is the rod average heat emission and A_c is the total cladding external heat transfer area in the active fuel length region. The axial peaking factor is given in Table 5.5.1.

As described previously, the maximum local water temperature was computed. Within each fuel assembly sub-channel, water is continuously heated by the cladding as it moves axially upwards under laminar flow conditions. Rohsenow and Hartnett [5.6.1] report a Nusselt-number for laminar flow heat transfer in a heated channel. The film temperature driving force (ΔT_f) at the peak cladding flux location is calculated as follows:

$$\begin{aligned} \Delta T_f &= \frac{q_c}{h_f} \\ h_f &= Nu \frac{K_w}{D_h} \end{aligned} \quad (5-5)$$

where h_f is the waterside film heat transfer coefficient, D_h is sub-channel hydraulic diameter, K_w is water thermal conductivity and Nu is the Nusselt number for laminar flow heat transfer.

In order to introduce some additional conservatism in the analysis, we assume that the fuel cladding has a crud deposit resistance R_c (equal to $0.0005 \text{ ft}^2\text{-hr-}^\circ\text{F/Btu}$), which covers the entire surface. Thus, including the temperature drop across the crud resistance, the cladding to water local temperature difference (ΔT_c) is given by the equation $\Delta T_c = \Delta T_f + R_c \times q_c$.

5.7 RESULTS

This section contains results from the analyses performed for the postulated offload scenarios.

5.7.1 Decay Heat

For the offload/cooling scenarios described in Section 5.3, the calculated SFP decay heat loads are summarized in Table 5.7.1. Given the conservatisms incorporated into the calculations, actual decay heat loads will be lower than these calculated values. Figures 5.7.1 and 5.7.2 each present profiles of net decay heat load versus time for the evaluated transient scenarios.

5.7.2 Minimum Time-to-Boil and Maximum Boiloff Rate

For the offload/cooling described in Section 5.3, the calculated times-to-boil and maximum boil-off rates are summarized in Table 5.7.2. These results show that, in the extremely unlikely event of a failure of forced cooling to the SFP, there would be at least 1.55 hours available for corrective actions prior to SFP boiling. Given the conservatisms incorporated into the calculations, actual times-to-boil will be higher than these calculated values. It should be noted that a complete failure of forced cooling is extremely unlikely. The maximum water boiloff rate is less than 90 gpm.

5.7.3 Local Water and Fuel Cladding Temperatures

Consistent with our approach to make conservative assessments of temperature, the local water temperature calculations are performed for a SFP with a total decay heat generation equal to the calculated decay heat load coincident with the maximum SFP bulk temperature. Thus, the local water temperature evaluation is a calculation of the temperature increment over the theoretical spatially uniform value due to local hot spots (due to the presence of highly heat emissive fuel assemblies). As described in Subsection 5.6, the peak fuel clad superheats (i.e., the maximum clad-to-local water temperature difference) are determined. The resultant bounding superheat values were used to calculate bounding maximum fuel clad temperatures.

The numeric results of the maximum local water temperature and the bounding fuel cladding temperature evaluations are presented in Table 5.7.3. Figure 5.7.3 presents converged

temperature contours in a vertical slice through the hot fuel region. Figure 5.7.4 presents converged velocity vectors in a vertical slice through the hot fuel region.

Both the maximum local water temperatures and the bounding fuel cladding temperatures are substantially lower than the 240 °F local boiling temperature at the top of the SFSRs. These results demonstrate that boiling, including nucleate boiling on clad surfaces, cannot occur anywhere within the ANO Unit 2 SFP while the SFC system is operating.

Under a postulated accident scenario of the loss of all cooling, the water temperature will rise. Assuming a temperature of 212 °F at the inlet to the rack cells, and conservatively using the bounding bulk-to-local and local-to-clad temperature differences from Table 5.7.3, the maximum possible cladding temperature will be 272.5 °F, which is greater than the saturation temperature at the top of the active fuel length. Due to the low maximum assembly heat flux (approximately 7000 W/m²) and the critical heat flux required for departure from nucleate boiling (on the order of 10⁶ W/m²), it can be concluded that the fuel cladding will not be subjected to departure from nucleate boiling even under the postulated accident scenario of the loss of all SFP cooling and the cladding integrity would be maintained.

5.8 REFERENCES

- [5.3.1] "QA Documentation for DECOR," Holtec Report HI-971734, Revision 0.
- [5.3.2] A.G. Croff, "ORIGEN2 - A Revised and Updated Version of the Oak Ridge Isotope Generation and Depletion Code," ORNL-5621, Oak Ridge National Laboratory, 1980.
- [5.4.1] Balzhiger, R.E. and Samuels, M. R. "Engineering Thermodynamics", Appendix B Steam Tables, Prentice Hall Inc., (1977)
- [5.5.1] Batchelor, G.K., "An Introduction to Fluid Dynamics", Cambridge University Press, 1967.
- [5.5.2] "Validation of FLUENT Version 5.1", Holtec Report HI-992276, Revision 0.
- [5.6.1] Rohsenow, N.M., and Hartnett, J.P., "Handbook of Heat Transfer", McGraw Hill Book Company, New York, 1973.

Table 5.3.1

Key Input Data for Decay Heat Computations

Input Data Parameter	Value
Reactor Thermal Power (MWt)	3100
Number of Assemblies in Reactor Core	177
Maximum Number of Storage Cells in SFP	988
Bounding Discharge Schedule	Table 5.3.2
Minimum In-Core Hold Time (hr)	100
Fuel Discharge Rate	5 per hour

Table 5.3.2

Theoretical Bounding* Fuel Discharge History

CYCLE NUMBER	CYCLE LENGTH* (Months)	NUMBER OF DISCHARGED ASSEMBLIES
Cycle 1	24	90
Cycle 2	24	90
Cycle 3	24	90
Cycle 4	24	90
Cycle 5	24	90
Cycle 6	24	90
Cycle 7	24	90
Cycle 8	24	90
Cycle 9	24	90
Cycle 10	24	90

* To conservatively overestimate background decay heat, the refuel batch size and fuel burnup are maximized. Because a great bulk of the total pool decay heat is contributed by the freshly discharged fuel, the overall impact of this overestimation on pool temperatures is quite modest.

* While historic (ca. 2002) offloads were on 18-month cycles, the use of the longer 24-month cycle will have a negligible impact on the total SFP heat load. This is due to the use of bounding burnups, initial enrichments and offload batch sizes for the historic offloads, as well as the extremely long cooling times for these fuel assemblies at the point in time where the SFP becomes filled.

Table 5.4.1

Key Input Data for Time-To-Boil Evaluation

SFP Surface Area	753.25 ft²
Minimum Pool Water Depth	39.4 feet
SFP Net Water Volume	17,071 ft³

Table 5.5.1

Key Input Data for Local Temperature Evaluation

Axial Peaking Factor	1.248
Number of Fuel Assemblies	988
Cooled SFP Water Flow Rate through SFPCS Heat Exchanger	1000 gpm*
Fuel Assembly Type	CE 16x16
Fuel Rod Outer Diameter	0.382 inches
Active Fuel Length	149.61 inches
Number of Rods per Assembly	236 rods
Rack Cell Inner Dimension	8.58 inches
Rack Cell Length	188.9 inches
Modeled Bottom Plenum Height	3 inches

* The SFP cooling system has two pumps, each with a capacity of 2000 gpm. Conservatively, only 1000 gpm of cooling water flow has been credited in the local temperature analysis.

Table 5.7.1

Result of SFP Decay Heat Calculations

Heat Load Component	Partial Core Offload Value (Btu/hr)	Full Core Offload Value (Btu/hr)
Previously Discharged Fuel	5.85×10^6	5.85×10^6
Recently Discharged Fuel at End of Transfer	19.655×10^6	36.503×10^6
Total Bounding Decay Heat	25.505×10^6	42.353×10^6

Table 5.7.2

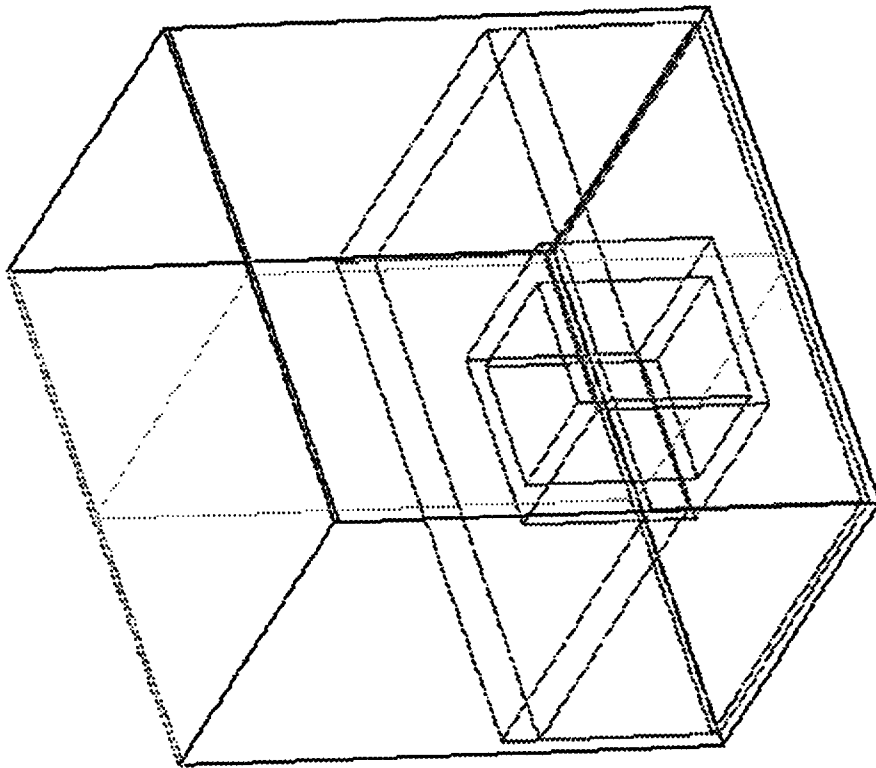
Results of Loss-of-Forced Cooling Evaluations

Calculate Result Parameter	Partial Core Offload Value	Full Core Offload Value
Minimum Time-to-Boil	3.82 hours	1.55 hours
Maximum Boiloff Rate	2.63×10^4 lb/hour	4.36×10^4 lb/hour
Minimum Time for Water to Drop to Top of Racks	42.65 hours	24.93 hours

Table 5.7.3

Results of Maximum Local Water and Fuel Cladding Temperature Evaluations

Parameter	Value
Peak Local Water Temperature	187.5 °F
Peak Cladding Superheat	23 °F
Peak Local Fuel Cladding Temperature	210.5 °F



Grid

Feb 18, 2002
FLUENT 5.5 (3d, segregated, ke)

Figure 5.5.1 Schematic of the CFD Model of the ANO Unit 2 SFP.

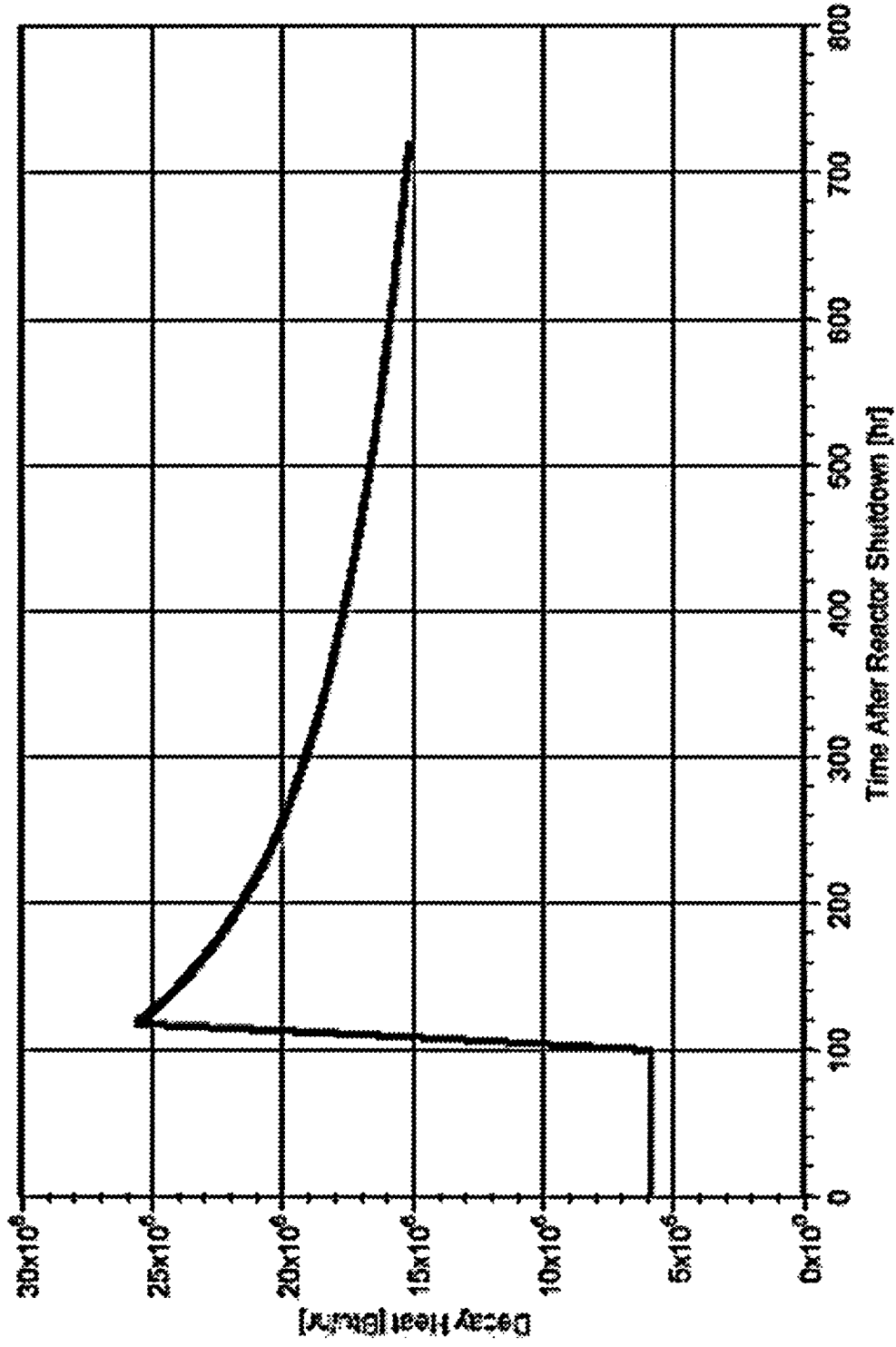


Figure 5.7.1: ANO Unit 2 Pool Decay Heat Plot (Partial Core Discharge)

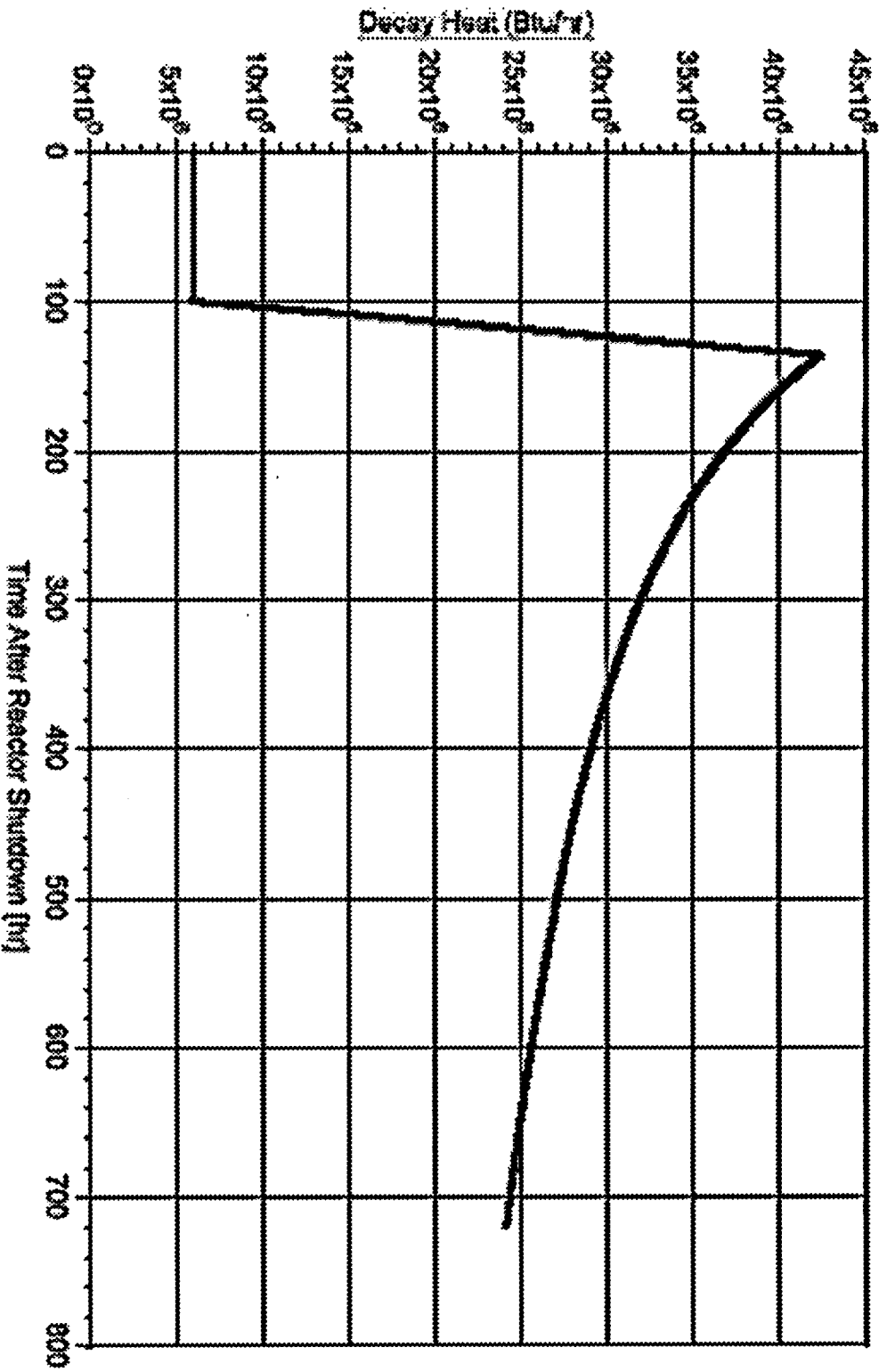
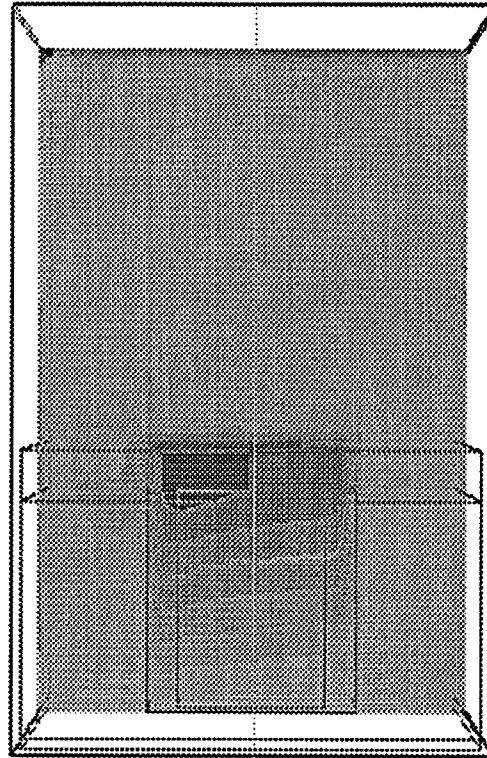
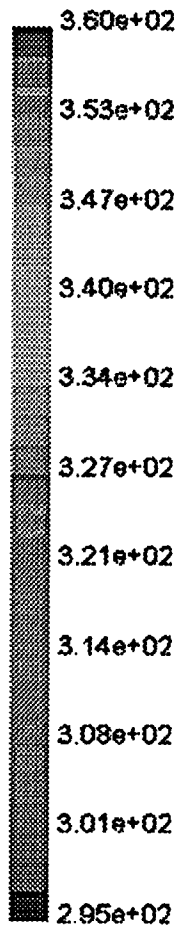


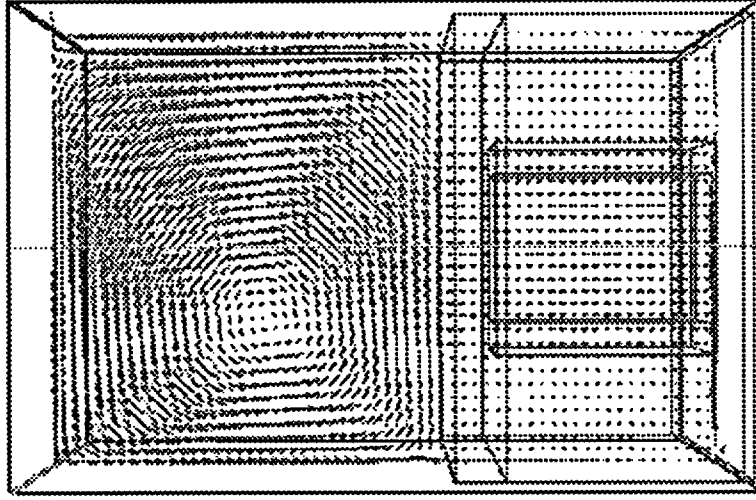
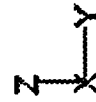
Figure 5.7.2: ANO Unit 2 Decay Heat Curve (Full Core Discharge)



Contours of Static Temperature (k) Sep 20, 2002
FLUENT 5.5 (3d, segregated, ke)

Figure 5.7.3 Contours of Static Temperature In a Vertical Plane Through the Center of the SFP.

5.96e-01
 5.36e-01
 4.77e-01
 4.17e-01
 3.58e-01
 2.98e-01
 2.38e-01
 1.79e-01
 1.19e-01
 5.97e-02
 8.55e-05



Velocity Vectors Colored By Velocity Magnitude (m/s)

Sep 20, 2002
 FLUENT 5.5 (3d, segregated, ke)

Figure 5.7.4: Velocity Vector Plot in a Vertical Plane Through the Center of the SFP.

6.0 STRUCTURAL/SEISMIC CONSIDERATIONS

6.1 INTRODUCTION

This section considers the structural adequacy of the existing spent fuel racks with new poison inserts under all loadings postulated for normal and seismic conditions at ANO-2. The module layout is illustrated in Figure 6.1.1, along with the X and Y coordinate axes used to identify displacement orientation.

The analyses undertaken to confirm the structural integrity of the racks and the poison inserts, are performed in compliance with the OT Position Paper [6.1.2], ANO Specification No. AP&L-C-2502 [6.1.3], and the ANO Unit 2 SAR [6.1.4]. An abstract of the methodology, modeling assumptions, key results, and summary of the parametric evaluation is presented. Delineation of the relevant criteria is discussed in the text associated with each analysis.

6.2 OVERVIEW OF RACK STRUCTURAL ANALYSIS METHODOLOGY

The response of a freestanding rack module to seismic inputs is highly nonlinear and involves a complex combination of motions (sliding, rocking, twisting, and turning), resulting in potential impacts and friction effects. Some of the unique attributes of the rack dynamic behavior include a large fraction of the total structural mass in a confined rattling motion, friction support of rack pedestals against lateral motion, and large fluid coupling effects due to deep submergence and independent motion of closely spaced adjacent structures.

Linear methods, such as modal analysis and response spectrum techniques, cannot accurately simulate the structural response of such a highly nonlinear structure to seismic excitation. An accurate simulation is obtained only by direct integration of the nonlinear equations of motion with the three pool slab acceleration time-histories applied as the forcing functions acting simultaneously.

Whole Pool Multi-Rack (WPMR) analysis is the vehicle utilized in this project to simulate the dynamic behavior of the complex storage rack structures. The following sections provide the basis for this selection and discussion on the development of the methodology.

6.2.1 Background of Analysis Methodology

Reliable assessment of the stress field and kinematic behavior of the rack modules calls for a conservative dynamic model incorporating all key attributes of the actual structure. This means that the model must feature the ability to execute the concurrent motion forms compatible with the freestanding installation of the modules.

The model must possess the capability to effect momentum transfers which occur due to rattling of fuel assemblies inside storage cells and the capability to simulate lift-off and subsequent impact of support pedestals with the pool liner (or bearing pad). The contribution of the water mass in the interstitial spaces around the rack modules and within the storage cells must be modeled in an accurate manner, since erring in quantification of fluid coupling on either side of the actual value is no guarantee of conservatism.

The Coulomb friction coefficient at the pedestal-to-pool liner (or bearing pad) interface may lie in a rather wide range and a conservative value of friction cannot be prescribed without analyzing this effect. In fact, a review of the results of rack dynamic analyses in numerous docket (Table 6.2.1) indicates that an upper bound value of the coefficient of friction often maximizes the computed rack displacements as well as the equivalent elastostatic stresses.

In short, there are a large number of parameters with potential influence on the rack kinematics. The comprehensive structural evaluation must deal with all of these without sacrificing conservatism.

The three-dimensional single rack dynamic model introduced by Holtec International in the Enrico Fermi Unit 2 rack project (ca. 1980) and used in some 50 rerack projects since that time (Table 6.2.1) addresses most of the abovementioned array of parameters. The details of this methodology are also published in the permanent literature [6.2.1]. Despite the versatility of the 3-D seismic model, the accuracy of the single rack simulations has been suspect due to one key element; namely, hydrodynamic participation of water around the racks. During dynamic rack motion, hydraulic energy is either drawn from or added to the moving rack, modifying its submerged motion in a significant manner. Therefore, the dynamics of one rack affects the motion of all others in the pool.

A dynamic simulation, which treats only one rack, or a small grouping of racks, is intrinsically inadequate to predict the motion of rack modules with any quantifiable level of accuracy. Three-dimensional Whole Pool Multi-Rack analyses carried out on several previous plants demonstrate that single rack simulations may under predict rack displacement during seismic responses [6.2.2].

Briefly, the 3-D rack model dynamic simulation, involving one or more spent fuel racks, handles the array of variables as follows:

Interface Coefficient of Friction Parametric runs are made with upper bound and lower bound values of the coefficient of friction. The limiting values are based on experimental data which have been found to be bounded by the values 0.2 and 0.8. Simulations are also performed with the array of pedestals having randomly chosen coefficients of friction in a Gaussian distribution with a mean of 0.5 and lower and upper limits of 0.2 and 0.8, respectively. In the fuel rack simulations, the Coulomb friction interface between rack support pedestal and liner is simulated by piecewise linear (friction) elements. These elements function only when the pedestal is physically in contact with the pool liner or bearing pad.

Rack Beam Behavior Rack elasticity, relative to the rack base, is included in the model by introducing linear springs to represent the elastic bending action, twisting, and extensions.

Impact Phenomena Compression-only gap elements are used to provide for opening and closing of interfaces such as the pedestal-to-bearing pad interface, and the fuel assembly-to-cell wall interface. These interface gaps are modeled using nonlinear spring elements. The term "nonlinear spring" is a generic term used to denote the mathematical representation of the condition where a restoring force is not linearly proportional to displacement.

Fuel Loading Scenarios The fuel assemblies are conservatively assumed to rattle in unison which exaggerates the contribution of impact against the cell wall.

Fluid Coupling Holtec International extended Fritz's classical two-body fluid coupling model to multiple bodies and utilized it to perform the first two-dimensional multi-rack analysis (Diablo Canyon, ca. 1987). Subsequently, laboratory experiments were conducted to validate the multi-

rack fluid coupling theory. This technology was incorporated in the computer code DYNARACK [6.2.4] which handles simultaneous simulation of all racks in the pool as a Whole Pool Multi-Rack 3-D analysis. This development was first utilized in Chinshan, Oyster Creek, and Shearon Harris plants [6.2.1, 6.2.3] and, subsequently, in numerous other rerack projects. The WPMR analyses have corroborated the accuracy of the single rack 3-D solutions in predicting the maximum structural stresses, and also serve to improve predictions of rack kinematics.

For closely spaced racks, demonstration of kinematic compliance is verified by including all modules in one comprehensive simulation using a WPMR model. Additional more conservative single rack analyses are performed to confirm kinematic stability under the most adverse conditions such as fuel loading eccentricities and interim reracking configurations. In WPMR analysis, all rack modules are modeled simultaneously and the coupling effect due to this multi-body motion is included in the analysis. Due to the superiority of this technique in predicting the dynamic behavior of closely spaced submerged storage racks, the Whole Pool Multi-Rack analysis methodology is used for this project.

6.3 DESCRIPTION OF RACKS

The storage racks are analyzed as follows:

RACK WEIGHT DATA

Rack #	Array Size	# of Cells	# of Poison Inserts	Dry Weight of Rack w/o Poison Inserts (lb)	Total Weight of Rack plus Poison Inserts [†] (lb)
1	9 x 9	81	144	15,550	29,950
2	9 x 10	90	0	17,250	17,250
3	9 x 10	90	0	17,250	17,250
4	9 x 9	81	0	18,000	18,000
5	9 x 9	81	144	15,550	29,950
6	9 x 10	90	0	17,250	17,250
7	9 x 10	90	0	17,250	17,250
8	9 x 9	81	0	18,000	18,000
9	8 x 9	72	127	13,850	26,550
10	8 x 10	80	0	15,350	15,350
11	8 x 10	80	0	15,350	15,350
12	8 x 9	72	0	16,600	16,600

[†] Poison inserts are conservatively assumed to weigh 100 lb each. The actual weight of a poison insert plus a lead-in device is approximately 43 lb total.

For the purpose of modeling, the racks are numbered 1 through 12 as shown in Figure 6.1.1.

The Cartesian coordinate system utilized within the rack dynamic model has the following nomenclature:

- x = Horizontal axis along plant South
- y = Horizontal axis along plant East
- z = Vertical axis upward from the rack base

6.4 SYNTHETIC TIME-HISTORIES

The synthetic time-histories in three orthogonal directions (N-S, E-W, and vertical) are generated in accordance with the provisions of SRP [6.1.2], Section 3.7.1. In order to prepare an acceptable set of acceleration time-histories, Holtec International's proprietary code GENEQ [6.4.1] is utilized.

A preferred criterion for the synthetic time-histories in SRP 3.7.1 calls for both the response spectrum and the power spectral density corresponding to the generated acceleration time-history to envelope their target (design basis) counterparts with only finite enveloping infractions. The time-histories for the pools have been generated to satisfy this preferred criterion. The seismic files also satisfy the requirements of statistical independence mandated by SRP 3.7.1.

Figures 6.4.1 through 6.4.3 provide plots of the time-history accelerograms which were generated over a 20 second duration for the DBE event. Figures 6.4.4 through 6.4.6 provide plots of the time-history accelerograms which were generated over a 20 second duration for the OBE event. These artificial time-histories are used in all non-linear dynamic simulations of the racks.

Results of the correlation function of the three time-histories are given in Table 6.4.1. Absolute values of the correlation coefficients are shown to be less than 0.15, indicating that the desired statistical independence of the three data sets has been met.

6.5 WPMR METHODOLOGY

Recognizing that the analytical work effort must deal with both stress and displacement criteria, the sequence of model development and analysis steps that are undertaken are summarized in the following:

- a. Prepare 3-D dynamic models suitable for a time-history analysis of the maximum density racks. These models include the assemblage of all rack modules in each pool. Include all fluid coupling interactions and mechanical coupling appropriate to performing an accurate non-linear simulation. This 3-D simulation is referred to as a Whole Pool Multi-Rack model.

- b. Perform 3-D dynamic analyses on various physical conditions (such as coefficient of friction and extent of cells containing fuel assemblies). Archive appropriate displacement and load outputs from the dynamic model for post-processing.
- c. Perform stress analysis of high stress areas for the limiting case of all the rack dynamic analyses. Demonstrate compliance with ANO Specification No. AP&L-C-2502 [6.1.3] and ANO Unit 2 SAR [6.1.4] limits on stress and displacement.

6.5.1 Model Details for Spent Fuel Racks

The dynamic modeling of the rack structure is prepared with special consideration of all nonlinearities and parametric variations. Particulars of modeling details and assumptions for the Whole Pool Multi-Rack analysis of racks are given in the following:

6.5.1.1 Assumptions

- a. The fuel rack structure motion is captured by modeling the rack as a 12 degree-of-freedom structure. Movement of the rack cross-section at any height is described by six degrees-of-freedom of the rack base and six degrees-of-freedom at the rack top. In this manner, the response of the module, relative to the base-plate, is captured in the dynamic analyses once suitable springs are introduced to couple the rack degrees-of-freedom and simulate rack stiffness.
- b. Rattling fuel assemblies within the rack are modeled by five lumped masses located at H , $.75H$, $.5H$, $.25H$, and at the rack base (H is the rack height measured above the base-plate). Each lumped fuel mass has two horizontal displacement degrees-of-freedom. Vertical motion of the fuel assembly mass is assumed equal to rack vertical motion at the base-plate level. The centroid of each fuel assembly mass can be located off-center, relative to the rack structure centroid at that level, to simulate a partially loaded rack.

- c. **Seismic motion of a fuel rack is characterized by random rattling of fuel assemblies in their individual storage locations. All fuel assemblies are assumed to move in-phase within a rack. This exaggerates computed dynamic loading on the rack structure and, therefore, yields conservative results.**
- d. **Fluid coupling between the rack and fuel assemblies, and between the rack and wall, is simulated by appropriate inertial coupling in the system kinetic energy. Inclusion of these effects uses the methods of [6.5.2, 6.5.3] for rack/assembly coupling and for rack-to-rack coupling.**
- e. **Sloshing is negligible 20 feet below the surface of the pool, where the racks reside, and it is, therefore, neglected in the analysis of the rack.**
- f. **Potential impacts between the cell walls of the racks and the contained fuel assemblies are accounted for by appropriate compression-only gap elements between masses involved. The possible incidence of rack-to-wall or rack-to-rack impact is simulated by gap elements at the top and bottom of the rack in two horizontal directions. Bottom gap elements are located at the base-plate elevation. The initial gaps reflect the presence of baseplate extensions, and the rack stiffnesses are chosen to simulate local structural detail.**
- g. **Pedestals are modeled by gap elements in the vertical direction and as "rigid links" for transferring horizontal stress. Each pedestal support is linked to the pool liner (or bearing pad) by two friction springs. The spring rate for the friction springs includes any lateral elasticity of the stub pedestals. Local pedestal vertical spring stiffness accounts for floor elasticity and for local rack elasticity just above the pedestal.**
- h. **Rattling of fuel assemblies inside the storage locations causes the gap between fuel assemblies and cell wall to change from a maximum of twice the nominal gap to a theoretical zero gap. Fluid coupling coefficients are based on the nominal gap in order to provide a conservative measure of fluid resistance to gap closure.**

- i. The model for the rack is considered supported, at the base level, on four pedestals modeled as non-linear compression only gap spring elements and eight piecewise linear friction spring elements. These elements are properly located with respect to the centerline of the rack beam, and allow for arbitrary rocking and sliding motions. In reality each rack has 14 pedestals. This assumption increases the load transmitted to a single pedestal, thereby resulting in higher pedestal stresses.

- j. The mass of the poison inserts, which is conservatively assumed as 100 lb per insert, is lumped with the mass of the rack. Although the model does not allow the poison inserts to move inside the flux traps, the potential impact force between the poison inserts and the flux trap walls has a negligible effect on the dynamic behavior of the rack. Moreover, the potential impacts involving the poison inserts are bounded by the conservative accounting of the poison insert weight.

6.5.1.2 Element Details

Figure 6.5.1 shows a schematic of the dynamic model of a single rack. The schematic depicts many of the characteristics of the model including all of the degrees-of-freedom and some of the spring restraint elements.

Table 6.5.1 provides a complete listing of each of the 22 degrees-of-freedom for a rack model. Six translational and six rotational degrees-of-freedom (three of each type on each end) describe the motion of the rack structure. Rattling fuel mass motions (shown at nodes 1°, 2°, 3°, 4°, and 5° in Figure 6.5.1) are described by ten horizontal translational degrees-of-freedom (two at each of the five fuel masses). The vertical fuel mass motion is assumed (and modeled) to be the same as that of the rack baseplate.

Figure 6.5.2 depicts the fuel to rack impact springs (used to develop potential impact loads between the fuel assembly mass and rack cell inner walls) in a schematic isometric. Only one of the five fuel masses is shown in this figure. Four compression only springs, acting in the horizontal direction, are provided at each fuel mass.

Figure 6.5.3 provides a 2-D schematic elevation of the storage rack model, discussed in more detail in Section 6.5.3. This view shows the vertical location of the five storage masses and some of the support pedestal spring members.

Figure 6.5.4 shows the modeling technique and degrees-of-freedom associated with rack elasticity. In each bending plane a shear and bending spring simulate elastic effects [6.5.4]. Linear elastic springs coupling rack vertical and torsional degrees-of-freedom are also included in the model.

Figure 6.5.5 depicts the inter-rack impact springs (used to develop potential impact loads between racks or between rack and wall).

6.5.2 Fluid Coupling Effect

In its simplest form, the so-called "fluid coupling effect" [6.5.2, 6.5.3] can be explained by considering the proximate motion of two bodies under water. If one body (mass m_1) vibrates adjacent to a second body (mass m_2), and both bodies are submerged in frictionless fluid, then Newton's equations of motion for the two bodies are:

$$\begin{aligned}(m_1 + M_{11}) A_1 + M_{12} A_2 &= \text{applied forces on mass } m_1 + O(X_1^2) \\ M_{21} A_1 + (m_2 + M_{22}) A_2 &= \text{applied forces on mass } m_2 + O(X_2^2)\end{aligned}$$

A_1 and A_2 denote absolute accelerations of masses m_1 and m_2 , respectively, and the notation $O(X^2)$ denotes nonlinear terms.

M_{11} , M_{12} , M_{21} , and M_{22} are fluid coupling coefficients which depend on body shape, relative disposition, etc. Fritz [6.5.3] gives data for M_{ij} for various body shapes and arrangements. The fluid adds mass to the body (M_{11} to mass m_1), and an inertial force proportional to acceleration of the adjacent body (mass m_2). Thus, acceleration of one body affects the force field on another. This force field is a function of inter-body gap, reaching large values for small gaps. Lateral motion of a fuel assembly inside a storage location encounters this effect. For example, fluid coupling behavior will be experienced between nodes 2 and 2* in Figure 6.5.1. The rack analysis also contains inertial fluid coupling terms, which model the effect of fluid in the gaps between adjacent racks.

Terms modeling the effects of fluid flowing between adjacent racks in a single rack analysis suffer from the inaccuracies described earlier. These terms are usually computed assuming that all racks adjacent to the rack being analyzed are vibrating in-phase or 180° out of phase. The WPMR analyses do not require any assumptions with regard to phase.

Rack-to-rack gap elements have initial gaps set to 100% of the physical gap between the racks or between outermost racks and the adjacent pool walls.

6.5.2.1 Multi-Body Fluid Coupling Phenomena

During the seismic event, all racks in the pool are subject to the input excitation simultaneously. The motion of each freestanding module would be autonomous and independent of others as long as they did not impact each other and no water were present in the pool. While the scenario of inter-rack impact is not a common occurrence and depends on rack spacing, the effect of water (the so-called fluid coupling effect) is a universal factor. As noted in Ref. [6.5.2, 6.5.4], the fluid forces can reach rather large values in closely spaced rack geometries. It is, therefore, essential that the contribution of the fluid forces be included in a comprehensive manner. This is possible only if all racks in the pool are allowed to execute 3-D motion in the mathematical model. For this reason, single rack or even multi-rack models involving only a portion of the racks in the pool, are inherently inaccurate. The Whole Pool Multi-Rack model removes this intrinsic limitation of the rack dynamic models by simulating the 3-D motion of all modules simultaneously. The fluid coupling effect, therefore, encompasses interaction between every set of racks in the pool, i.e., the motion of one rack produces fluid forces on all other racks and on the pool walls. Stated more formally, both near-field and far-field fluid coupling effects are included in the analysis.

The derivation of the fluid coupling matrix [6.5.5] relies on the classical inviscid fluid mechanics principles, namely the principle of continuity and Kelvin's recirculation theorem. While the derivation of the fluid coupling matrix is based on no artificial construct, it has been nevertheless verified by an extensive set of shake table experiments [6.5.5].

6.5.3 Stiffness Element Details

Three element types are used in the rack models. Type 1 elements are linear elastic elements used to represent the beam-like behavior of the integrated rack cell matrix. Type 2 elements are the piece-wise linear friction springs used to develop the appropriate forces between the rack pedestals and the supporting bearing pads. Type 3 elements are non-linear gap elements, which model gap closures and subsequent impact loadings i.e., between fuel assemblies and the storage cell inner walls, and rack outer periphery spaces.

If the simulation model is restricted to two dimensions (one horizontal motion plus one vertical motion, for example), for the purposes of model clarification only, then Figure 6.5.3 describes the configuration. This simpler model is used to elaborate on the various stiffness modeling elements.

Type 3 gap elements modeling impacts between fuel assemblies and racks have local stiffness K_i in Figure 6.5.3. Support pedestal spring rates K_s are modeled by type 3 gap elements. Local compliance of the concrete floor is included in K_s . The type 2 friction elements are shown in Figure 6.5.3 as K_f . The spring elements depicted in Figure 6.5.4 represent type 1 elements.

Friction at support/liner interface is modeled by the piecewise linear friction springs with suitably large stiffness K_f up to the limiting lateral load μN , where N is the current compression load at the interface between support and liner. At every time-step during transient analysis, the current value of N (either zero if the pedestal has lifted off the liner, or a compressive finite value) is computed.

The gap element K_s , modeling the effective compression stiffness of the structure in the vicinity of the support, includes stiffness of the pedestal, local stiffness of the underlying pool slab, and local stiffness of the rack cellular structure above the pedestal.

The previous discussion is limited to a 2-D model solely for simplicity. Actual analyses incorporate 3-D motions.

6.5.4 Coefficients of Friction

To eliminate the last significant element of uncertainty in rack dynamic analyses, multiple simulations are performed to adjust the friction coefficient ascribed to the support pedestal/pool bearing pad interface. These friction coefficients are chosen consistent with the two bounding extremes from Rabinowicz's data [6.5.1]. Simulations are also performed by imposing friction coefficients developed by a random number generator with Gaussian normal distribution characteristics. The assigned values are then held constant during the entire simulation in order to obtain reproducible results.[†] Thus, in this manner, the WPMR analysis results are brought closer to the realistic structural conditions.

The coefficient of friction (μ) between the pedestal supports and the pool floor is indeterminate. According to Rabinowicz [6.5.1], results of 199 tests performed on austenitic stainless steel plates submerged in water show a mean value of μ to be 0.503 with standard deviation of 0.125. Upper and lower bounds (based on twice standard deviation) are 0.753 and 0.253, respectively. Analyses are therefore performed for coefficient of friction values of 0.2 (lower limit) and 0.8 (upper limit), as well as for random friction values clustered about a mean of 0.5. The bounding values of $\mu = 0.2$ and 0.8 have been found to envelope the upper limit of module response in previous rerack projects.

6.5.5 Governing Equations of Motion

Using the structural model discussed in the foregoing, equations of motion corresponding to each degree-of-freedom are obtained using Lagrange's Formulation [6.5.4]. The system kinetic energy includes contributions from solid structures and from trapped and surrounding fluid. The final system of equations obtained has the matrix form:

$$[M] \left[\frac{d^2 q}{dt^2} \right] = [Q] + [G]$$

[†] It is noted that DYNARACK has the capability to change the coefficient of friction at any pedestal at each instant of contact based on a random reading of the computer clock cycle. However, exercising this option would yield results that could not be reproduced. Therefore, the random choice of coefficients is made only once per run.

where:

[M] = total mass matrix (including structural and fluid mass contributions). The size of this matrix will be $22n \times 22n$ for a WPMR analysis (n = number of racks in the model).

q = the nodal displacement vector relative to the pool slab displacement (the term with q indicates the second derivative with respect to time, i.e., acceleration)

[G] = a vector dependent on the given ground acceleration

[Q] = a vector dependent on the spring forces (linear and nonlinear) and the coupling between degrees-of-freedom

The above column vectors have length $22n$. The equations can be rewritten as follows:

$$\left[\frac{d^2 q}{dt^2} \right] = [M]^{-1} [Q] + [M]^{-1} [G]$$

This equation set is mass uncoupled, displacement coupled at each instant in time. The numerical solution uses a central difference scheme built into the proprietary computer program DYNARACK [6.2.4].

6.6 STRUCTURAL EVALUATION OF SPENT FUEL RACK DESIGN

6.6.1 Kinematic and Stress Acceptance Criteria

There are two sets of criteria to be satisfied by the rack modules:

a. Kinematic Criteria

According to Section 3.8.5 of Ref. [6.1.1], the minimum required safety margins against overturning under the OBE and DBE events are 1.5 and 1.1, respectively.

The maximum rotations of the rack (about the two principal axes) are obtained from a post processing of the rack time history response output. The margin of safety against overturning is given by the ratio of the rotation required to produce incipient tipping in either principal plane to the actual maximum rotation in that plane predicted by the time history solution.

$$\text{Margin of Safety} = \frac{\theta \text{ required for overturning}}{\theta \text{ predicted}}$$

All ratios for the OBE and DBE events should be greater than 1.5 and 1.1, respectively, to satisfy the regulatory acceptance criteria. However, to be conservative, the OBE safety factor of 1.5 is applied to the worst case displacements from DBE. This is conservative, since the displacement for the DBE simulations exceed those for the OBE simulation.

b. Stress Limit Criteria

Stress limits must not be exceeded under the postulated load combinations provided herein.

6.6.2 Stress Limit Evaluations

The stress limits presented below apply to the rack structure and are derived from the ASME Code, Section III, Article XVII [6.6.1]. Parameters and terminology are in accordance with the ASME Code. Material properties are obtained from the ASME Code Appendices [6.6.2], and are listed in Table 6.3.1. The yield and ultimate strengths are taken at 150°F, which is based on the maximum normal operating allowable temperature for ANO Spent Fuel Pools. Therefore, 150 °F is an appropriate temperature for the determination of material properties.

(i) Normal & Upset Conditions (Levels A & B)

- a. Allowable stress in tension on a net section is:

$$F_t = 0.6 S_y$$

where S_y = yield stress at temperature and F_t is equivalent to primary membrane stress.

- b. Allowable stress in shear on a net section is:

$$F_v = .4 S_y$$

- c. Allowable stress in compression on a net section is:

$$F_a = S_y \left(.47 - \frac{kl}{444 r} \right)$$

where kl/r for the main rack body is based on the full height and cross section of the honeycomb region and does not exceed 120 for all sections.

l = unsupported length of component

k = length coefficient which gives influence of boundary conditions. The following values are appropriate for the described end conditions:

1 (simple support both ends)

2 (cantilever beam)

½ (clamped at both ends)

$r =$ radius of gyration of component

- d. Maximum allowable bending stress at the outermost fiber of a net section, due to flexure about one plane of symmetry is:

$$F_b = 0.60 S_y \quad (\text{equivalent to primary bending})$$

- e. Combined bending and compression on a net section satisfies:

$$\frac{f_a}{F_a} + \frac{C_{mx} f_{bx}}{D_x F_{bx}} + \frac{C_{my} f_{by}}{D_y F_{by}} < 1$$

where:

f_a = Direct compressive stress in the section

f_{bx} = Maximum bending stress along x-axis

f_{by} = Maximum bending stress along y-axis

C_{mx} = 0.85

C_{my} = 0.85

D_x = $1 - (f_a/F'_{ex})$

D_y = $1 - (f_a/F'_{ey})$

$F'_{ex,ey}$ = $(\pi^2 E)/(2.15 (kl/r)_{x,y}^2)$

E = Young's Modulus

and subscripts x,y reflect the particular bending plane.

- f. Combined flexure and compression (or tension) on a net section:

$$\frac{f_a}{0.6 S_y} + \frac{f_{bx}}{F_{bx}} + \frac{f_{by}}{F_{by}} < 1.0$$

The above requirements are to be met for both direct tension and compression.

- g. Welds

Allowable maximum shear stress on the net section of a weld is given by:

$$F_w = 0.3 S_u$$

where S_u is the weld material ultimate strength at temperature. For fillet weld legs in contact with base metal, the shear stress on the gross section is limited to $0.4S_y$, where S_y is the base material yield strength at temperature.

(ii) Faulted Conditions (Level D)

Per ANO Specification No. AP&L-C-2502 [6.1.3], the stress limits for DBE conditions are the stress limits for Levels A and B, as defined above, multiplied by 1.5.

Exceptions to the above general multiplier are the following:

- a) Stresses in shear shall not exceed $0.5S_y$.
- b) The maximum allowable stress in bending and tension is $0.9S_y$.
- c) For this licensing application, AISC N-690 is conservatively used for welds and the limit on weld shear stress is set as:

$$\text{Weld Allowable} = (0.3 \times S_u) \times 1.4$$

6.6.3 Dimensionless Stress Factors

For convenience, the stress results are in dimensionless form. Dimensionless stress factors are defined as the ratio of the actual developed stress to the specified limiting stress value. Based on the stress limits of ASME Code Article XVII for Level A and Level D conditions, the limiting value of each stress factor is 1.0. For this evaluation, however, the stress limits defined in ANO Specification No. AP&L-C-2502 [6.1.3] for Level D conditions are more restrictive than the ASME Code. As a result, the limiting values for the stress factors are less than 1.0 under DBE conditions. The following table provides the list of dimensionless stress factors along with the limiting values for OBE and DBE.

Dimensionless Stress Factors	Limiting Value	
	OBE	DBE
R_1 = Ratio of direct tensile or compressive stress on a net section to its allowable value (note pedestals only resist compression)	1.0	0.75
R_2 = Ratio of gross shear on a net section in the x-direction to its allowable value	1.0	0.694
R_3 = Ratio of maximum bending stress due to bending about the x-axis to its allowable value for the section	1.0	0.75
R_4 = Ratio of maximum bending stress due to bending about the y-axis to its allowable value for the section	1.0	0.75
R_5 = Combined flexure and compression factor (as defined in Section 3.4.1.5 above)	1.0	0.75
R_6 = Combined flexure and tension (or compression) factor (as defined in Section 3.4.1.6 above)	1.0	0.75
R_7 = Ratio of gross shear on a net section in the y-direction to its allowable value	1.0	0.694

6.6.4 Loads and Loading Combinations for Spent Fuel Racks

The applicable loads and their combinations, which are considered in the seismic analysis of rack modules, are excerpted from the OT Position Paper [6.1.2], ANO Specification No. AP&L-C-2502 [6.1.3], the Unit 2 SAR, and Section 3.8.4 of the USNRC Standard Review Plan (SRP) [6.1.1]. The SRP load combinations are not required to be met by ANO. However, for thoroughness the load equations outlined in SRP 3.8.4 are used. The load combinations considered are identified below:

Loading Combination	Service Level [†]	Section Reference
D + L D + L + T _o D + L + T _o + E	Level A	6.11 6.11, 6.13.2 6.8, 6.9, 6.13.2
D + L + T _a + E D + L + T _o + P _f	Level B	6.13.2 6.14
D + L + T _a + E' D + L + T _o + F _d	Level D The functional capability of the fuel racks must be demonstrated.	6.8, 6.9 7.0

[†] The allowable stress limits for Service Levels A, B, and D are given in Section 6.6.2.

Where:

- D = Dead weight-induced loads
- L = Live Load (including stored fuel assemblies, poison inserts, and miscellaneous equipment loads)
- P_f = Upward force on the racks caused by postulated stuck fuel assembly
- F_d = Impact force from accidental drop of the heaviest load from the maximum possible height.
- E = Operating Basis Earthquake (OBE)
- E' = Safe Shutdown Earthquake (DBE)
- T_o = Differential temperature induced loads (normal operating or shutdown condition based on the most critical transient or steady state condition)

T_a = Differential temperature induced loads (the highest temperature associated with the postulated abnormal design conditions) T_a and T_o produce local thermal stresses. The worst thermal stress field in a fuel rack is obtained when an isolated storage location has a fuel assembly generating heat at maximum postulated rate and surrounding storage locations contain no fuel. Heated water makes unobstructed contact with the inside of the storage walls, thereby producing maximum possible temperature difference between adjacent cells. Secondary stresses produced are limited to the body of the rack; that is, support pedestals do not experience secondary (thermal) stresses.

6.7 PARAMETRIC SIMULATIONS

The multiple rack models employ the fluid coupling effects for all racks in the pool, as discussed above, and these simulations are referred to as WPMR evaluations. In addition, single rack models are also developed for additional study of the effect of various parameters on rack displacement. The models are described as follows:

(I) Whole Pool Multi Rack Model

An array of twelve racks is modeled with proper interface fluid gaps and a coefficient of friction at the support interface locations with the bearing pad generated by a Gaussian distribution random number generator with 0.5 as the mean and 0.15 standard deviation. The response to both DBE and OBE seismic excitation is determined.

(II) Single Rack Model

A single rack model is employed to study the effect of top loading the rack with miscellaneous equipment, which represents a future storage possibility. Rack number 9 is chosen for this simulation because it is both the smallest and lightest rack in the pool, which makes it most susceptible to overturning. The top loaded rack simulation (Case 7) is performed using the 0.8 coefficient of friction and the DBE event since this combination generally produces the largest rack top displacements. A fictitious 2,000 lbf mass, with three translational degrees of freedom, is rigidly attached to the rack 24" above the top of

the cell structure. The displacements calculated from the single rack run are used as a further check for kinematic stability.

The Whole Pool and Single Rack simulations listed in the following table have been performed to investigate the structural integrity of the rack array, including the new poison inserts.

LIST OF WPMR AND SINGLE RACK SIMULATIONS				
<u>Case</u>	<u>Model</u>	<u>Load Case</u>	<u>COF</u>	<u>Event</u>
1	WPMR	All racks fully loaded	Random	OBE
2	WPMR	All racks fully loaded	0.2	OBE
3	WPMR	All racks fully loaded	0.8	OBE
4	WPMR	All racks fully loaded	Random	DBE
5	WPMR	All racks fully loaded	0.2	DBE
6	WPMR	All racks fully loaded	0.8	DBE
7	Single	Fully loaded rack w/ 2,000 lb load overhead	0.8	DBE

where Random = Gaussian distribution with a mean coeff. of friction of 0.5.

(upper and lower limits of 0.8 and 0.2, respectively)

COF = Coefficient of Friction

6.8 TIME HISTORY SIMULATION RESULTS

The results from the DYNARACK runs may be seen in the raw data output files. However, due to the huge quantity of output data, a post-processor is used to scan for worst case conditions and develop the stress factors discussed in subsection 6.6.3. Further reduction in this bulk of information is provided in this section by extracting the worst case values from the parameters of interest; namely displacements, support pedestal forces, impact loads, and stress factors. This section also summarizes additional analyses performed to develop and evaluate structural member stresses which are not determined by the post processor.

6.8.1 Rack Displacements

The maximum rack displacements are obtained from the time histories of the motion of the upper and lower four corners of each rack in each of the simulations. The maximum absolute value of displacement in the two horizontal directions, relative to the pool slab, is determined by the post-processor for each rack, at the top and bottom corners. The maximum displacements in either direction reported from the WPMR analyses is 0.749" at the top of Rack 4 during the DBE events and 0.650" at the top of Rack 12 during the OBE events. The maximum displacement in either direction reported from the single rack analysis is 0.361", which was performed for Rack 9. It is obvious from these small displacements at the top of the racks that the safety factors for tipping are met.

6.8.2 Pedestal Vertical Forces

The maximum vertical pedestal force obtained in the WPMR simulations was 150,000 lbf for Rack 6 under DBE conditions. The maximum vertical pedestal force obtained in the OBE simulation was 159,000 lbf for Rack 3.

6.8.3 Pedestal Friction Forces

The maximum interface shear force value in any direction bounding all pedestals in the WPMR simulations is 51,800 lbf for Rack 11 in Case 6.

6.8.4 Rack Impact Loads

A freestanding rack, by definition, is a structure subject to potential impacts during a seismic event. Impacts arise from rattling of the fuel assemblies in the storage rack locations and, in some instances, from localized impacts between the racks, or between a peripheral rack and the pool wall. The following sections discuss the bounding values of these impact loads.

6.8.4.1 Rack to Rack Impacts

Gap elements track the potential for impacts between adjacent racks. The results for each simulation have been scanned for non-zero impact forces. The simulation results show that no

gap element between any two racks closes. Thus, there are no rack-to-rack impacts.

6.8.4.2 Rack to Wall Impacts

The storage racks do not impact the pool walls under any simulation.

6.8.4.3 Fuel to Cell Wall Impact Loads

A review of all simulations performed allows determination of the maximum instantaneous impact load between fuel assembly and fuel cell wall at any modeled impact site. The maximum fuel/cell wall impact loads are 922 lbf in Rack 4 in the DBE case of the WPMR analyses and 865 lbf for the OBE case in Rack 8. The cell wall integrity under this instantaneous impact load has been evaluated and shown to remain intact with no permanent damage.

The permissible lateral load on an irradiated spent fuel assembly has been studied by the Lawrence Livermore National Laboratory. The LLNL report [6.8.1] states that "...for the most vulnerable fuel assembly, axial buckling varies from 82g's at initial storage to 95g's after 20 years' storage. In a side drop, no yielding is expected below 63g's at initial storage to 74g's after 20 years' [dry] storage". The most significant load on the fuel assembly arises from rattling during the seismic event. For the five lumped mass model, the limiting lateral load, therefore, is equal to F_e , where

$$F_e = (w \times a)/4$$

where:

w = weight of one fuel assembly (upper bound value = 1700 lbs)

a = permissible lateral acceleration in g's (a = 63)

Therefore, $F_e = 26,775$ lbs

The maximum fuel-to-storage cell rattling force from the WPMR runs is 922 lbs. Therefore, the nominal factor of safety against fuel failure is roughly equal to 29.

6.9 RACK STRUCTURAL EVALUATION

6.9.1 Rack Stress Factors

The time history results from the DYNARACK solver provide the pedestal normal and lateral interface forces, which may be converted to the limiting bending moment and shear force at the bottom baseplate-pedestal interface. In particular, maximum values for the previously defined stress factors are determined for every pedestal in the array of racks. With this information available, the structural integrity of the pedestal can be assessed and reported. The net section maximum (in time) bending moments and shear forces can also be determined at the bottom baseplate-rack cellular structure interface for each spent fuel rack in the pool. Using these forces and moments, the maximum stress in the limiting rack cell (box) can be evaluated.

The stress factor results for male and female pedestals, and for the entire spent fuel rack cellular cross section just above the baseplate have been determined. These factors are reported for every rack in each simulation, and for each pedestal in every rack. These locations are the most heavily loaded net sections in the structure so that satisfaction of the stress factor criteria at these locations ensures that the overall structural criteria set forth in Section 6.6 are met.

The maximum pedestal stress factor for OBE is 0.330, which occurs in Rack 3 during Case 1, and for DBE is 0.171, which occurs in Rack 7 during Case 6. The maximum cell wall stress factor is computed to be 0.428 for OBE in Rack 3 during Case 1 and 0.203 for DBE in Rack 6 during Case 4. An evaluation of the stress factors, for all of the simulations performed, leads to the conclusion that all stress factors are less than the limits specified in Section 6.6.3. Therefore, the requirements of Section 6.6.2 are indeed satisfied for the load levels considered for every limiting location in the rack.

6.9.2 Pedestal Thread Shear Stress

From the WPMR simulations, the maximum thread engagement stresses under seismic conditions for every pedestal for every rack in the pool are 9,490 psi under DBE conditions and 10,059 psi under OBE conditions. The yield stress for the pedestal material is 27,500 psi. The allowable shear stress for Level B conditions is 0.4 times the yield stress, which gives 11,000 psi. Since 10,059 psi (occurs during OBE run) is less than the OBE allowable of 11,000 psi, the male pedestal threads are shown to be acceptable. The maximum shear stress in the pedestal threads under DBE conditions is 9,490 psi, which is less than $0.5S_y$ (or 13,750 psi).

6.9.3 Local Stresses Due to Impacts

Impact loads at the pedestal base (discussed in subsection 6.8.4.1) produce stresses in the pedestal for which explicit stress limits are prescribed in the Code. However, impact loads on the cellular region of the racks, as discussed in subsection 6.8.4.3 above, produce stresses which attenuate rapidly away from the loaded region. This behavior is characteristic of secondary stresses.

Even though limits on secondary stresses are not prescribed in the Code for class 3 NF structures, evaluations are made to ensure that the localized impacts do not lead to plastic deformations in the storage cells which affect the sub-criticality of the stored fuel array.

a. Impact Loading Between Fuel Assembly and Cell Wall

Local cell wall integrity is conservatively estimated from peak impact loads. Plastic analysis is used to obtain the limiting impact load which would lead to gross permanent deformation. The limiting impact load of 3,438 lbf (including a safety factor of 2.0) is much greater than the highest calculated impact load value of 922 lbf (see subsection 6.8.4.3) obtained from any of the rack analyses. Therefore, fuel impacts do not represent a significant concern with respect to fuel rack cell deformation.

b. Impacts Between Adjacent Racks

As may be seen from subsection 6.8.4.1, no impacts are predicted between adjacent racks.

6.9.4 Weld Stresses

Weld locations subjected to significant seismic loading are at the bottom of the rack at the baseplate-to-cell connection, at the top of the pedestal support at the baseplate connection, and at cell-to-cell connections. Bounding values of resultant loads are used to qualify the connections.

a. Baseplate-to-Rack Cell Welds

For Level A or B conditions, Ref. [6.6.1] permits an allowable weld stress of $\tau = .3 S_u = 21900$ psi. As stated in subsection 6.6.2, the allowable may be increased for Level D by an amplification factor which is equal to 1.4. The allowable stress increase factor of 1.4 greatly exceeds the ratio of maximum DBE to OBE stresses. Therefore, Level B becomes the governing condition.

Weld dimensionless stress factors are produced through the use of a simple conversion (ratio) factor applied to the corresponding stress factor in the adjacent rack material. The ratio 0.956 is developed from the differences in material thickness and length versus weld throat dimension and length:

$$\begin{aligned} \text{RATIO} &= (\text{Cell wall thickness} * \text{Avg. Cell Wall Length}) / (\text{Effective Weld Size} * \text{Weld Length}) \\ &= (0.075 * 8.655) / (0.12 * 0.7071 * 8.0) \end{aligned}$$

The highest predicted cell to baseplate weld stress is calculated based on the highest R6 value for the rack cell region tension stress factor and R2 and R7 values for the rack cell region shear stress factors. Refer to subsection 6.6.3 for definition of these factors. These cell wall stress factors may be converted into weld stress values as follows:

$$[R6 * (0.6) + R2 * (0.4) + R7 * (0.4)] * S_y * \text{Ratio} =$$
$$[0.428 * (0.6) + 0.032 * (0.4) + 0.031 * (0.4)] * (27,500) * 0.956 = 7,414 \text{ psi}$$

This calculation is conservative for the following reasons:

- 1) The directional stresses associated with the normal stress σ_y and the two shear stresses τ_x and τ_y should be combined using SRSS instead of direct summation.
- 2) The maximum stress factors used above do not all occur at the same time instant, in the same storage rack, or during the same simulation.

The OBE condition governs since it has a higher calculated stress and a lower allowable stress limit. The maximum weld stress is less than the OBE allowable for base metal shear stress, which is 11,000 psi. Therefore, the welds are acceptable, with a safety factor of $(11,000/7,414) = 1.48$.

b. Baseplate-to-Pedestal Welds

The weld between baseplate and support pedestal is checked using finite element analysis to determine that the maximum weld stresses. The maximum weld stresses under OBE and DBE conditions are 17,020 psi and 16,960 psi, respectively. Both of these calculated stress values are below the OBE weld allowable of 21,900 psi. Therefore, these welds have been determined to be acceptable.

The maximum shear stresses in the base metal adjacent to the weld are 1,151 psi and 1,176 psi, respectively, under OBE and DBE conditions. Both of these calculated stress values are well below the OBE base metal allowable of 11,000 psi.

c. Cell-to-Cell Welds

Cell-to-cell connections are by a series of connecting welds along the cell height. Stresses in storage cell to cell welds develop due to fuel assembly impacts with the cell wall. These weld stresses are conservatively calculated by assuming that fuel assemblies in adjacent cells are moving out of phase with one another so that impact loads in two adjacent cells are in opposite directions; this tends to separate the two cells from each other at the weld.

Table 6.9.1 gives the computed results for the maximum allowable load that can be transferred by these welds based on the available weld area. The upper bound on the applied load transferred is also given in Table 6.9.1. This upper bound value is very conservatively obtained by applying the bounding rack-to-fuel impact load from any simulation in two orthogonal directions simultaneously, and multiplying the result by 2 to account for the simultaneous impact of two assemblies in adjacent cells moving in opposing directions. An equilibrium analysis at the connection then yields the upper bound load to be transferred. As shown in Table 6.9.1, the calculated shear stress in the base metal adjacent to the weld is 10,920 psi under OBE conditions and 11,660 psi under DBE conditions. These values are less than the allowable OBE and DBE stress limits of 11,000 psi and 13,750 psi, respectively.

6.10 POISON INSERT STRUCTURAL EVALUATION

A structural evaluation will be performed to demonstrate that the stresses in the poison insert, under normal and accident conditions, meet the appropriate stress limits from ANO Specification No. AP&L-C-2502 [6.1.3] and the ANO Unit 2 SAR [6.1.4]. The design details of the poison insert are provided in Section 2.5. The minimum calculated safety factor for the poison insert for all loading conditions will be greater than 1.0.

6.11 LEVEL A EVALUATION

The stress allowables are the same for Level A and Level B conditions. The Upset (OBE) condition controls over normal (Gravity) condition. Therefore, no further evaluation is required for these load cases.

6.12 HYDRODYNAMIC LOADS ON POOL WALLS

The hydrodynamic pressures that develop between adjacent racks and the pool walls can be computed from the archived results produced by the WPMR analysis. Of the racks next to the SFP walls, the one that resulted in the maximum displacement generates the maximum hydrodynamic load on its adjacent wall. The maximum hydrodynamic pressure is considered as individual load in the structural qualification of the spent fuel pool. The pressure plots on the four walls of the SFP at the time of maximum (in absolute value) instantaneous hydrodynamic pressure for the DBE event are shown in Figure 6.11.1.

6.13 LOCAL STRESS CONSIDERATIONS

This section presents the results of evaluations for the possibility of cell wall buckling and the secondary stresses produced by temperature effects.

6.13.1 Cell Wall Buckling

The allowable local buckling stresses in the fuel cell walls are obtained by using classical plate buckling analysis. The evaluation for cell wall buckling is based on the applied stress being uniform along the entire length of the cell wall. In the actual fuel rack, the compressive stress comes from consideration of overall bending of the rack structures during a seismic event, and as such is negligible at the rack top, and maximum at the rack bottom.

The critical buckling stress is determined to be 7,458 psi. The average compressive stress in the cell wall, based on the R6 stress factor, is 7,062 psi. Therefore, there is a 5.6% margin of safety against local cell wall buckling.

6.13.2 Thermal Loads

The rack is freestanding; thus, there is minimal or no restraint against free thermal expansion of the rack. The high thermal conductivity of the stainless steel material, the buoyancy driven flow of the SFP water, and the thin sheet metal construction tend to diminish the thermal gradients in the spent fuel racks. Thermal loads applied to the rack are, therefore, not included in the stress combinations.

6.14 EVALUATION OF POSTULATED STUCK FUEL ASSEMBLY

The ability of the spent fuel racks to withstand the uplift forces due to a postulated stuck fuel assembly is also evaluated. Strength of materials formulas are used to determine the effects of a 5,000 lb force, which bounds the fuel handling crane's cut-off limit, applied at various locations on the storage cell. For a load applied vertically anywhere along a cell wall, the tensile stress is 7,770 psi, which is below the yield stress of the material. When the load is applied at a 45 degree angle to the top of a cell wall, the damaged region extends downward, from the top of the rack, no more than 2.14 inches, which is well short of the poison insert.

6.15 CONCLUSION

Seven discrete freestanding dynamic simulations of maximum density spent fuel storage racks have been performed to establish the structural margins of safety. Of the seven parametric analyses, six simulations consisted of modeling all 12 fuel racks in the pool in one comprehensive Whole Pool Multi Rack (WPMR) model. The remaining run was carried out with the classical single rack 3-D model. The parameters varied in the different runs consisted of the rack/pool liner interface coefficient of friction and the type of seismic input (DBE or OBE). Maximum (maximum in time and space) values of pedestal vertical, shear forces, displacements and stress factors have been post-processed from the array of runs and summarized in tables in this chapter. The results show that:

- (i) All stresses are well below the specified allowable limits.
- (ii) There is no rack-to-rack or rack-to-wall impact anywhere in the cellular region of the rack modules

- (iii) The factor of safety against overturning of a rack is in excess of 60.

An evaluation of the thermal (secondary) stress produced by the condition of maximum thermal gradient (obtained when a maximum heat emitting fuel assembly is stored in a cell surrounded by empty storage locations wherein no heat is generated) was performed. The thermal stresses, for which no statutory limit in the code (Section III, Article XVII, Class 3 Structures) exists, are found to be limited to 11,020 psi, which is below the allowable limit of 13,750 psi.

In conclusion, all evaluations of structural safety, mandated by the OT Position Paper [6.1.2] and the contemporary fuel rack structural analysis practice have been carried out. They demonstrate consistently large margins of safety in all storage modules.

6.16 REFERENCES

- [6.1.1] USNRC NUREG-0800, Standard Review Plan, June 1987.
- [6.1.2] (USNRC Office of Technology) "OT Position for Review and Acceptance of Spent Fuel Storage and Handling Applications", dated April 14, 1978, and January 18, 1979 amendment thereto.
- [6.1.3] Technical Specification for Earthquake Resistance Design of Structures and / or Components Located in the Auxiliary Building for the Arkansas Nuclear One Unit 2 Power Plant, Arkansas Power and Light Company, Little Rock, Arkansas, Specification Number AP&L-C-2502, revision 2.
- [6.1.4] Arkansas Nuclear One Unit 2 Safety Analysis Report (SAR).
- [6.2.1] Soler, A.I. and Singh, K.P., "Seismic Responses of Free Standing Fuel Rack Constructions to 3-D Motions", Nuclear Engineering and Design, Vol. 80, pp. 315-329 (1984).
- [6.2.2] Soler, A.I. and Singh, K.P., "Some Results from Simultaneous Seismic Simulations of All Racks in a Fuel Pool", INNM Spent Fuel Management Seminar X, January, 1993.
- [6.2.3] Singh, K.P. and Soler, A.I., "Seismic Qualification of Free Standing Nuclear Fuel Storage Racks - the Chin Shan Experience, Nuclear Engineering International, UK (March 1991).
- [6.2.4] Holtec Proprietary Report HI-961465 - WPMR Analysis User Manual for Pre&Post Processors & Solver, August, 1997.
- [6.4.1] Holtec Proprietary Report HI-89364 - Verification and User's Manual for Computer Code GENEQ, January, 1990.

- [6.5.1] Rabinowicz, E., "Friction Coefficients of Water Lubricated Stainless Steels for a Spent Fuel Rack Facility," MIT, a report for Boston Edison Company, 1976.
- [6.5.2] Singh, K.P. and Soler, A.I., "Dynamic Coupling in a Closely Spaced Two-Body System Vibrating in Liquid Medium: The Case of Fuel Racks," 3rd International Conference on Nuclear Power Safety, Keswick, England, May 1982.
- [6.5.3] Fritz, R.J., "The Effects of Liquids on the Dynamic Motions of Immersed Solids," Journal of Engineering for Industry, Trans. of the ASME, February 1972, pp 167-172.
- [6.5.4] Levy, S. and Wilkinson, J.P.D., "The Component Element Method in Dynamics with Application to Earthquake and Vehicle Engineering," McGraw Hill, 1976.
- [6.5.5] Paul, B., "Fluid Coupling in Fuel Racks: Correlation of Theory and Experiment", (Proprietary), NUSCO/Holtec Report HI-88243.
- [6.6.1] ASME Boiler & Pressure Vessel Code, Section III, Article XVII, 1980 Edition with Winter 1981 Addenda.
- [6.6.2] ASME Boiler & Pressure Vessel Code, Section III, Appendix I, Table I-3, 1980 Edition with Winter 1981 Addenda.
- [6.6.3] Kopp, L., "Guidance on the Regulatory Requirements for Criticality Analysis of Fuel Storage at Light Water Reactor Power Plants," USNRC Internal Memorandum, 1998.
- [6.8.1] Chun, R., Witte, M. and Schwartz, M., "Dynamic Impact Effects on Spent Fuel Assemblies," UCID-21246, Lawrence Livermore National Laboratory, October 1987.

- [6.9.1] ACI 349-85, Code Requirements for Nuclear Safety Related Concrete Structures, American Concrete Institute, Detroit, Michigan, 1985.**
- [6.9.2] ACI 318-95, Building Code requirements for Structural Concrete," American Concrete Institute, Detroit, Michigan, 1995.**
- [6.9.3] Holtec report HI-89330, Rev. 1, "Seismic Analysis of High Density Fuel Racks; Part III: Structural Design Calculations - Theory."**
- [6.10.1] ASME Boiler & Pressure Vessel Code, Section III, Subsection NF, 1998 Edition.**

Table 6.2.1

Partial Listing of Fuel Rack Applications Using Dynarack

PLANT	DOCKET NUMBER(s)	YEAR
Enrico Fermi Unit 2	USNRC 50-341	1980
Quad Cities 1 & 2	USNRC 50-254, 50-265	1981
Rancho Seco	USNRC 50-312	1982
Grand Gulf Unit 1	USNRC 50-416	1984
Oyster Creek	USNRC 50-219	1984
Pilgrim	USNRC 50-293	1985
V.C. Summer	USNRC 50-395	1984
Diablo Canyon Units 1 & 2	USNRC 50-275, 50-323	1986
Byron Units 1 & 2	USNRC 50-454, 50-455	1987
Braidwood Units 1 & 2	USNRC 50-456, 50-457	1987
Vogtle Unit 2	USNRC 50-425	1988
St. Lucie Unit 1	USNRC 50-335	1987
Millstone Point Unit 1	USNRC 50-245	1989
Chinshan	Taiwan Power	1988
D.C. Cook Units 1 & 2	USNRC 50-315, 50-316	1992
Indian Point Unit 2	USNRC 50-247	1990
Three Mile Island Unit 1	USNRC 50-289	1991
James A. FitzPatrick	USNRC 50-333	1990
Shearon Harris Unit 2	USNRC 50-401	1991
Hope Creek	USNRC 50-354	1990
Kuosheng Units 1 & 2	Taiwan Power Company	1990
Ulchin Unit 2	Korea Electric Power Co.	1990
Laguna Verde Units 1 & 2	Comision Federal de Electricidad	1991

Table 6.2.1**Partial Listing of Fuel Rack Applications Using Dynarack**

PLANT	DOCKET NUMBER(s)	YEAR
Zion Station Units 1 & 2	USNRC 50-295, 50-304	1992
Sequoyah	USNRC 50-327, 50-328	1992
LaSalle Unit 1	USNRC 50-373	1992
Duane Arnold Energy Center	USNRC 50-331	1992
Fort Calhoun	USNRC 50-285	1992
Nine Mile Point Unit 1	USNRC 50-220	1993
Beaver Valley Unit 1	USNRC 50-334	1992
Salem Units 1 & 2	USNRC 50-272, 50-311	1993
Limerick	USNRC 50-352, 50-353	1994
Ulchin Unit 1	KINS	1995
Yonggwang Units 1 & 2	KINS	1996
Kori-4	KINS	1996
Connecticut Yankee	USNRC 50-213	1996
Angra Unit 1	Brazil	1996
Sizewell B	United Kingdom	1996
Waterford 3	USNRC 50-382	1997
J.A. Fitzpatrick	USNRC 50-333	1998
Callaway	USNRC 50-483	1998
Nine Mile Unit 1	USNRC 50-220	1998
Chin Shan	Taiwan Power Company	1998
Vermont Yankee	USNRC 50-271	1998
Millstone 3	USNRC 50-423	1998
Byron/Braidwood	USNRC 50-454, 50-455, 50-567, 50-457	1999

Table 6.2.1**Partial Listing of Fuel Rack Applications Using Dynarack**

PLANT	DOCKET NUMBER(s)	YEAR
Wolf Creek	USNRC 50-482	1999
Plant Hatch Units 1 & 2	USNRC 50-321, 50-366	1999
Harris Pools C and D	USNRC 50-401	1999
Davis-Besse	USNRC 50-346	1999
Enrico Fermi Unit 2	USNRC 50-341	2000
Kewaunee	USNRC 50-305	2001

Table 6.3.1 Rack Material Data (150°F) (ASME - Section III, Appendix I, Table I-3)			
Stainless Steel Material	Young's Modulus E (psi)	Yield Strength S_y (psi)	Ultimate Strength S_u (psi)
SA240, Type 304 (cell boxes)	27.9 x 10 ⁶	27,500	73,000
Support Material Data (150°F)			
SA240, Type 304 (upper part of support feet)	27.9 x 10 ⁶	27,500	73,000
SA479, Type 304 (lower part of support feet)	27.9 x 10 ⁶	27,500	73,000

Table 6.4.1	
Time-History Statistical Correlation Results	
OBE	
Data1 to Data2	0.051
Data1 to Data3	0.005
Data2 to Data3	0.050
DBE	
Data1 to Data2	0.026
Data1 to Data3	0.006
Data2 to Data3	0.084

Data1 corresponds to the time-history acceleration values along the X axis (South)

Data2 corresponds to the time-history acceleration values along the Y axis (East)

Data3 corresponds to the time-history acceleration values along the Z axis (Vertical)

Table 6.5.1
Degrees-of-Freedom

<u>LOCATION (Node)</u>	<u>DISPLACEMENT</u>			<u>ROTATION</u>		
	U_x	U_y	U_z	θ_x	θ_y	θ_z
1	p_1	p_2	p_3	q_4	q_5	q_6
2	p_7	p_8	p_9	q_{10}	q_{11}	q_{12}
<p>Node 1 is assumed to be attached to the rack at the bottom most point. Node 2 is assumed to be attached to the rack at the top most point. Refer to Figure 6.5.1 for node identification.</p>						
2*	p_{13}	p_{14}				
3*	p_{15}	p_{16}				
4*	p_{17}	p_{18}				
5*	p_{19}	p_{20}				
1*	p_{21}	p_{22}				
<p>where the relative displacement variables p_i are defined as:</p> <p>$p_i = q_i(t) + U_x(t) \quad i = 1,7,13,15,17,19,21$ $= q_i(t) + U_y(t) \quad i = 2,8,14,16,18,20,22$ $= q_i(t) + U_z(t) \quad i = 3,9$ $= q_i(t) \quad i = 4,5,6,10,11,12$</p> <p>$p_i$ denotes absolute displacement with respect to inertial space q_i denotes relative rotation with respect to the floor slab $U(t)$ are the three known earthquake displacements</p> <p>* denotes fuel mass nodes</p>						

Table 6.9.1		
Comparison of Bounding Calculated Stresses vs. Code Allowables at Impact Locations and at Welds		
	OBE[†]	
Item/Location	Calculated	Allowable
Rack/baseplate weld, psi	7,414	11,000
Female pedestal/baseplate weld, psi	17,020	21,900
Cell/cell welds, psi ^{††}	10,920	11,000

[†] OBE controls over DBE.

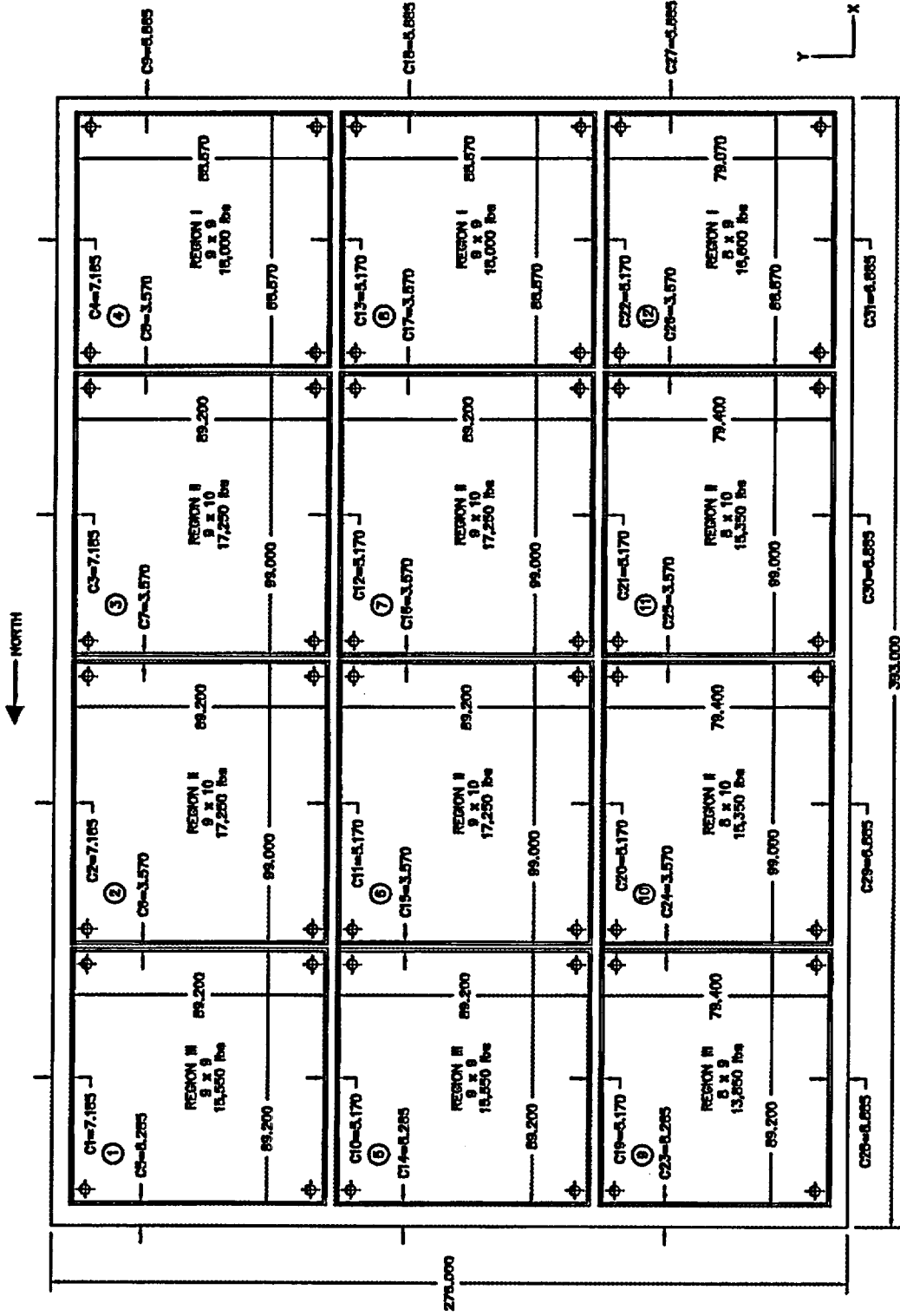


Figure 6.1.1 - ANO Unit 2 Spent Fuel Pool Layout

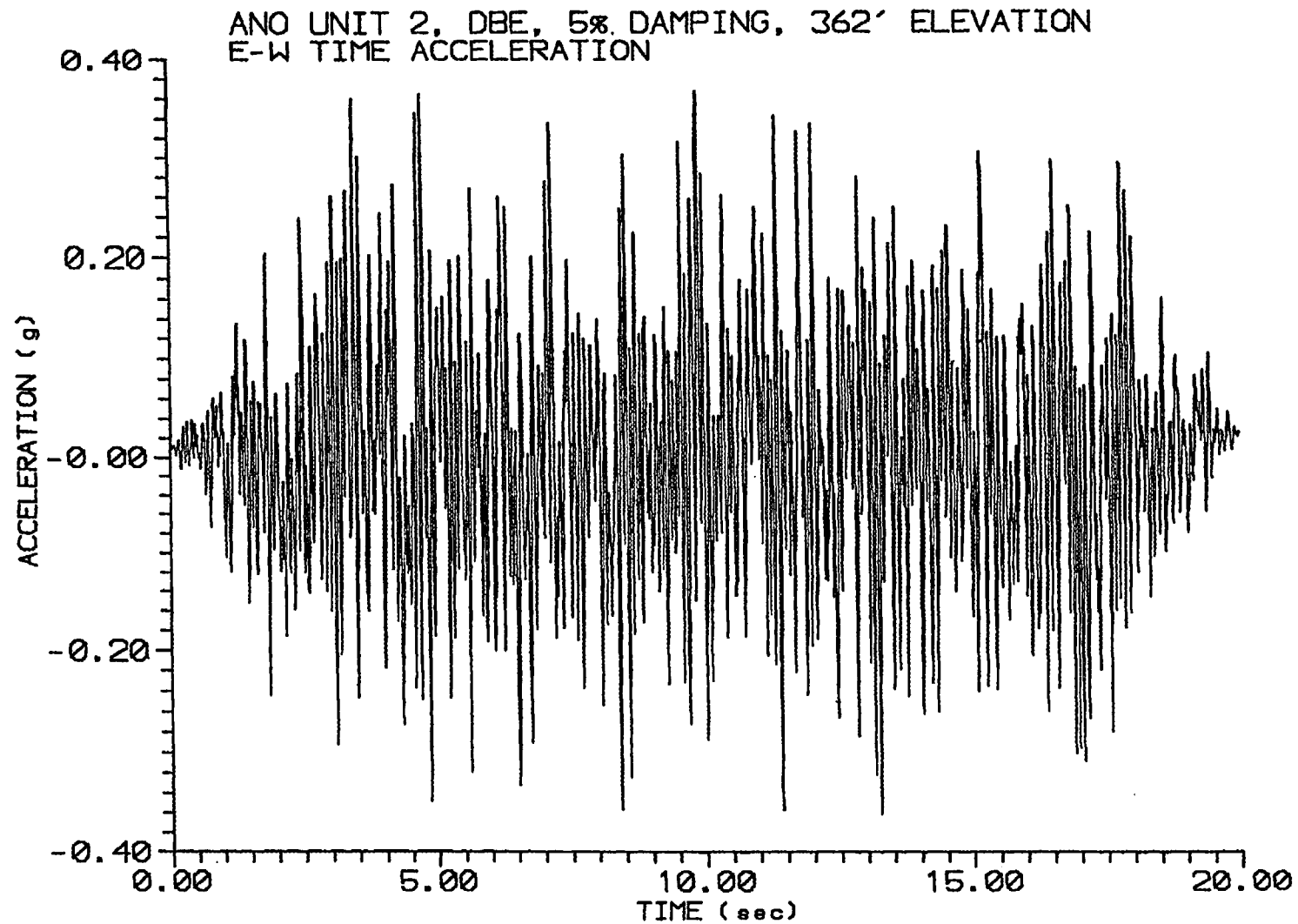


Figure 6.4.1

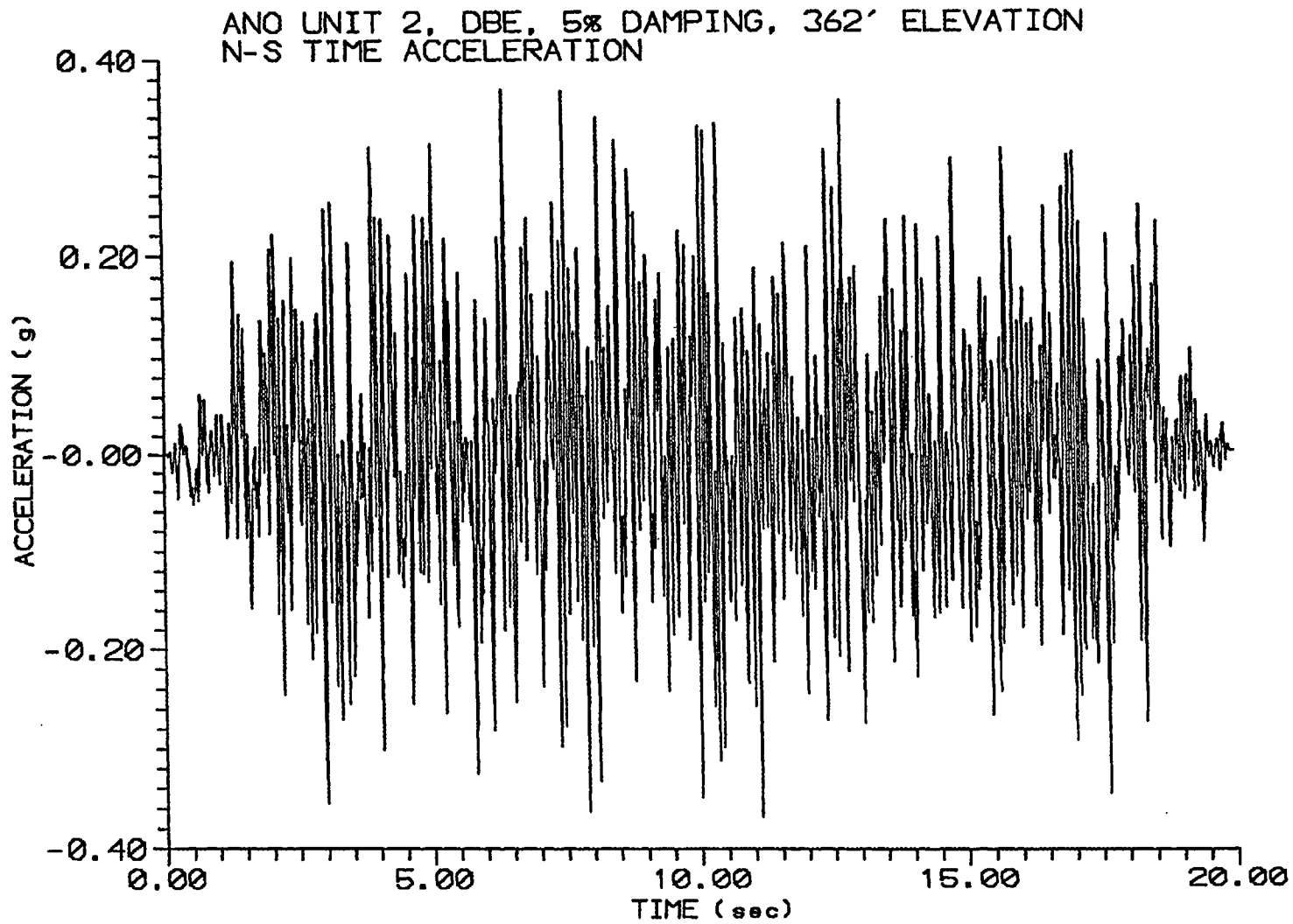


Figure 6.4.2

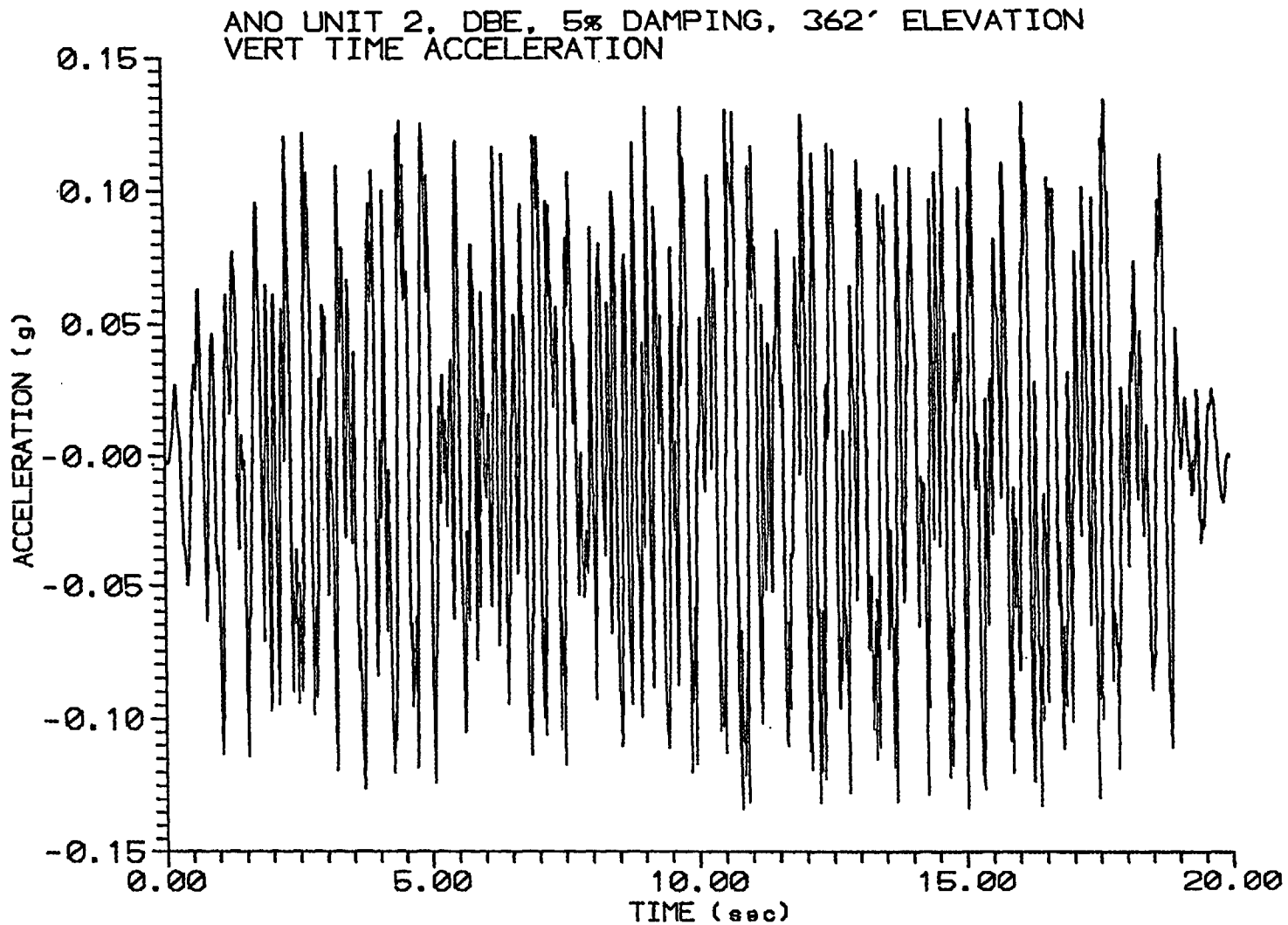


Figure 6.4.3

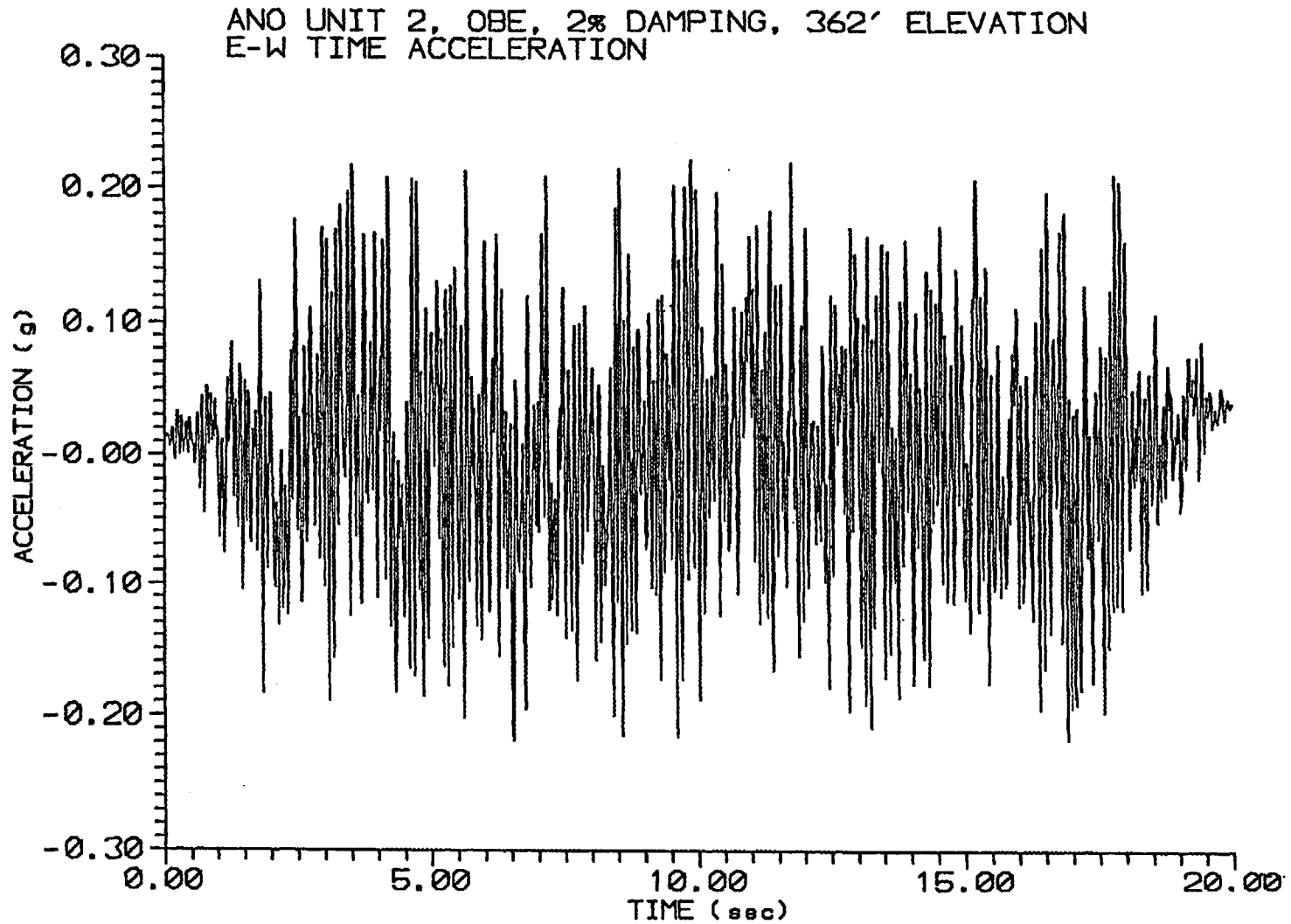


Figure 6.4.4

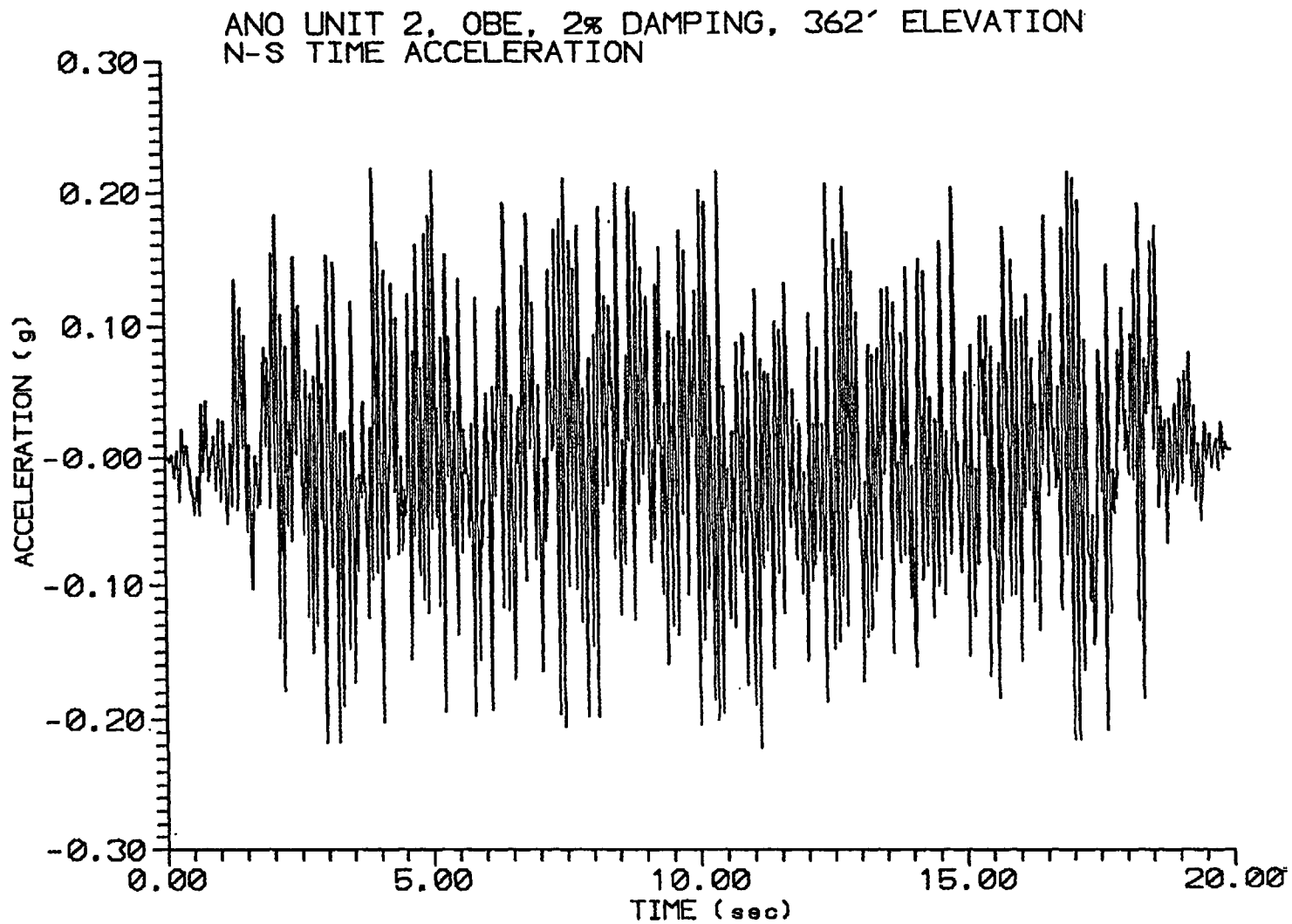


Figure 6.4.5

ANO UNIT 2, OBE, 2% DAMPING, 362' ELEVATION
VERT TIME ACCELERATION

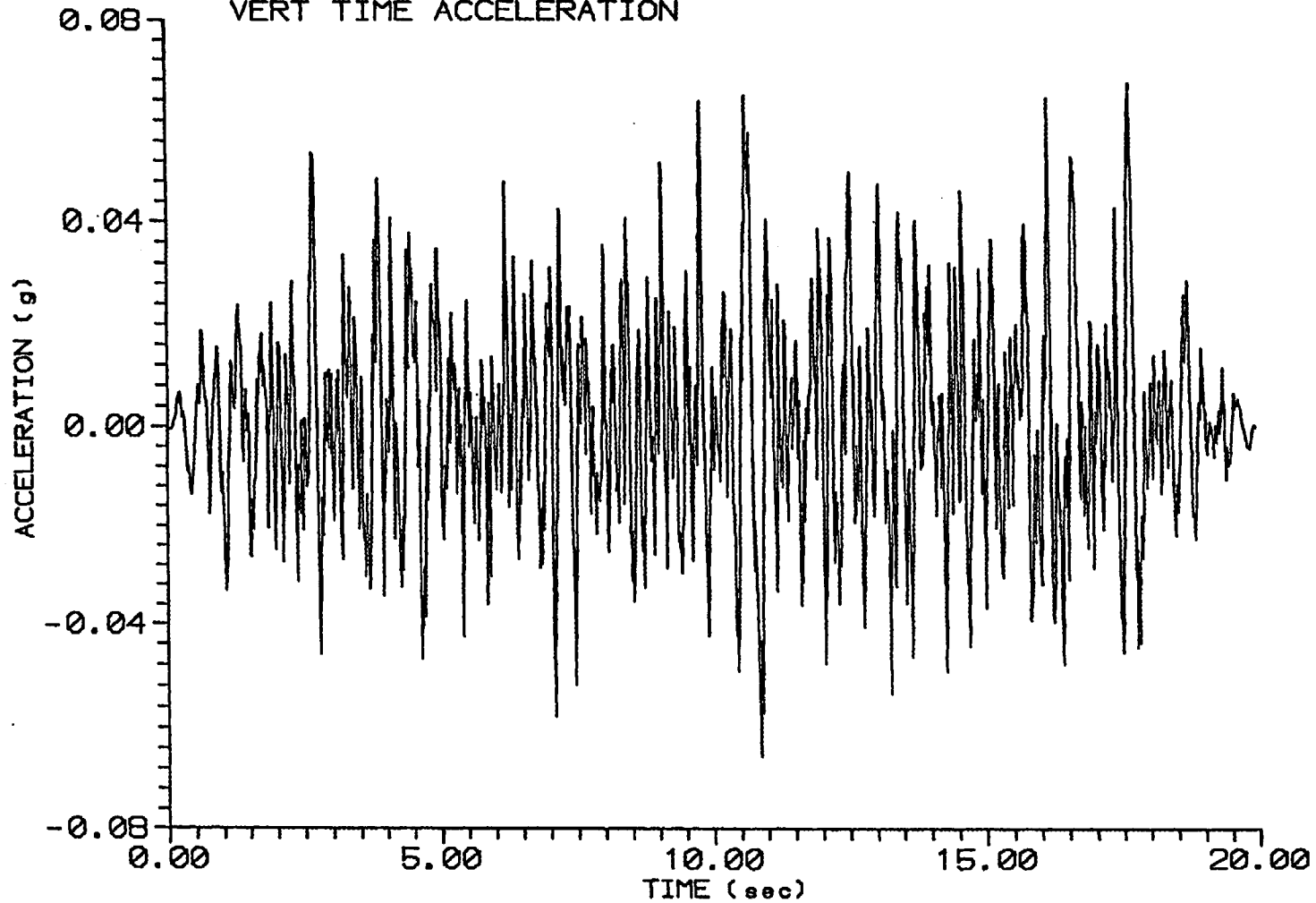


Figure 6.4.6

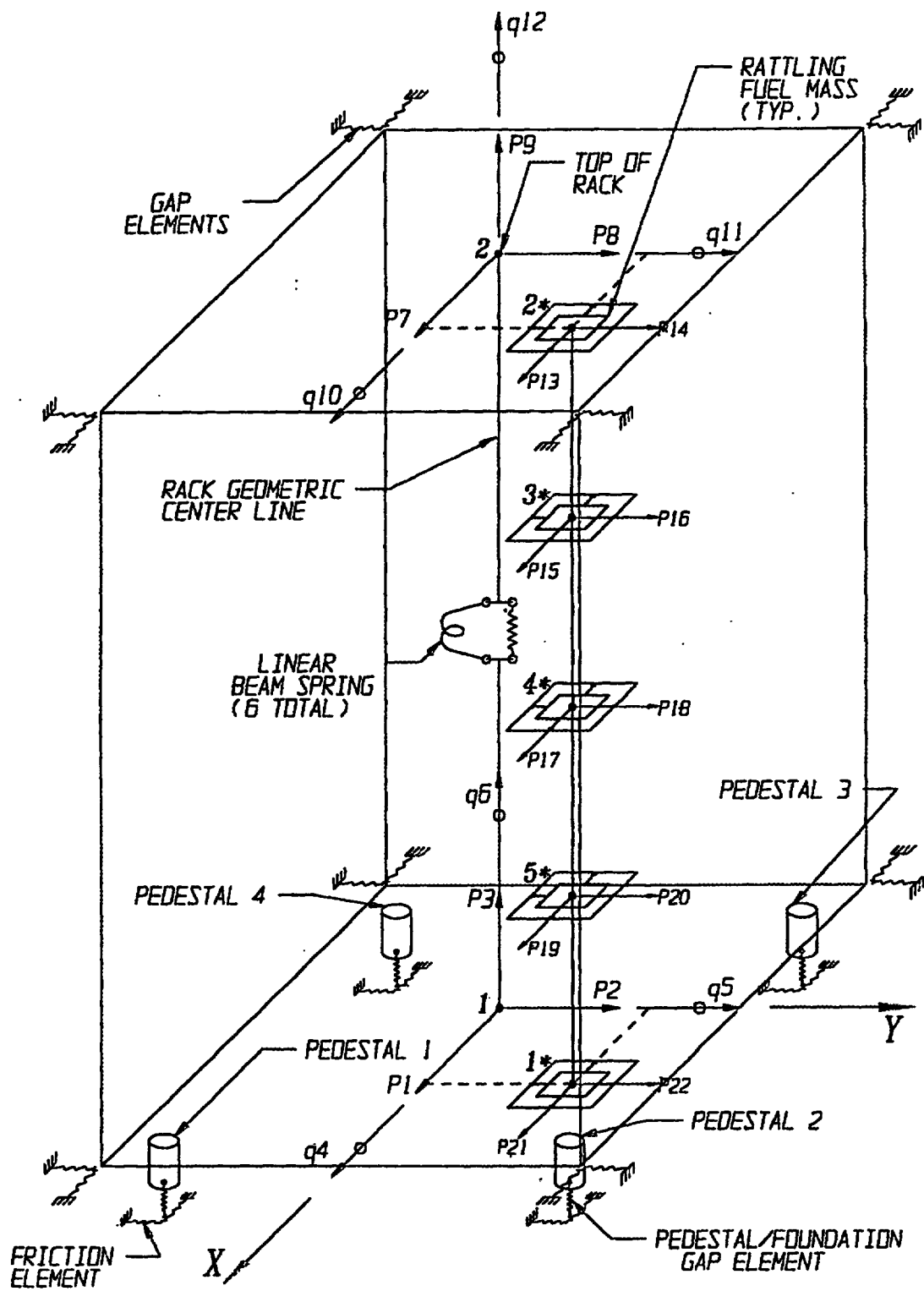


Figure 6.5.1 – Schematic of Single Rack Dynamic Model Used in Dynarack

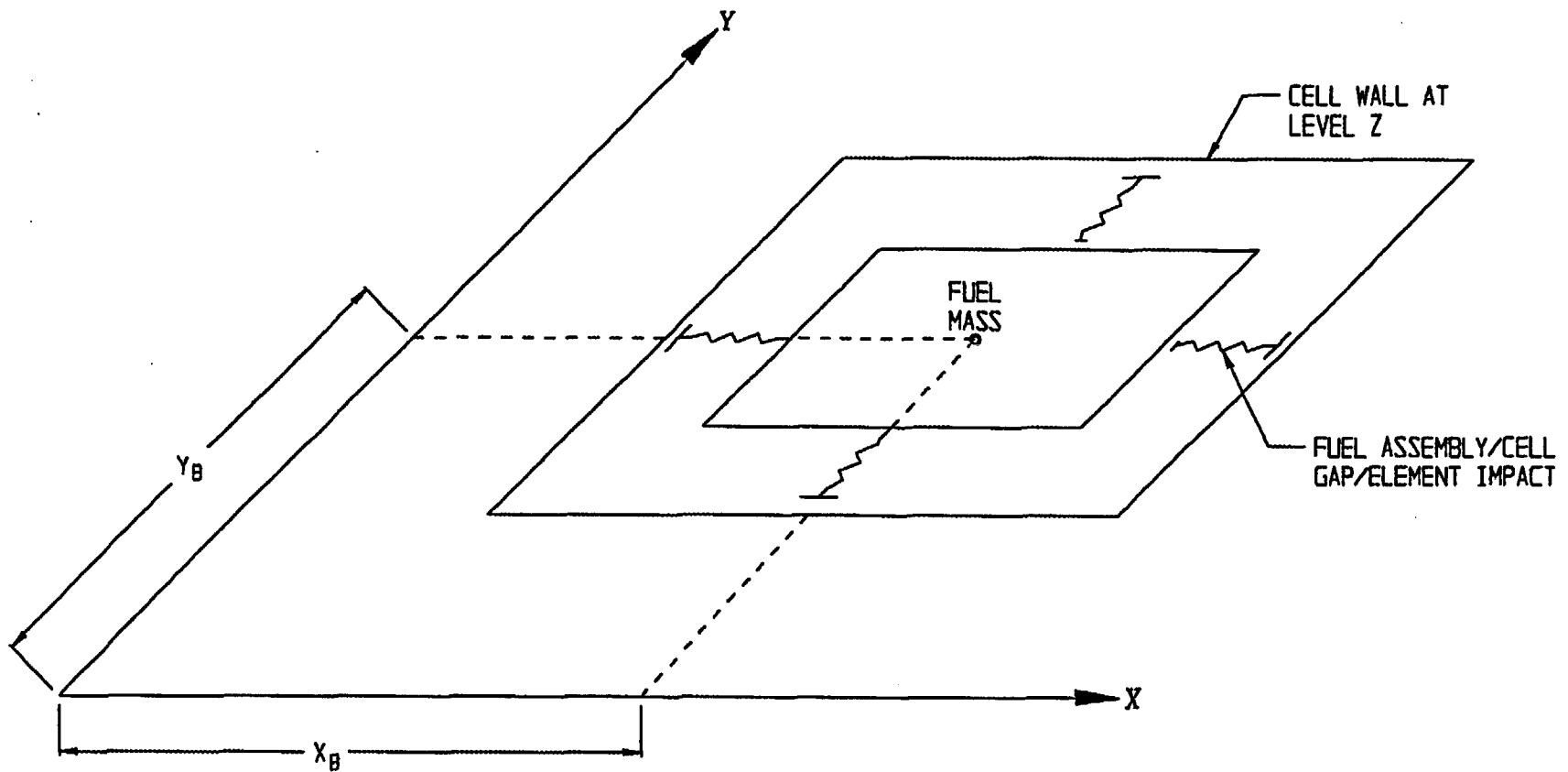


Figure 6.5.2 – Fuel-to-Rack Gap/Impact Elements at Level of Rattling Mass

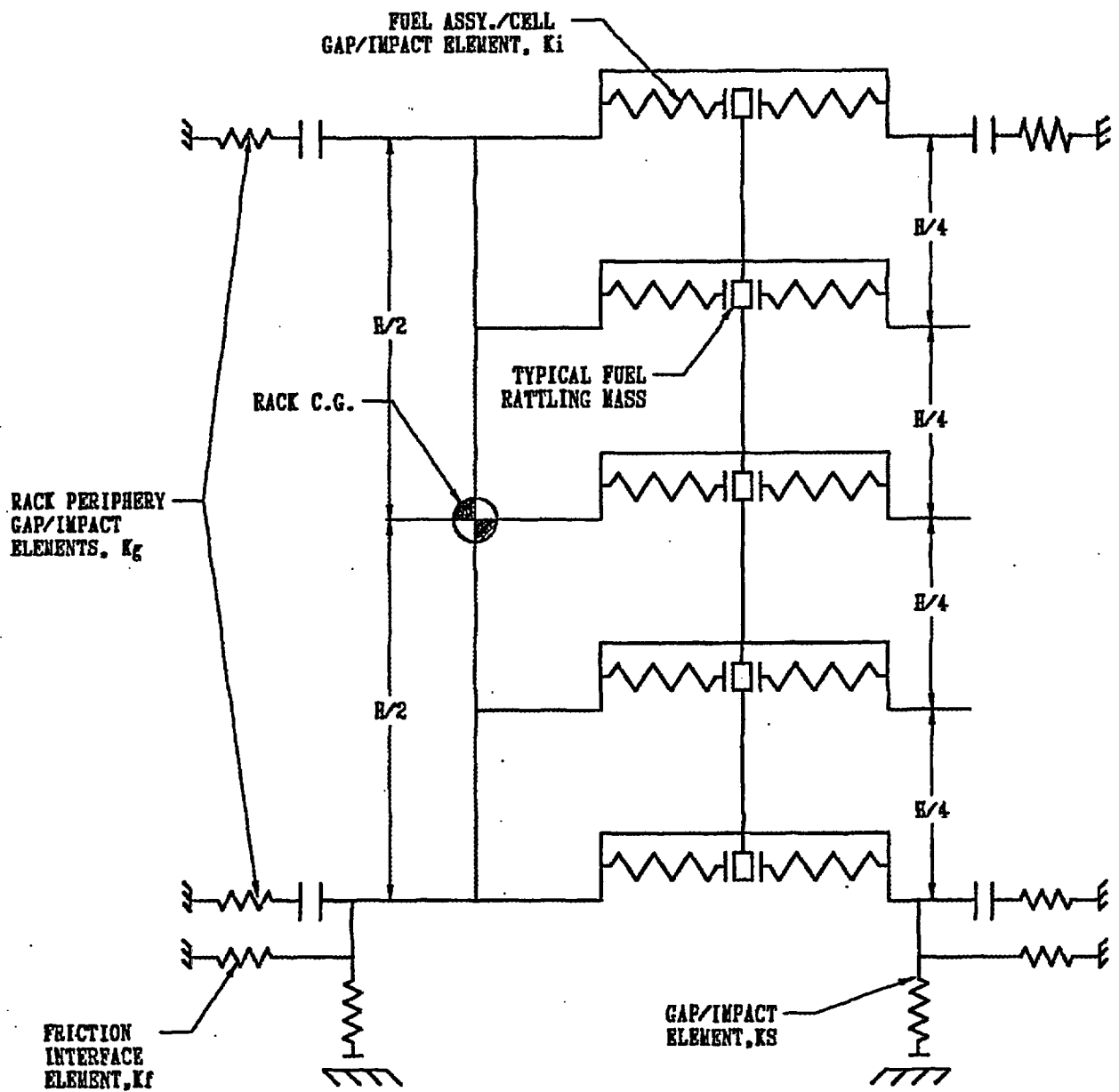
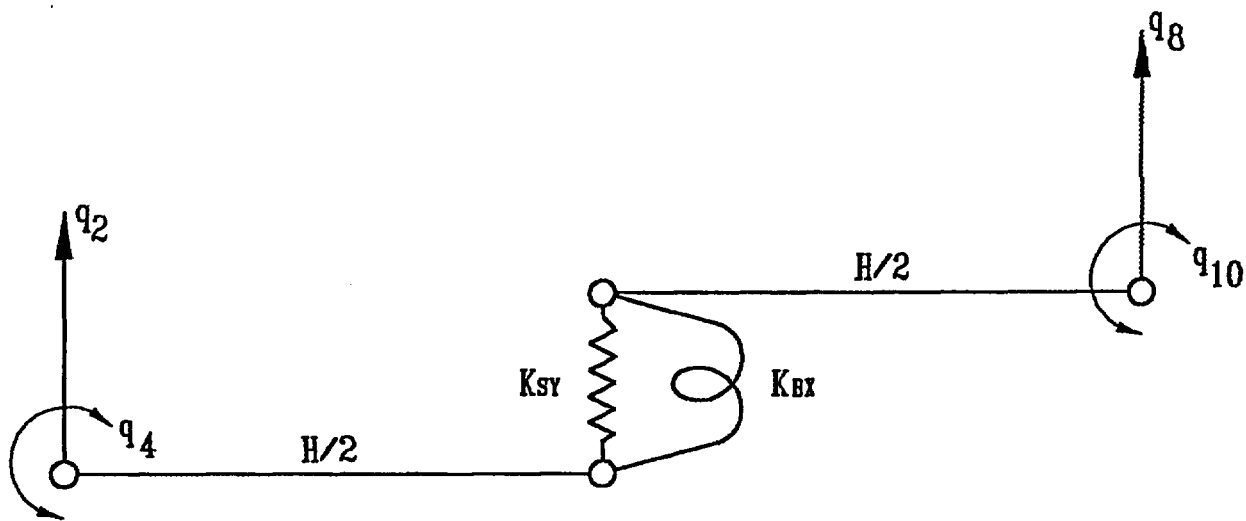
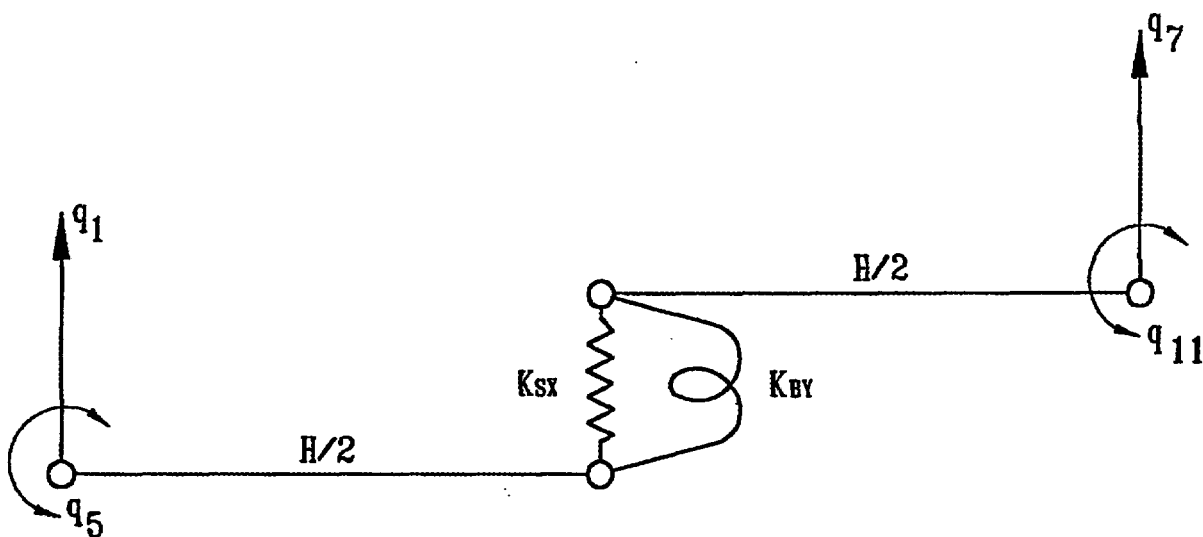


Figure 6.5.3 – Two Dimensional View of Spring-Mass Simulation



RACK DEGREES-OF-FREEDOM FOR Y-Z PLANE BENDING WITH SHEAR AND BENDING SPRING



RACK DEGREES-OF-FREEDOM FOR X-Z PLANE BENDING WITH SHEAR AND BENDING SPRING

Figure 6.5.4 – Shear and Bending Springs Representing Rack Elasticity in X-Z and Y-Z Planes

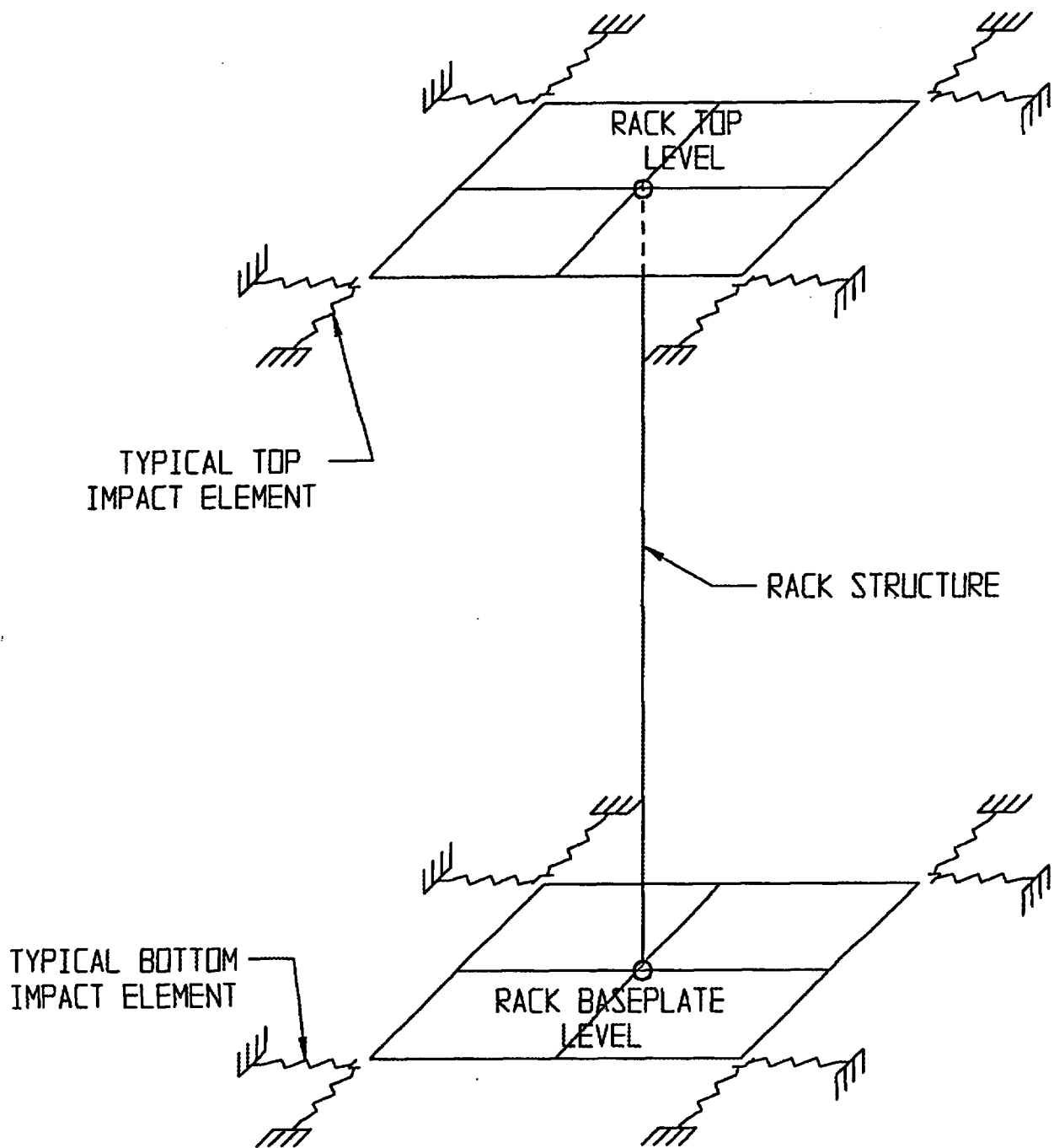
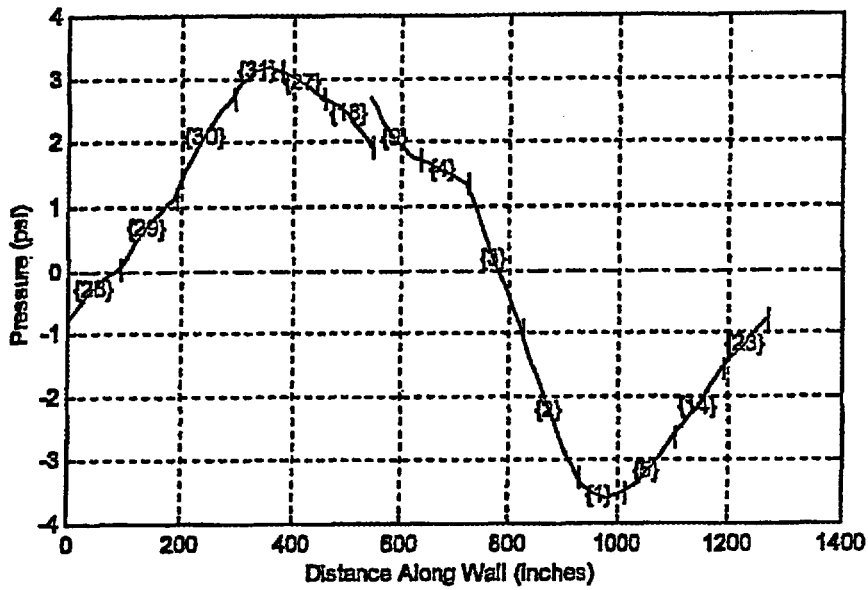


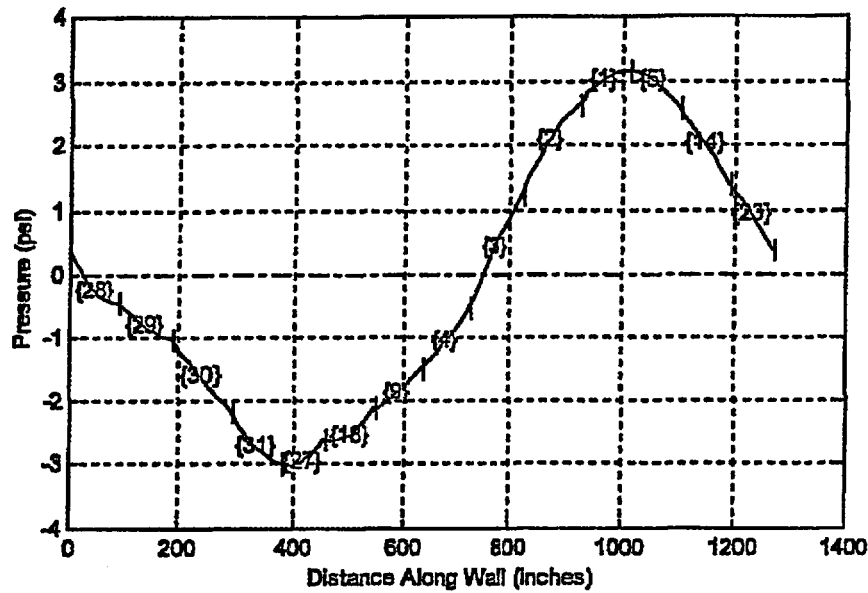
Figure 6.5.5 – Rack Periphery Gap/Impact Elements

Pressures by Prog. CHAPLS10 at time = 17.11
 {n} Denotes Channel n; "I" Marks Channel Ends



UNIT 2, OBE, COF = 0.2

Pressures by Prog. CHAPLS10 at time = 3.5
 {n} Denotes Channel n; "I" Marks Channel Ends



UNIT 2, DBE, RANDOM COF

Figure 6.11.1 – Maximum Instantaneous Hydrodynamic Pressures

7.0 MECHANICAL ACCIDENTS

7.1 INTRODUCTION

The USNRC OT position paper [7.1.1] specifies that the design of the rack must ensure the functional integrity of the spent fuel racks under all credible drop events.

The postulated fuel drop events on the ANO-2 spent fuel pool Region 3 racks, which will be inserted with Metamic® material in the rack flux traps with lead-ins installed on the top of flux traps, are evaluated.

The proposed change to the rack does not impact conclusions in the current licensing basis on the potential fuel damage due to mechanical accidents.

7.2 DESCRIPTION OF MECHANICAL ACCIDENTS

The postulated drop accidents assume that a fuel assembly, along with the portion of handling tool will drop vertically and hit the top of the rack at one of two enveloping locations: the cell wall edge, or the cell wall corner intersection. The weight and drop height in the postulated fuel drop accident are conservatively assumed to be 2,580 lbs and 29.25 inches, respectively. This compares conservatively with the actual Unit 2 weight and drop height values of 1915 lbs and 14.9 inches.

7.3 EVALUATION OF MECHANICAL ACCIDENTS

To obtain conservative results, the postulated mechanical drop accidents were evaluated based on the maximum impact energy, a thinner rack wall thickness, weakest weld size and configuration, and worst case fabrication tolerance for the ANO-2 Region 3 racks. The evaluation of the postulated drop events demonstrated that, with the previously described conservative considerations, the postulated mechanical drop accidents would result in significant damage to the impacted cell wall down into the active region, leading to the failure of Metamic® inserts inside the flux trap.

7.4 CONCLUSION

The fuel assembly drop events postulated for the ANO-2 spent fuel pool Region 3 racks were very conservatively evaluated and found that the poison inserts, as well as the cell wall, of the impacted rack cell could be significantly damaged under the postulated accidental events. To ensure the functional integrity of the rack, the criticality safety evaluation (reported in Section 4.0) conservatively analyzed the Region 3 racks under the postulated assumption that all poison inserts in the impacted cell are damaged. The racks were determined to remain subcritical even under this extremely conservative postulate, when credit was taken for the proposed technical specification limit of 2000 ppm soluble boron in the pool.

7.5 REFERENCES

[7.1.1] "OT Position for Review and Acceptance of Spent Fuel Storage and Handling Applications," dated April 14, 1978, and addendum dated 1979.

Attachment 5

2CAN010304

**Evaluation of Spent Fuel Pool Structural Integrity
for
Increased Loads from Spent Fuel Racks**

Evaluation of Spent Fuel Pool Structural Integrity for Increased Loads from Spent Fuel Racks

The ANO-2 spent fuel pool consists of 6'-0" thick reinforced concrete walls and a 5'-6" thick floor slab. The pool is supported below by thick foundation walls. Concrete compressive strength for the ANO-2 spent fuel pool is 3000 psi and reinforcement used was Grade 60.

The spent fuel pool was originally designed by Bechtel Corp. in accordance with the ACI 318-63 reinforced concrete building code, for loadings including deadweight of the structure, water, and spent fuel racks, hydrodynamic pressure from the water, operating thermal, accident thermal, seismic, tornado and flood loads. Rack loads were treated as a uniform load spread across the pool floor slab. Finite element models were used for this analysis. During a review of the structural drawings to the as-built pool structure, it was determined that insufficient anchorage existed for some of the reinforcement on the inside face of the pool. This was taken into account in the Bechtel analysis, and two pipe struts were added between the walls of the refueling canal. The North pool wall is common with the refueling canal. The purpose of the struts was to relieve high indicated transverse shear loads.

In 1981-1982, a reanalysis of the spent fuel pool structure including the foundation walls, refueling canal and cask storage area was performed by Structural Dynamics Inc. in support of the re-rack project for ANO-2. Finite element methodology was used for this analysis. The same loads as described above in the Bechtel design were included in the analysis, plus a pre-load for the struts. The loads from the spent fuel racks included their deadweight (treated as live load on the pool floor slab) and vertical and horizontal seismic load effects. Rack loads were provided by Westinghouse Corp. This analysis, again used the acceptance criteria in the ACI 318-63 code, but supplemented the strength design methodology using provisions from the ACI 349-80 Nuclear Structure Reinforced Concrete Code. The load combinations used were in accordance with Standard Review Plan, Section 3.8.

The dominant load effects were due to thermal expansion from the accident thermal loading for both analyses of the ANO-2 Spent Fuel Pool.

The recent evaluation of the spent fuel racks by Holtec International was performed to evaluate the effects on three of the racks for the additional weight of proposed poison inserts for three of the racks. This evaluation included analyses of the racks as described in Sections 3 through 6, and resulted in revised loads imparted from the racks to the pool floor slab. ANO engineering also conservatively redefined the total deadweight of all the racks. Additionally, Holtec specified a conservative hydrodynamic pressure resulting from the seismic displacement of the racks, which loads the pool walls for the height of the racks.

A review of the pool structure was performed using the 1981-1982 analysis by Structural Dynamics with the applied loads including the rack load effects. These effects were amplified using conservatively determined factors to account for the increased loads from the racks. Specifically, the deadweight loading of the racks was factored up by the ratio of the maximum increase for any of the racks. The seismic load contribution (which consisted of combined seismic effects for the pool structure, the water, plus the rack seismic loads) was factored in its entirety, by the maximum ratio calculated for the worst case rack in either the horizontal or vertical directions. This also conservatively accounted for the added hydrodynamic pressure on the pool walls.

The 1981-1982 analysis checked 21 points for section moment, transverse shear, and in-plane shear. These 21 points were the highest stressed points for the various elements of the pool structure (e.g. the highest stressed points for each direction for the pool floor slab, the highest stressed point in each of the pool walls, etc.). Of these locations, two were for the pool floor slab and three were for the pool foundation walls. The spent fuel racks are supported only by the pool floor slab, which transmits load effects from the racks to the foundation walls, to the ground. Above the pool slab level, the rack loads have little impact on the pool structural elements.

Hence, the five critical locations for the pool floor slab and foundation walls were reviewed in detail, with the rack deadweight (live load case) and the seismic loading combinations factored as described above. The following table summarizes the results of the review of these five locations.

Summary of Section Strength Review of Selected Locations

Location	Section Strength Parameter	Previous Analysis Ratio to Code Allowable	Conservative Estimate of Ratio to Code Allowable for Increased Rack Loads
Pool Floor Slab East-West Section	Moment	0.54	0.545
	Transverse Shear	0.27	0.301
	In-Plane Shear	0.15	0.187
Pool Floor Slab North-South Section	Moment	0.49	0.494
	Transverse Shear	0.37	0.479
	In-Plane Shear	0.21	0.252
Pool Foundation North Wall	Moment	0.18	0.200
	Transverse Shear	0.29	0.301
	In-Plane Shear	0.40	0.503
Pool Foundation East Wall	Moment	0.30	0.339
	Transverse Shear	0.26	0.171
	In-Plane Shear	0.76	0.806
Pool Foundation West Wall	Moment	0.36	0.387
	Transverse Shear	0.29	0.288
	In-Plane Shear	0.64	0.728

The greatest change was found for transverse shear for the north-south section, which previously had a ratio of applied shear to allowable of 0.37, and with the conservative review has a ratio of 0.479. This is a 29.5% increase, but still shows significant capacity. The highest indicated section strength value was for the Pool East Foundation Wall, for in-plane shear, with a ratio of applied shear to allowable of 0.806. Previously, the ratio was 0.76. This is a 6.1% increase, and also shows significant margin remains.

It should be noted that the added poison inserts increase the deadweight for only three of the racks by a total of about 14525 pounds, which is about a 3.5% increase in deadweight for these racks. For the review performed however, the weights for all racks were effectively increased about 31.5%. Additionally, the factored seismic loads included factoring the pool structural seismic loads as well, which have not changed. Hence in general, it can be seen that the

increased load effects as applied for this review resulted in only slight increases, and if only the added poison inserts were considered, the changes would be very small.

The results of this review demonstrate that the indicated increased loads from the racks have minimal effects on the pool structural elements, and that the structural integrity of the pool structure is maintained.

Attachment 6

2CAN010304

Commitments

List of Regulatory Commitments

The following table identifies those actions committed to by Entergy in this document. Any other statements in this submittal are provided for information purposes and are not considered to be regulatory commitments.

COMMITMENT	TYPE (Check one)		SCHEDULED COMPLETION DATE (If Required)
	ONE- TIME ACTION	CONT. COMPL.	
Upon approval of this amendment, Entergy will establish a Coupon Sampling Program to ensure that the physical and chemical properties of Metamic behave in a similar manner to that found at the test facilities.		X	September 19, 2003
Entergy will complete the analysis of the structural integrity of the poison panel inserts for normal and seismic conditions considering the finalized design modification.	X		September 19, 2003
A SAR change will be submitted to Licensing reflecting the changes made by this amendment.	X		September 19, 2003